

Evaluating the applicability of an alkaline amino acid leaching process for base and precious metal leaching from printed circuit board waste

by

Cara Philipa Broeksma

Thesis presented in partial fulfilment
of the requirements for the Degree

of

MASTER OF ENGINEERING
(EXTRACTIVE METALLURGICAL ENGINEERING)



in the Faculty of Engineering
at Stellenbosch University

UNIVERSITEIT
STELLENBOSCH
UNIVERSITY

100

1918-2018
Supervisor

Prof. C. Dorfling

Co-Supervisor

Prof. J.J. Eksteen

March 2018

Declaration

By submitting this thesis electronically, I declare that the entirety of the work contained therein is my own, original work, that I am the sole author thereof (save to the extent explicitly otherwise stated), that reproduction and publication thereof by Stellenbosch University will not infringe any third party rights and that I have not previously in its entirety or in part submitted it for obtaining any qualification.

Date: March 2018

Copyright © March 2018 Stellenbosch University
All rights reserved

Abstract

The recovery of metals from waste printed circuit boards (PCBs), a key component in electronic equipment, is beneficial from both an environmental and economic perspective. Current hydrometallurgical processing routes utilise strong mineral acids and cyanide or halides, which pose environmental hazards. Amino acids have been proposed as alternative lixiviants with a lower environmental impact. This project aimed to evaluate the applicability of the amino acid leaching process for the dissolution of metals from PCB waste.

Bench-scale leach tests were performed to determine the rate, extent and selectivity of base and precious metal leaching at different conditions. Glycine, the simplest amino acid, was used as lixiviant. The relatively low solubility of copper in the glycine system limited the pulp density during base metal leach tests to 25 g PCBs/L.

When air was used as oxidant, copper dissolution was initially independent of both temperature and glycine concentration. It was suggested that initial copper dissolution in the air system, at 1 M glycine, was limited by oxygen diffusion through the solid-liquid boundary layer. As the reaction progressed, oxygen diffusion through the CuO intermediate was believed to be rate-limiting. Increasing the temperature and glycine concentration in the presence of air, increased the rate of CuO removal through copper-glycine complex formation, which, in turn, reduced the resistance to oxygen diffusion to the reaction surface.

When pure oxygen was used as oxidant, increasing the temperature from 25°C to 60°C increased copper dissolution after 22 hours by approximately 50%. Increasing the glycine concentration above 1 M, in the presence of pure oxygen, had no effect on copper dissolution. 81% copper dissolution was achieved after 22 hours at the optimal conditions of 60°C, 1 M glycine, using pure oxygen as oxidant. At these conditions, co-extraction of gold was 1.3%.

Precious metal leach tests were performed using the residue from the base metal leach tests as feed, with H₂O₂ fed continuously as oxidant. Increasing the temperature (up to 90°C), glycine concentration (0.1 M to 0.5 M) and pH (11.5 to 12.5) had no significant effect on gold extraction, with less than 2% gold dissolution achieved after 96 hours. Further tests were performed on pure gold foils to determine whether the presence of copper in the PCBs inhibited

gold dissolution. Leaching from gold foils, however, did not improve gold dissolution and it was concluded that gold leaching with glycine is not technically feasible.

A suggested flowsheet for metal extraction was validated experimentally. Small pilot-scale leach tests were performed at the optimal conditions identified from the bench-scale base metal leach tests (60°C, 1 M glycine, with pure oxygen as oxidant). Due to poor mass transfer of oxygen into solution in the small pilot-scale leach tests, two stages (each with a duration of 41 – 52 hours) were required to achieve 78% copper dissolution. In a subsequent leaching stage, 38% gold dissolution was achieved after 96 hours, with the addition of 0.04 M NaCN to 0.13 M glycine at 25°C, using air as oxidant. Further optimisation of process variables are required to maximise gold leaching in the glycine-cyanide system.

Opsomming

Die herwinning van metale vanuit afval gedrukte stroombaan borde (GSBs), 'n sleutel onderdeel van elektroniese apparaat, is voordelig vanuit beide omgewings en ekonomiese oogpunte. Onlangse hidrometallurgiese prosesroetes gebruik sterk mineraalsure en sianied of haliede, wat omgewingsgevaar inhou. Aminosure is al voorgestel as plaasvervanger loogmiddels met 'n verminderde impak op die omgewing. Hierdie projek het beoog om die toepaslikheid van die aminosuur loogproses op die loging van metale vanuit GSB-afval te evalueer.

Kleinskaalse loogtoetse is uitgevoer om die tempo, hoeveelheid en selektiwiteit van basis- en edelmetaal loging onder verskillende omstandighede te bepaal. Glisien, die eenvoudigste aminosuur, is gebruik as loogmiddel. Die betreklike lae oplosbaarheid van koper in die glisienstelsel het die pulpdigtheid tydens basismetaal loogtoetse tot 25 g GSBs/L beperk.

Met lug as oksidant was die loging van koper aanvanklik onafhanklik van beide temperatuur en glisien-konsentrasie. Daar is aangevoer dat aanvanklike koper-loging in die lugstelsel, teen 1 M glisien, deur suurstof diffusie deur die grenslaag beperk is. Met die vordering van die reaksie, het die suurstof diffusie deur die CuO-intermediêr tempo-beperkend geword. Verhoging van die temperatuur en 'n toename in die glisien-konsentrasie in die aanwesigheid van lug het die CuO-verwydering deur koper-glisien kompleks vorming versnel, wat op sy beurt die weerstand teen suurstof diffusie na die reaksie-oppervlak verminder het.

Met die gebruik van suiwer suurstof as oksidant het die verhoging in temperatuur van 25°C tot 60°C koper-loging na 22 uur met ongeveer 50% vermeerder. Die vermeerdering van glisien tot bokant 1 M, in die aanwesigheid van suurstof, het geen invloed op koper-loging gehad nie. 81% koper-loging is bereik na 22 uur in die gunstigste toestande van 60°C, 1 M glisien-konsentrasie, met die gebruik van suiwer suurstof as oksidant. In hierdie toestande is die mede-ekstraksie van goud 1.3%.

Edelmetaal loogtoetse is uitgevoer deur die oorblyfsels van die basismetaal loogtoetse as voermiddel te gebruik, met 'n kontinue voer van H₂O₂ as oksidant. Verhoging van die temperatuur (tot 90°C), glisien-konsentrasie (0.1 M tot 0.5 M) en pH (11.5 tot 12.5) het geen

noemenswaardige uitwerking op goud-ekstraksie gehad nie, met minder as 2% goud-loging na 96 uur. Verdere toetse is op suiwer goudfoelie gedoen om te bepaal of die aanwesigheid van koper in die GSBs goud-loging inperk. Die logging vanuit goudfoelie het egter nie die goud-loging verbeter nie en die slotsom is bereik dat goudlogging met glisien nie tegnies lewensvatbaar is nie.

‘n Voorgestelde prosesroete vir metaal ekstraksie is eksperimenteel bevestig. Grootskaalse loogtoetse in optimale toestande, bepaal deur die kleinskaalse basismetale loogtoetse (60°C, 1 M glisien, met suiwer suurstof as oksidant), is uitgevoer. As gevolg van die skamele massa oordrag van suurstof tot in oplossing gedurende die grootskaalse loogtoetse, was twee fases (wat elk 41 – 52 uur duur) nodig om 78% koper-loging te bereik. In ‘n opvolgende loofase is 38% goud-loging bereik na 96 uur, met die byvoeging van 0.04 NaCN by 0.13 M glisien teen 25°C, met lug as oksidant. Verdere optimering van proses veranderlikes word benodig om die goudlogging in die glisien-sianied stelsel te maksimeer.

Acknowledgements

I would like to express my gratitude and appreciation to the following people:

- My supervisor, Prof Christie Dorfling, for his technical advice, guidance, support and patience.
- The technical and administrative staff at the Department of Process Engineering at Stellenbosch University for their assistance.
- The staff at Stellenbosch University's Central Analytical Facility, for conducting ICP-MS and for technical assistance during Scanning Electron Microscopy work.
- My family and friends, particularly my parents, Albert and Kinoet Broeksma, and Michen Haller, for their love, support and encouragement.

This work was supported by the Waste RDI Roadmap, funded by the Department of Science and Technology (DST).

Table of Contents

Declaration.....	i
Abstract.....	ii
Opsomming.....	iv
Acknowledgements.....	vi
List of Figures.....	xi
List of Tables.....	xvi
Nomenclature.....	xx
1. Introduction.....	1
1.1 Background.....	1
1.2 Motivation.....	2
1.3 Objectives.....	2
1.4 Approach and scope.....	3
1.5 Thesis outline.....	4
2. Literature Review.....	5
2.1 Introduction.....	5
2.2 Process overview.....	7
2.3 Leaching of metals from PCBs.....	9
2.3.1 Base metals.....	9
2.3.2 Precious metals.....	11
2.3.3 Material characterisation.....	13
2.4 Amino acid leaching.....	13
2.4.1 Background.....	13
2.4.2 Amino acid chemistry.....	15

2.4.3	Dissolution of copper	17
2.4.4	Dissolution of other base metals	23
2.4.5	Dissolution of precious metals	27
2.5	Reaction kinetics	29
2.6	Variables influencing rate and extent of leaching	33
2.6.1	Oxidising agent	36
2.6.2	Temperature	37
2.6.3	Glycine concentration	38
2.6.4	pH.....	39
2.6.5	Catalytic ions	40
2.6.6	Pulp density.....	42
3.	Experimental	43
3.1	Experimental planning	43
3.1.1	Base metal leaching	43
3.1.2	Precious metal leaching	47
3.2	Materials.....	50
3.2.1	Feed preparation.....	50
3.2.2	PCB characterisation.....	51
3.2.3	Leaching reagents	52
3.3	Equipment	53
3.3.1	Bench-scale leach tests	53
3.3.2	Small pilot-scale leach tests	54
3.4	Experimental procedure	55
3.4.1	Bench-scale leach tests	55

3.4.2	Small pilot-scale leach tests	55
3.5	Analytical techniques and data interpretation	56
4.	Results and discussion	58
4.1	PCB Characterisation	58
4.2	Base metal leaching.....	59
4.2.1	Preliminary tests.....	59
4.2.2	Experimental design.....	62
4.2.3	Additional tests	82
4.2.4	Bench-scale test recommendations	86
4.2.5	Variability in feed composition	87
4.2.6	Small pilot-scale leach tests	88
4.3	Precious metal leaching.....	91
4.3.1	Experimental design for preliminary tests	91
4.3.2	Additional tests	96
4.3.3	Glycine-cyanide test.....	97
4.3.4	Gold foil tests.....	98
4.3.5	Conclusions.....	100
4.4	Hydrometallurgical flowsheet	101
5.	Conclusions and Recommendations	103
5.1	Base metal leaching.....	103
5.2	Precious metal leaching.....	104
5.3	Suggested flowsheet.....	104
5.4	Recommendations	105
6.	References.....	107

Appendix A: Supplementary material	117
Appendix B: PCB Characterisation	118
B.1 Acid digestion results	118
B.2 SEM Images	122
Appendix C: Experimental data.....	124
C.1 Base metal leach tests.....	124
C.1.1 Preliminary tests	124
C.1.2 Experimental design.....	124
C.1.3 Additional tests.....	131
C.1.4 Feed composition for bench-scale tests.....	134
C.1.5 Small pilot-scale leach tests	135
C.2 Precious metal leach tests.....	136
C.2.1 Experimental design.....	136
C.2.2 Additional tests.....	137
C.2.2 Silver dissolution.....	138
Appendix D: Sample calculations.....	139
D.1 Mass balance to determine feed composition	139
D.2 Percentage dissolution.....	139
D.3 Rate calculations	140

List of Figures

Figure 1.1. Overview of experimental approach.	4
Figure 2.1. General structure of the common amino acids (redrawn from Lehninger, 1988). 15	
Figure 2.2. Ionic forms of glycine (adapted from Garret and Grisham, 2012).....	16
Figure 2.3. Speciation of glycine as a function of pH in a glycine-water system at 25°C.	17
Figure 2.4. Pourbaix diagram for a copper-water system at 25°C, with 0.43 M copper.	19
Figure 2.5. Pourbaix diagram for a copper-water-glycine system at 25°C, with 1 M glycine and 0.43 M copper.	20
Figure 2.6. Pourbaix diagram for an iron-water-glycine system at 25°C, with 1 M glycine and 0.07 M iron.....	24
Figure 2.7. Pourbaix diagram for a nickel-water-glycine system at 25°C, with 1 M glycine and 0.01 M nickel.	25
Figure 2.8. Pourbaix diagram for a lead-water-glycine system at 25°C, with 1 M glycine and 0.024 M lead.	25
Figure 2.9. Pourbaix diagram for a zinc-water-glycine system at 25°C, with 1 M glycine and 0.057 M zinc.	26
Figure 2.10. Pourbaix diagram for a tin-water system at 25°C, with 1 M glycine and 0.026 M tin.	27
Figure 2.11. Oxygen solubility in pure water as a function of temperature at atmospheric pressure using (a) pure oxygen as source ($P_{O_2} = 1$ atm), (b) air as source ($P_{O_2} = 0.21$ atm) [adapted from Xing et al. (2014) and Jackson (1986)].	30
Figure 2.12. Concentration profile of reactant at solid-solution interface [Redrawn from Jackson, (1986)]......	31
Figure 3.1. Schematic representation of the three different material characterisation methods investigated: (a) Aqua regia only, (b) 55 wt% (11.7 M) HNO_3 followed by aqua regia, (c) 30 wt% (5.6 M) HNO_3 followed by aqua regia.	52
Figure 3.2. Diagram of experimental setup for bench-scale leach tests.	54

Figure 4.1. Mass of copper extracted as a function of leaching time, temperature and glycine concentration for tests performed using air as oxidant, initial pH of 11, with a pulp density of 100 g PCBs/L (approximately 23 g Cu in the feed).....	61
Figure 4.2. Percentage copper dissolution as a function of leaching time and temperature, using 1 M glycine, with air as oxidant.....	63
Figure 4.3. Percentage copper dissolution as a function of leaching time and temperature, using 2 M glycine, with air as oxidant.....	64
Figure 4.4. Percentage copper dissolution as a function of leaching time and temperature, using 1 M glycine, with pure oxygen as oxidant.....	65
Figure 4.5. Percentage copper dissolution as a function of leaching time and temperature, using 2 M glycine, with pure oxygen as oxidant.....	66
Figure 4.6. pH as a function of time and temperature with air as oxidant for glycine concentrations of (a) 1 M and (b) 2 M.....	68
Figure 4.7. pH as a function of time and temperature with pure oxygen as oxidant for glycine concentrations of (a) 1 M and (b) 2 M.....	68
Figure 4.8. Percentage copper dissolution as a function of time and glycine concentration at 25°C for two different oxidants (a) air and (b) O ₂	70
Figure 4.9. Percentage copper dissolution as a function of time and glycine concentration at 40°C for two different oxidants (a) air and (b) O ₂	71
Figure 4.10. Percentage copper dissolution as a function of time and glycine concentration at 60°C for two different oxidants (a) air and (b) O ₂	71
Figure 4.11. Percentage copper dissolution as a function of time and oxidant type at 25°C for glycine concentrations of (a) 1 M and (b) 2 M.....	74
Figure 4.12. Percentage copper dissolution as a function of time and oxidant type at 40°C for glycine concentrations of (a) 1 M and (b) 2 M.....	74
Figure 4.13. Percentage copper dissolution as a function of time and oxidant type at 60°C for glycine concentrations of (a) 1 M and (b) 2 M.....	75
Figure 4.14. Plots for determining the rate of copper dissolution as a function of time, for tests performed at 1 M glycine, with air as oxidant. Trendlines are fitted to the period of rapid	

leaching, to ensure that the data used for estimating the rate of dissolution follows a linear trend.	76
Figure 4.15. Percentage gold dissolution as a function of leaching time, glycine concentration and oxidant type for tests performed at 60°C.....	79
Figure 4.16. Percentage silver dissolution as a function of leaching time, glycine concentration and oxidant type for tests performed at 60°C.....	79
Figure 4.17. Percentage dissolution of base metals as a function of leaching time at 60°C, 1 M glycine, with pure oxygen as oxidant.	81
Figure 4.18. Percentage copper dissolution as a function of leaching time and glycine concentration for tests performed at 60°C, with pure oxygen as oxidant.....	83
Figure 4.19. Percentage copper dissolution as a function of time and H ₂ O ₂ flowrate for tests performed at 60°C, with 1 M glycine.	84
Figure 4.20. (a) Percentage copper dissolution and (b) pH, as a function of time and oxidant type for tests performed at 60°C, with 1 M glycine.....	85
Figure 4.21. Percentage gold and silver dissolution as a function of H ₂ O ₂ flowrate for tests performed at 60°C and 1 M glycine.....	86
Figure 4.22. Mass of copper extracted as a function of time and glycine concentration, for tests performed at 60°C using air as oxidant. 95% Confidence intervals are shown to illustrate the variability in feed composition (CL refers to confidence limit).	88
Figure 4.23. Percentage copper dissolution as a function of time for tests performed at 60°C, 1 M glycine, using O ₂ as oxidant for the bench-scale test (test 2i), and two small pilot-scale leach tests, each with two stages.	90
Figure 4.24. pH as a function of time for tests performed at 60°C, 1 M glycine, using O ₂ as oxidant for the bench-scale test (test 2i), and the first stage of each of the two small pilot-scale leach tests.	90
Figure 4.25. Percentage gold dissolution after 48 hours as a function of temperature, glycine concentration and pH, for precious metal tests performed using H ₂ O ₂ as oxidant, fed continuously at 4 mL/hr.	93

Figure 4.26. Percentage silver dissolution after 48 hours as a function of temperature, glycine concentration and pH, for precious metal tests performed using H ₂ O ₂ as oxidant, fed continuously at 4 mL/hr.	94
Figure 4.27. Percentage copper dissolution as a function of time and temperature for precious metal tests performed using H ₂ O ₂ as oxidant, fed continuously at 4 mL/hr.	94
Figure 4.28. Percentage dissolution as a function of time temperature and peroxide flowrate, for the tests performed at pH 12.5 and 0.5 M glycine.	96
Figure 4.29. Percentage gold dissolution as a function of time for a mixture of 2 g/L NaCN, and 10 g/L glycine, at 25°C, initial pH 11.5, using air as oxidant.	98
Figure 4.30. Mass of gold extracted as a function of time for tests using gold foil, at 60°C, 0.5 M glycine and initial pH 12.5.	99
Figure 4.31. Flowsheet for base and precious metal leaching of PCB waste.	102
Figure B.1. Ag extraction from 20 g PCB samples, using: (A) Aqua regia only, (B) 55 wt% HNO ₃ followed by aqua regia, (C) 30 wt% HNO ₃ followed by aqua regia.	118
Figure B.2. Al extraction from 20 g PCB samples, using: (A) Aqua regia only, (B) 55 wt% HNO ₃ followed by aqua regia, (C) 30 wt% HNO ₃ followed by aqua regia.	118
Figure B.3. Au extraction from 20 g PCB samples, using: (A) Aqua regia only, (B) 55 wt% HNO ₃ followed by aqua regia, (C) 30 wt% HNO ₃ followed by aqua regia.	119
Figure B.4. Cu extraction from 20 g PCB samples, using: (A) Aqua regia only, (B) 55 wt% HNO ₃ followed by aqua regia, (C) 30 wt% HNO ₃ followed by aqua regia.	119
Figure B.5. Fe extraction from 20 g PCB samples, using: (A) Aqua regia only, (B) 55 wt% HNO ₃ followed by aqua regia, (C) 30 wt% HNO ₃ followed by aqua regia.	119
Figure B.6. Ni extraction from 20 g PCB samples, using: (A) Aqua regia only, (B) 55 wt% HNO ₃ followed by aqua regia, (C) 30 wt% HNO ₃ followed by aqua regia.	120
Figure B.7. Pb extraction from 20 g PCB samples, using: (A) Aqua regia only, (B) 55 wt% HNO ₃ followed by aqua regia, (C) 30 wt% HNO ₃ followed by aqua regia.	120

Figure B.8. Sn extraction from 20 g PCB samples, using: (A) Aqua regia only, (B) 55 wt% HNO₃ followed by aqua regia, (C) 30 wt% HNO₃ followed by aqua regia. 120

Figure B.9. Zn extraction from 20 g PCB samples, using: (A) Aqua regia only, (B) 55 wt% HNO₃ followed by aqua regia, (C) 30 wt% HNO₃ followed by aqua regia. 121

Figure B.10. SEM image of fresh feed showing incomplete liberation of copper from non-metallic material: (a) EDS layered map (b) Individual element maps for Si, Al, O and Cu. 122

Figure B.11. SEM image of fresh feed showing almost complete liberation of copper from non-metallic material: (a) EDS layered map (b) Individual element maps for Si, Al, O, Cu and Si 123

Figure C.1. Percentage silver dissolution as a function of time temperature and peroxide flowrate, for the tests performed at pH 12.5 and 0.5 M glycine. 138

List of Tables

Table 2.1. Reported composition of PCBs from different types of electronic equipment.....	7
Table 2.2. Particle sizes of crushed PCBs at which sufficient metal liberation has been reported.	8
Table 2.3. Summary of optimal leaching parameters from previous studies on base metal dissolution from PCBs.	10
Table 2.4. Disadvantages of cyanide alternatives used for precious metal leaching.....	11
Table 2.5. Summary of optimal leaching parameters from previous studies on precious metal dissolution from PCBs.	12
Table 2.6. Stability constants for copper-glycine complexes at 25°C and 1 atm (Aksu and Doyle, 2001; Martell and Smith, 1974).	18
Table 2.7. Stability constants for complexes of glycine with base metals other than copper at 25°C and 1 atm (Martell and Smith, 1974).	23
Table 2.8. Stability constants for gold and silver glycine complexes at 25°C and 1 atm.	28
Table 2.9. Leach rate of gold from pure gold foil at 0.5 M glycine, 1% H ₂ O ₂ , pH 11, 60°C (Oraby and Eksteen, 2015a).	28
Table 2.10. Summary of publications on the alkaline amino acid leaching of base metals. ...	34
Table 2.11. Summary of publications on the alkaline amino acid leaching of precious metals.	35
Table 2.12. Precious metal leach rates from gold and gold-silver foils after 168 hours at 60°C, 1 M glycine, 1% H ₂ O ₂ , pH 10 (Oraby & Eksteen, 2015a).	41
Table 3.1. Temperature and glycine concentration values for preliminary base metal leach tests.	44
Table 3.2. Fixed parameters for preliminary base metal leach tests.	45
Table 3.3. Experimental design to determine effect of temperature, glycine concentration and oxidant type on base metal leaching.	46

Table 3.4. Experimental conditions for base metal leach tests according to the experimental design in Table 3.3, and additional test at a reduced glycine concentration.....	46
Table 3.5. Hydrogen peroxide flowrates for tests performed at 60°C, 1 M glycine.....	47
Table 3.6. Feed material for each of the small pilot-scale leach tests – performed at 60°C, 1 M glycine, using pure oxygen as oxidant.....	47
Table 3.7. Experimental design for preliminary tests to determine the effect of temperature, glycine concentration and pH on precious metal leaching.	48
Table 3.8. Fixed parameters for the precious metal leach tests outlined in Table 3.7.....	48
Table 3.9. Experimental conditions for precious metal leach tests according to the experimental design given in Table 3.7.....	49
Table 3.10. Parameters for additional precious metal leach tests.....	50
Table 3.11. Parameters for precious metal leach tests performed using gold foil.....	50
Table 3.12. Reagents used for leaching and material characterisation.....	53
Table 4.1. Average composition of three 20 g PCB samples with standard deviation, for each of the three different acid digestion methods, at 60°C with S/L = 1/10: (A) Aqua regia only, (B) 55 wt% (11.7 M) HNO ₃ followed by aqua regia, (C) 30 wt% (5.6 M) HNO ₃ followed by aqua regia.....	59
Table 4.2. Estimation of the copper dissolution rate during the rapid leaching period(s).....	78
Table 4.3. Description of tests performed at 60°C, 1 M glycine, using pure oxygen as oxidant, at a pulp density of 25 g/L, at pH 11.....	89
Table 4.4. Final base metal extraction achieved in each of the small pilot-scale leach tests. .	91
Table 4.5. Average composition of precious metal feed, with standard deviation.....	91
Table 4.6. Experimental conditions for precious metal leach tests according to the experimental design given in Table 3.7.....	92
Table 4.7. Percentage dissolution of metals after 96 hours for the test performed using 2 g/L NaCN and 10 g/L glycine, at 25°C, initial pH 11.5, using air as oxidant.....	98
Table 4.8. Gold dissolution expected based on leach rates reported in literature.....	100

Table A.1. Metal content in the feed to base metal leach tests, with corresponding stoichiometric glycine concentration, at pulp densities of 100 g/L and 25 g/L.	117
Table C.1. Copper concentration and mass extracted during preliminary tests at t = 24 hours	124
Table C.2. ICP results for test 2a.	124
Table C.3. ICP results for test 2b.	125
Table C.4. ICP results for test 2c.	125
Table C.5. ICP results for test 2d.	126
Table C.6. ICP results for test 2e.	126
Table C.7. ICP results for test 2f.	127
Table C.8. ICP results for test 2g.	127
Table C.9. ICP results for test 2h.	128
Table C.10. ICP results for test 2i.	128
Table C.11. ICP results for test 2j.	129
Table C.12. ICP results for test 2k.	129
Table C.13. ICP results for test 2l.	130
Table C.14. ICP results for precious metal co-extraction.	130
Table C.15. ICP results for test 2m.	131
Table C.16. ICP results for test 3a.	131
Table C.17. ICP results for test 3b.	132
Table C.18. ICP results for test 3c.	132
Table C.19. ICP results for test 3d.	133
Table C.20. ICP results for precious metal co-extraction.	133
Table C.21. Feed composition for bench-scale base metal leach tests.	134

Table C.22. ICP results for test 4a(i).	135
Table C.23. ICP results for test 4b(i).	135
Table C.24. ICP results for test 4a(ii).	136
Table C.25. ICP results for test 4b(ii).	136
Table C.26. ICP results for experimental design tests, at t = 48 hours.	136
Table C.27. ICP results for glycine tests without the addition of cyanide.	137
Table C.28. ICP results for test 6c (cyanide-glycine test), with initial volume of 500 mL. ...	137

Nomenclature

Symbols		
A	Interfacial area	m^2
c_R	Concentration of reactant R in the bulk solution	mol/m^3
c_{RO}	Concentration of reactant R at the solid-solution interface	mol/m^3
D_R	Diffusion coefficient of reactant R	m^2/s
E_a	Activation energy	J/mol
k	Overall reaction rate constant	
k_0	Pre-exponential factor	
P_{O_2}	Oxygen partial pressure	atm
R	Ideal gas constant	$J/mol \cdot K$
T	Absolute temperature	K
t	Time	min or h
X	Fraction of metal dissolved	
δ	Boundary layer thickness	m

Abbreviations	
BFR	Brominated flame retardant
CMP	Chemical mechanical planarization
DO	Dissolved oxygen
EDS	Energy dispersive X-ray spectrometry
E-waste	Electronic waste
ICP-AES	Inductively coupled plasma atomic emission spectrometry
ICP-MS	Inductively coupled plasma mass spectrometry
S/L	Solid to liquid ratio
PCB	Printed circuit board
PLS	Pregnant leach solution
SEM	Scanning electron microscopy

1. Introduction

1.1 Background

The rate of electronic waste (e-waste) generation is increasing continuously due to rapid advances in technology and the subsequent reduced lifespan of electronic equipment. The recovery of metals from e-waste is important from both an environmental and economic perspective.

Printed circuit boards (PCBs) are key components in electronic equipment. One ton of PCB waste contains around 200 kg Cu and 250 g Au, which is significantly higher than the typical grade of these metals found in primary sources (5 – 10 kg Cu per ton of ore, and 1 – 10 g Au per ton of ore) (Tuncuk *et al.*, 2012). Of the metals contained in PCB waste, copper and gold are considered to have the greatest economic potential (Tuncuk *et al.*, 2012; Cui and Zhang, 2008).

Hydrometallurgical processes for the recovery of metals from PCBs are more selective and have lower capital cost than pyrometallurgical process routes (Ghosh *et al.*, 2015). Currently, hydrometallurgical processes used for metal recovery consist of a base metal dissolution stage using strong inorganic acids as lixiviant, followed by precious metal dissolution with cyanide or halides. These conventional leaching agents pose environmental hazards.

The Gold Technology Group of Curtin University, Australia, has developed an environmentally benign process for the hydrometallurgical recovery of metals using an alkaline amino acid as lixiviant. This process, predominantly tested on copper-gold concentrates and gold and silver foils, is disclosed in two patents (Eksteen and Oraby, 2016, 2014). It is proposed that copper can be selectively leached at ambient temperatures, while silver and gold are leached in a subsequent stage at elevated temperatures, in an oxidative environment.

This project aims to evaluate the applicability of the alkaline amino acid leaching process for the dissolution of metals from PCB waste.

1.2 Motivation

As stated in Section 1.1, the alkaline amino acid leaching process has predominantly been tested on copper-gold concentrates, and gold and silver foils. The effect of process variables on metal dissolution from these feed materials have been quantified, and optimal operating conditions have been identified. The amino acid leaching of metals from PCB waste is discussed by Eksteen and Oraby (2016) and Oraby and Eksteen (2016). However, only pH and amino acid concentration were varied in the base metal leach stage, and metal extraction was not optimised. Further study is required to investigate the effect of other process variables in order to improve metal dissolution. For precious metal leaching from PCBs, low concentrations of cyanide were added to the amino acid system (Oraby and Eksteen, 2016). Amino acid leaching at conditions favourable for precious metal extraction, without the addition of cyanide, was not reported.

Copper-gold concentrates contain metal-bearing oxide and sulphide minerals. In contrast, metals found in e-waste are present in pure form or as alloys (Ghosh *et al.*, 2015; Tuncuk *et al.*, 2012). Consequently, the leaching behaviour of metals from e-waste, as well as impurities present in the pregnant leach solution (PLS) is expected to be different compared to the leaching of metals from an ore concentrate. Knowing the composition of impurities present in the PLS is important in the purification and subsequent recovery of metals from solution. Furthermore, impurities in solution can interact with each other to either inhibit or enhance dissolution. Eksteen and Oraby (2015) and Oraby and Eksteen (2015a) reported the catalytic effect of silver and copper ions on the dissolution of gold in amino acid solutions.

1.3 Objectives

In order to evaluate the applicability of an alkaline amino acid leaching process for metal dissolution from PCB waste, the following objectives had to be achieved:

- Experimentally determine the effect of key process variables on the rate, extent and selectivity of the respective leaching stages. These process variables included temperature, oxidant type, amino acid concentration and pH.
 - For the base metal leaching stage, determine the conditions at which the greatest extent of copper dissolution is achieved, with minimal gold dissolution.

- For the precious metal leaching stage, determine the conditions at which the greatest extent of gold dissolution is achieved.
- From the experimental results, propose a flowsheet with suitable operating conditions for a multistage leaching process i.e. the selective dissolution of base metals followed by precious metal dissolution.

1.4 Approach and scope

Figure 1.1 illustrates the approach used for experimental work. Feed material for the leach tests were prepared by partially dismantling waste PCBs, followed by crushing to obtain particles of the desired size. Bench-scale base metal leach (BML) tests were performed to determine the effect of key process variables on base metal dissolution. From these tests, conditions were identified at which the greatest extent of copper dissolution was achieved, with minimal precious metal dissolution. At these conditions, small pilot-scale leach tests were performed. The solid residue from the small pilot-scale leach tests was used as feed for precious metal leach (PML) tests. Samples, taken at specific time intervals during the leaching tests, were analysed to determine the concentration of metals in solution. The residue from each of the bench-scale base and precious metal leach tests was digested in aqua regia, for complete dissolution of the remaining metals. This allowed the feed composition for each test to be quantified by means of a mass balance. Subsequently, the percentage dissolution of each metal could be calculated as a function of time. The concentration/purification of the resulting PLS and subsequent recovery of metals from solution was not considered in this project.

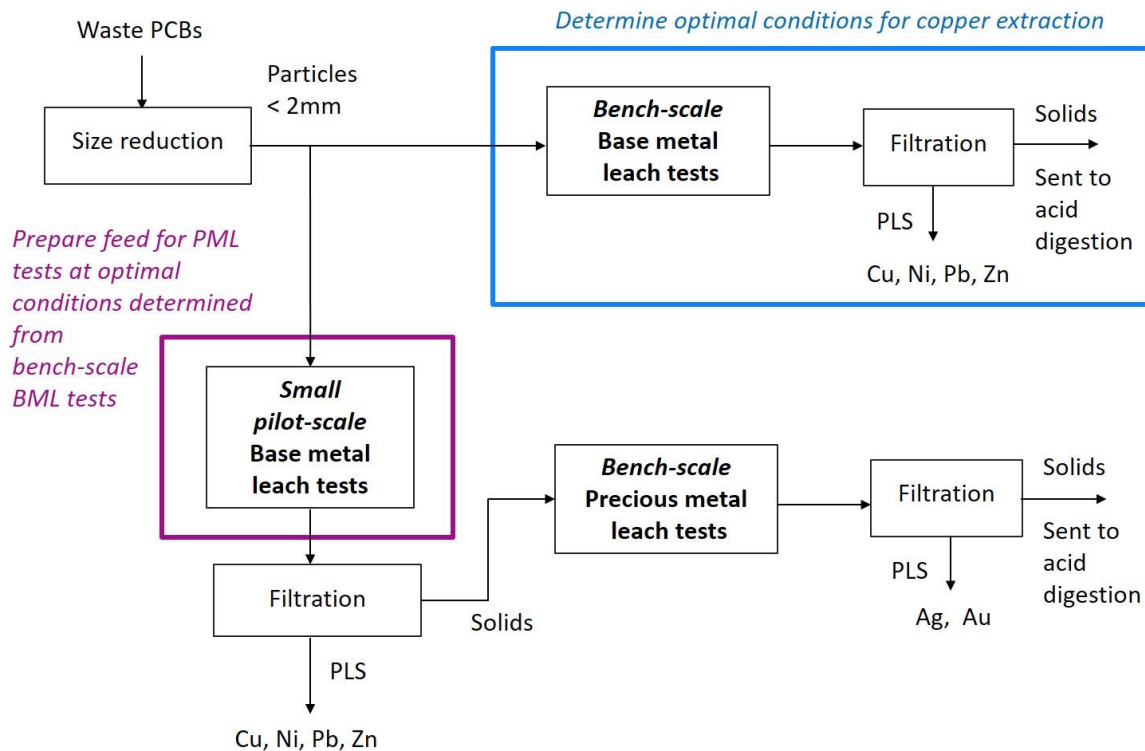


Figure 1.1. Overview of experimental approach.

1.5 Thesis outline

Section 2 presents an overview of the metal recovery from e-waste, including current lixiviants used in this process. This is followed by the chemistry of amino acid leaching, reaction kinetics and the effect of process variables on metal dissolution. The experimental planning, equipment and methodology are described in Section 3. Section 4 provides the experimental results and discussion, with conclusions and recommendations given in Section 5.

The appendices consist of supplementary material (Appendix A), material characterisation results (Appendix B), experimental data (Appendix C), and sample calculations (Appendix D).

2. Literature Review

2.1 Introduction

End-of-life electronic equipment contains a number of hazardous substances, notably heavy metals, such as mercury, cadmium and lead, and brominated flame retardants (BFRs). Consequently, if improperly managed, e-waste can pose a significant risk to the environment and to human health (Tsydenova and Bengtsson, 2011).

Conventional waste treatment methods, such as landfilling and incineration, are not adequate for the handling of e-waste. During landfilling, heavy metals present in e-waste can leach into the groundwater and soil. In the thermal treatment of e-waste, either to dispose of municipal solid waste or for pyrometallurgical recovery of metals, the metals present can act as catalyst, generating toxic compounds such as dioxins and furans from BFRs (Ghosh *et al.*, 2015). Off-gas treatment is required to prevent the emission of these substances (Hagelucken, 2006).

Hydrometallurgical methods for metal recovery are considered to have a number of benefits over pyrometallurgical process routes. Hydrometallurgical process routes are considered to be more economically viable on a smaller scale, more selective with respect to recovery of target metals over gangue, and do not give off toxic gases associated with the combustion of BFRs (Akcil *et al.*, 2014; Tuncuk *et al.*, 2012).

In addition to the environmental benefits of the proper treatment of e-waste, considerable value can be gained from the recovery of metals from waste PCBs (Tuncuk *et al.*, 2012; Chatterjee and Kumar, 2009; Cui and Zhang, 2008). PCBs are key parts in electronic equipment and typically contain 40% metals, 30% plastics and 30% ceramics by weight (Ogunniyi *et al.*, 2009; Cui and Forssberg, 2003).

A typical PCB has the following structure (Ghosh *et al.*, 2015; Kaya, 2016):

- Non-conducting substrate, composed of fibreglass-reinforced epoxy resin and ceramics.
- Conductive copper tracks printed on and/or between layers of substrate.

- Electronic components, such as chips, connectors, and capacitors, mounted on the substrate, containing a variety of base and precious metals, plastics and ceramics.
- Solder, composed of lead or tin, which bind components to the substrate.

This complex heterogeneous nature of PCBs poses a challenge to the recovery of metals (Cui and Anderson, 2016; Tuncuk *et al.*, 2012). Metals in PCBs are present in pure form, or as alloys (Tuncuk *et al.*, 2012). The plating of gold directly onto copper is sometimes used as a surface finish (Uyemura International, 2017; Le Solleu, 2010).

The ceramics and fibreglass present in PCBs typically consist of SiO_2 and Al_2O_3 , with CaO and MgO used in some cases. The plastics, including the epoxy resin, are comprised of C-H-O polymers and halogenated polymers (Ogunniyi *et al.*, 2009).

Reported compositions of PCBs from different types of electronic equipment is given in Table 2.1. The composition of e-waste varies significantly, depending on the equipment type, age and manufacturer (Cui and Zhang, 2008). Table 2.1 shows that PCBs from televisions typically have a lower metal content than PCBs from computers and mobile phones. Copper and gold are considered to have the greatest economic potential based on the value and relative amounts of these metals in PCBs (Tuncuk *et al.*, 2012; Cui and Zhang, 2008).

Table 2.1. Reported composition of PCBs from different types of electronic equipment.

Metal	Computer boards			Television boards		Mobile phone boards	
	Rossouw (2015)	Hageluken (2006)	Mecucci and Scott (2002)	Hageluken (2006)	Bas <i>et al.</i> (2014)	Hageluken (2006)	Ogunniyi and Vermaak (2009)
Cu (%)	27.6	20	21.9	10	11.2	13	23.47
Al (%)	4.5	5	-	10	0.3	1	1.33
Pb (%)	4.96	1.5	0.297	1	0.0126	0.3	0.99
Zn (%)	3.73	-		-	0.15	-	1.51
Ni (%)	0.68	1	0.003	0.3	0.02	0.1	2.35
Fe (%)	3.9	7	-	28	0.0043	5	1.22
Sn (%)	3.05	2.9	0.38	1.4	-	0.5	1.54
Ag (g/ton)	700	1000	53.7	280	48	1340	3301
Au (g/ton)	220	250	31.8	17	0.14	350	570
Pd (g/ton)	-	110	271.8	10	-	210	294

2.2 Process overview

Hydrometallurgical methods for the recovery of metals from PCBs typically consist of physical pre-treatment, including size reduction and mechanical separation, followed by selective leaching of metals using appropriate lixiviants. The resulting PLS is concentrated and purified using methods such as solvent extraction and ion exchange, with subsequent recovery of the metals from solution by electrolysis or precipitation (Ghosh *et al.*, 2015; Akcil *et al.*, 2014).

Whole PCBs are partially dismantled to remove hazardous or reusable components. Currently, disassembly of PCBs is largely a manual process (Ghosh *et al.*, 2015). The partially dismantled boards undergo size reduction, which is necessary to liberate metals from the non-metallic resin of the board, and to increase the surface area exposed to the leaching agent (Hageluken, 2006). Size reduction is achieved by shredding, crushing or grinding (Ghosh *et al.*, 2015).

Particle sizes at which sufficient liberation of metals from non-metals can be achieved is given in Table 2.2. Liberation has been reported across a wide range of particle sizes due to the significant variation in composition encountered in PCBs.

Table 2.2. Particle sizes of crushed PCBs at which sufficient metal liberation has been reported.

Particle size	Extent of liberation of metals from non-metals	Reference
<5 mm	96.5% - 99.5%	He <i>et al.</i> (2006)
<2 mm	> 99% Cu	Zhang and Forssberg (1997)
<1 mm	100%	Eswaraiah <i>et al.</i> (2008)
<0.6 mm	100%	Guo <i>et al.</i> (2011)
<0.59 mm	100%	Quan <i>et al.</i> (2012)
<0.5 mm	>98.7% Cu	Zhao <i>et al.</i> (2004)

Yang *et al.* (2011) reported high leaching efficiencies with PCB particles smaller than 1 mm. Decreasing the particle size below 0.5 mm did not increase leaching and led to a significant increase in energy consumption.

After size reduction, mechanical separation can be used to increase the grade of metal in the feed. This can be achieved by separating metals from non-metals or less valuable metals, such as iron, based on a variety of properties including electrical conductivity, magnetic susceptibility and specific gravity (Cui and Forssberg, 2003). While metals need to be completely liberated for efficient separation, and to avoid metal losses (Tuncuk *et al.*, 2012), ultrafine particles can hinder separation processes such as dense medium separation (Das *et al.*, 2009).

The mechanically pre-treated PCB feed typically undergoes a two-stage leaching process, with selective base metal dissolution, followed by the dissolution of precious metals in a subsequent stage. High concentrations of base metals can negatively affect precious metal leaching performance; hence the need for selective base metal dissolution. Native metals, such as copper, can act as a reducing surface for cementation gold. Base metals also tend to dissolve more readily than the noble precious metals; thereby decreasing the amount of reagents available for precious metal dissolution (Nguyen *et al.*, 1997).

Additionally, cyanide is relatively expensive compared to mineral acids used for base metal dissolution. Using cyanide as a leaching agent for less valuable metals, such as copper, renders leaching uneconomical (Eksteen and Oraby, 2014). Copper also competes with gold in the adsorption process causing a reduction in the gold loading capacity on activated carbon (Stewart and Kappes, 2012).

Lixivants commonly used in the recovery of metals from waste PCBs are discussed in the following section.

2.3 Leaching of metals from PCBs

2.3.1 Base metals

Strong mineral acids, such as nitric acid and sulphuric acid, are typically used for selective base metal dissolution (Zhang *et al.*, 2012). Sulphuric acid requires the addition of an oxidant, such as hydrogen peroxide, for base metal leaching, while nitric acid is a strong oxidising acid and effective alone (Bas *et al.*, 2014). These conventional mineral acids are not environmentally benign, and handling and disposal of these acids pose a risk to the environment. Optimal leaching parameters reported in previous studies using mineral acids for base metal leaching, are given in Table 2.3.

Biobleaching has been investigated for the recovery of base metals from e-waste (Bas *et al.*, 2013; Ilyas *et al.*, 2007; Brandl *et al.*, 2001). While biobleaching is environmentally benign, reaction rates are significantly slower than those achieved by chemical-leaching, and metals can be toxic to the microorganisms utilised for this application (Zhang *et al.*, 2012).

Table 2.3. Summary of optimal leaching parameters from previous studies on base metal dissolution from PCBs.

Leaching agent	Particle size (mm)	Pulp density (g/L)	T (°C)	Time (h)	% Dissolution achieved (Concentration of metal in solution)	Reference
1.6 M H ₂ SO ₄ + 0.8 M H ₂ O ₂	<0.1	13.33	68	0.5	>98% Cu (1.2 g/L)	Deveci <i>et al.</i> (2010)
2 M H ₂ SO ₄ + 0.2 M H ₂ O ₂	<0.8	100	80	8	85% Cu (40.4 g/L), 76% Zn 82% Fe, 77% Al, 70% Ni	Ficeriova (2011)
2 M H ₂ SO ₄ + 20 mL H ₂ O ₂	<3	100	30	3	76.1% Cu (23.27 g/L)	Birloaga <i>et al.</i> (2013)
2.5 M H ₂ SO ₄ + H ₂ O ₂ (30 wt%, 1.2 mL/min)	<2	160	25	8	92% Cu	Rossouw (2015)
1.2 M H ₂ SO ₄ + H ₂ O ₂ (10 vol%)	2 – 4	100	30	4	75.7% Cu (16.7 g/L)	Kumar <i>et al.</i> (2014)
3 M HNO ₃	2 – 4	100	90	5	96% Cu (21.1 g/L)	Kumar <i>et al.</i> (2014)
6 M HNO ₃	2.5	333.3	80	6	99% Cu (72.8 g/L), 99% Pb	Mecucci and Scott (2002)
3 M HNO ₃	<0.25	60	70	2	>98% Cu (6.7 g/L)	Bas <i>et al.</i> (2014)
1 M HCl + 1 M HNO ₃	<0.2	100	60	2	92.7% Cu (17.8 g/L)	Vijayaram <i>et al.</i> (2013)

2.3.2 Precious metals

Cyanide has conventionally been preferred as the main lixiviant for gold leaching due to its leaching performance. However, as a result of its toxicity and associated environmental management challenges, research is aimed at finding alternatives to replace cyanide (Hilson and Monhemius, 2006). The main cyanide alternatives investigated for e-waste leaching are thiosulphate, thiourea and halides (Tuncuk *et al.*, 2012; Zhang *et al.*, 2012). Disadvantages of these lixiviants are given in Table 2.4 (Eksteen and Oraby, 2014; Zhang *et al.*, 2012).

Table 2.4. Disadvantages of cyanide alternatives used for precious metal leaching

Lixiviant	Disadvantages
Halides (Chlorides, bromides, iodides)	Highly corrosive Environmental hazard; non-biodegradable
Thiourea, CS(NH ₂) ₂	Carcinogen; toxic High reagent consumption Expensive Cannot be produced on site
Thiosulphate (S ₂ O ₃ ²⁻)	High reagent consumption Expensive

Table 2.5 presents optimal leaching parameters for precious metal leaching from PCBs reported in previous studies.

Table 2.5. Summary of optimal leaching parameters from previous studies on precious metal dissolution from PCBs.

Leaching agent	Residual Cu in feed	Particle size (mm)	Pulp density (g/L)	T (°C)	pH	Time (h)	% Dissolution (Concentration of metal in solution)	Reference
0.1 M NaCN + pure O ₂	0.01% Cu	<0.3	200	20	11	24 h	97.1% Au (120 mg/L) 95.2% Ag (437 mg/L)	Quinet <i>et al.</i> (2005)
0.5 M (NH ₄) ₂ S ₂ O ₃ + 0.2 CuSO ₄ ·5H ₂ O + 1 NH ₃	8% Cu	<0.8	90	40	9	48 h	98% Au 93% Ag	Ficeriova <i>et al.</i> (2011)
0,2 M S ₂ O ₃ ²⁻ , 0.4 M NH ₃ , 0.02 M Cu ²⁺	1-10% Cu	<2	25	25	9-9.5	8	78.5% Au	Albertyn (2017)
0.1 3 M (NH ₄) ₂ S ₂ O ₃ + 20 mM Cu ²⁺	Negligible	<2	50	20	10	3	70% Au (5.9 mg/L) 55% Au	Camelino <i>et al.</i> (2015)
0.1 3 M (NH ₄) ₂ S ₂ O ₃ + 20 mM Cu ²⁺	15.6%	<2	50	20	10	3	55% Au	Camelino <i>et al.</i> (2015)
20 g/L CS(NH ₂) ₂ + 6 g/L Fe ³⁺ + 10 g/L H ₂ SO ₄	Not reported	<2	100	25	1.4	3.5	69% Au	Birloaga <i>et al.</i> (2014)
20 g/L CS(NH ₂) ₂ + 6 g/L Fe ³⁺ + 10 g/L H ₂ SO ₄	Negligible	<0.3	100	25	-	3	84.3% Au (15.5 mg/L) 71.4% Ag (71 mg/L)	Behnamfard <i>et al.</i> (2013)

2.3.3 Material characterisation

The metal content of PCBs is commonly determined by digesting PCBs in acid, followed by the analysis of metal concentration in solution. Aqua regia is a mixture of concentrated hydrochloric acid and nitric acid, with a volume ratio of HCl:HNO₃ of 3:1. It has the ability to completely dissolve the majority of metals contained in PCBs, including gold. As a result of this, aqua regia digestion has been used by a number of authors for determining the metal composition of PCBs (Bas *et al.*, 2014; Deveci *et al.*, 2010; Ogunniyi and Vermaak, 2009; Mecucci and Scott, 2002).

However, it has been reported that aqua regia is not suitable for complete silver dissolution, due to the formation of insoluble AgCl (Petter *et al.*, 2014; Lee *et al.*, 2011; Park and Fray, 2009). It has been proposed that nitric acid is more suitable for determining the silver content of PCBs (Petter *et al.*, 2014).

Ozmetin *et al.* (1998) investigated the effect of nitric acid concentration on the dissolution of metallic silver particles ranging from 1.7 mm – 2.36 mm. Nitric acid concentrations ranging from 7.22 M to 14.44 M were investigated. 95% silver dissolution was achieved after 20 minutes, using 7.22 M nitric acid, at 30°C and a pulp density of 20 g/L. By increasing the concentration of nitric acid, the rate of dissolution decreased. The formation of HNO₂ from HNO₃ was reported to have a catalytic effect on leaching. Increasing the concentration of nitric acid is believed to decrease the concentration of HNO₂, hence leading to decreased silver dissolution. Additionally, it was reported that at high nitric acid concentrations, formation of a saturated liquid film contributed to decreased rates of leaching.

2.4 Amino acid leaching

2.4.1 Background

As mentioned in Section 1.1, an environmentally benign leaching process, using an alkaline amino acid as lixiviant, has been developed and patented by Eksteen and Oraby (2016, 2014). A number of publications based on this patent predominantly uses glycine, the simplest amino acid, as lixiviant. Glycine is currently preferred over the other amino acids, due to its relatively low cost and bulk availability. In using other amino acids, any increase in leaching performance cannot be justified by the added costs (Eksteen and Oraby, 2016).

The leaching of copper from different types of copper-bearing minerals using glycine has been investigated by Eksteen *et al.* (2017), Tanda *et al.* (2017a) and Oraby and Eksteen (2014). Base and precious metal leaching from PCB waste is described by Eksteen and Oraby (2016) and Oraby and Eksteen (2016). Glycine leaching of precious metals from gold and silver foils was investigated by Eksteen and Oraby (2015) and Oraby and Eksteen (2015a). Further precious metals tests were performed using a glycine-cyanide mixture (Eksteen *et al.*, 2017b; Oraby *et al.*, 2017; Oraby and Eksteen, 2015b). In addition to leaching, the authors have also investigated the recovery of metals from glycine solutions. Tanda *et al.* (2017b) illustrated that copper can be recovered from aqueous copper-glycinate complexes using solvent extraction. It was also shown that gold and silver in amino acid solutions can be adsorbed onto activated carbon (Eksteen and Oraby, 2015; Oraby and Eksteen, 2015a).

Glycine offers a number of advantages over conventional leaching agents, as it is environmentally safe, stable, and readily biodegradable. It is currently used in the animal feed, food and beverages, and pharmaceutical industries, and is therefore commercially available. Glycine is produced by chemical synthesis, typically via the reaction of chloroacetic acid and ammonia (Araki and Ozeki, 2003).

Recent bulk prices show that glycine is significantly more expensive than mineral acids, but cheaper than sodium cyanide. Glycine costs 1700 USD/ton, compared to 460 USD/ton for nitric acid, and 275 USD/ton for sulphuric acid. The cost of sodium cyanide is 2380 USD/ton (Eksteen *et al.*, 2017b; Kemcore, 2017). Despite the relatively high cost of glycine, it has been reported that it can be recovered and reused (Eksteen and Oraby, 2014).

The alkaline amino acid leach process was predominantly developed for the use of metal recovery from ores. Copper deposits typically contain a high proportion of alkaline gangue minerals (such as calcite, magnesite, and dolomite) which dissolve readily in an acidic medium. Additionally, iron-bearing minerals, which dissolve partially in acidic solutions, are not expected to dissolve to a significant extent in alkaline solutions. Consequently, an alkaline leach system for copper dissolution is expected to improve the selectivity with respect to copper, and also decrease reagent consumption (Eksteen and Oraby, 2014).

As shown in Section 2.3, different lixivants are currently used for the base and precious metal leaching stages in the recovery of metals from PCB waste. The advantages of using the same

lixiviant for both leaching stages, as proposed in this project, include ease of washing between leaching stages, ease of inventory control and that similar construction materials can be used for both leaching stages (Eksteen and Oraby, 2014).

2.4.2 Amino acid chemistry

Amino acids are organic compounds which are the building blocks of protein. The 20 common amino acids, termed α -amino acids, have a carboxyl group (-COOH), amino group (-NH₂) and variable side chain (termed the R-group) attached to the same carbon atom (α carbon). Amino acids are classified according to the variable side chain, which gives each type of amino acid different properties (Lehninger, 1988). Under neutral conditions, the carboxyl group is present as -COO⁻ and the amino group as -NH₃⁺, resulting in a zwitterion (a neutral molecule with both a positive and a negative charge). The general structure of the common amino acids, in zwitterionic form, is given in Figure 2.1.

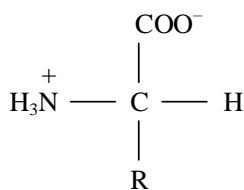


Figure 2.1. General structure of the common amino acids (redrawn from Lehninger, 1988).

The common amino acids are weak polyprotic acids, having two or more dissociable hydrogens. The degree of dissociation of the ionisable groups in aqueous solution depends on the pH of the medium (Garret and Grisham, 2012). This pH-dependent dissociation will be illustrated using glycine, the simplest amino acid. Glycine contains a single hydrogen atom as the R-group, with molecular formula NH₂CH₂COOH (Lehninger, 1988). At low pH, both carboxyl and amino groups are protonated resulting in a positively charged molecule, ⁺H₃NCH₂COOH (H₂L⁺). An increase in pH causes the carboxyl group to dissociate first, resulting in the zwitterion, ⁺H₃NCH₂COO⁻ (HL). Increasing the pH further causes the amino group to dissociate, yielding an anion, H₂NCH₂COO⁻ (L⁻). These different forms of glycine are illustrated in Figure 2.2.

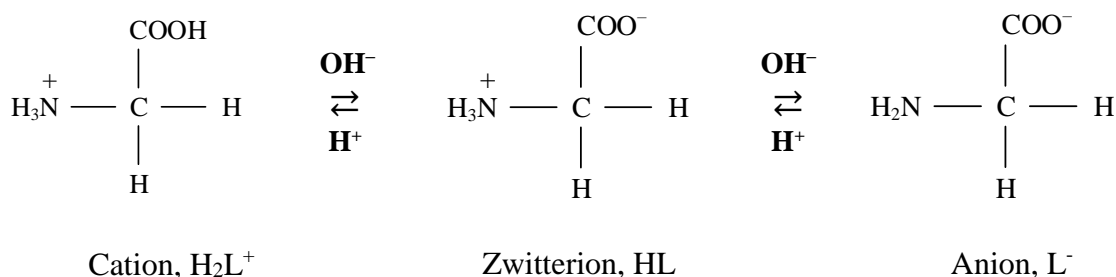


Figure 2.2. Ionic forms of glycine (adapted from Garret and Grisham, 2012).

The dissociation of a weak acid, HA, with dissociation constant, K_a , can be written as (Garret and Grisham, 2012):



The Henderson-Hasselbalch equation describes the dissociation of a weak acid in the presence of its conjugate base. For Equation 2.1, the Henderson-Hasselbalch equation can be written as:

$$pH = pK_a + \log\left(\frac{[A^-]}{[HA]}\right) \quad [2.2]$$

The dissociation of glycine is given in Equation 2.3 and 2.4. K_1 and K_2 are dissociation constants for the carboxyl group and amino acid group, respectively (Garret and Grisham, 2012; Choi, 2008):



Each type of amino acid has different values for the dissociation constants. For glycine at 25°C, $pK_1 = 2.35$ and $pK_2 = 9.78$ (Martell and Smith, 1974). The Henderson-Hasselbalch Equation, for Equation 2.3 and 2.4, can therefore be expressed as Equation 2.5 and 2.6, respectively:

$$pH = 2.35 + \log\left(\frac{[HL]}{[H_2L^+]}\right) \quad [2.5]$$

$$pH = 9.78 + \log\left(\frac{[L^-]}{[HL]}\right) \quad [2.6]$$

Figure 2.3 shows the speciation of glycine as a function of pH, based on Equation 2.5 and Equation 2.6. Below a pH of 2.35, glycine is predominantly in the cationic form. Between pH 2.35 and 9.78 the zwitterion predominates, and above pH 9.78 the anion predominates.

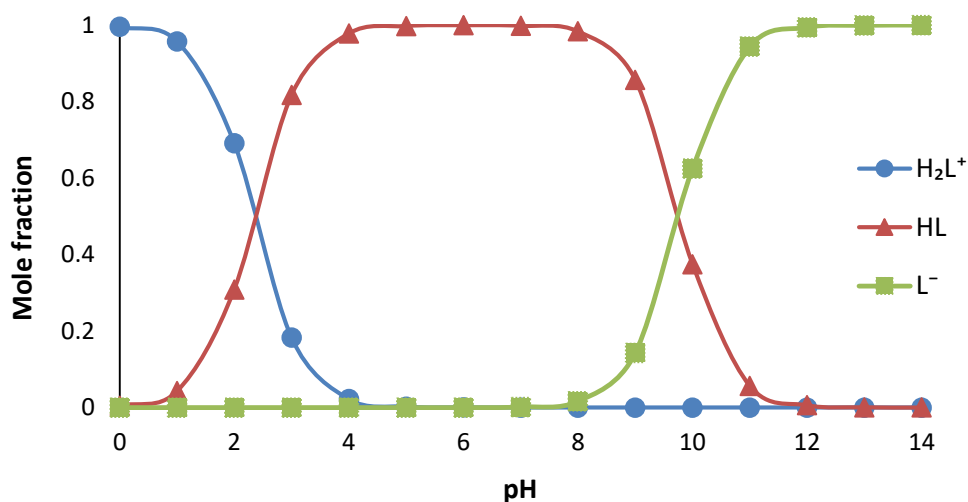


Figure 2.3. Speciation of glycine as a function of pH in a glycine-water system at 25°C.

2.4.3 Dissolution of copper

A glycine-peroxide system is commonly used as a polishing mixture in the fabrication of copper interconnects used in the electronic industry by means of chemical mechanical planarization (CMP). The glycine-peroxide mixture can effectively dissolve exposed metallic copper during CMP (Choi, 2008; Gorantla and Matijevic, 2005; Du *et al.*, 2004; Lu *et al.*, 2004; Aksu *et al.*, 2003).

Glycine forms a number of different soluble complexes with copper, as shown in Table 2.6. CuL₂ is the most stable complex, with a stability constant of 15.64. Solubility data for copper in glycine solutions could not be found in literature following a thorough search.

Table 2.6. Stability constants for copper-glycine complexes at 25°C and 1 atm (Aksu and Doyle, 2001; Martell and Smith, 1974).

Oxidation state of Cu	Complex		Log K
Cu ²⁺	$Cu(H_2NCH_2COO)^+$	CuL^+	8.56
	$Cu(H_2NCH_2COO)_2$	CuL_2	15.64
	$Cu(H_3NCH_2COO)^{2+}$	$CuHL^{2+}$	2.92
Cu ⁺	$Cu(H_2NCH_2COO)_2^-$	CuL_2^-	10.1

Pourbaix diagrams for base metals in aqueous glycine solutions were generated using HSC Chemistry version 7.1. Pourbaix diagrams show the most thermodynamically stable phases of a system at equilibrium at a particular redox potential (Eh) and pH. A limitation of these diagrams is that the kinetics of the respective reactions are not shown.

A system containing 1 M glycine and the metals content of 100 g of PCBs per litre of leach solution was defined, at a temperature of 25°C and pressure of 1 atm. The relative amounts of metals present in the PCBs were specified using the base metal composition of PCBs reported by Rossouw (2015) in Table 2.1. The Pourbaix diagrams for a copper-water system with and without glycine are given in this section, while Pourbaix diagrams for the other base metals are provided in Section 2.4.4.

Figure 2.4 shows the Pourbaix diagram for a copper-water system, in the absence of glycine. At a pH below 4, and Eh above 0.3 V, copper dissolves to form Cu²⁺ ions. With increasing pH, above a pH of 4, the solid copper surface is passivated by a copper oxide film, in the form of CuO(s) or Cu₂O(s). This illustrates that the dissolution of copper is only favoured in an acidic, oxidising environment.

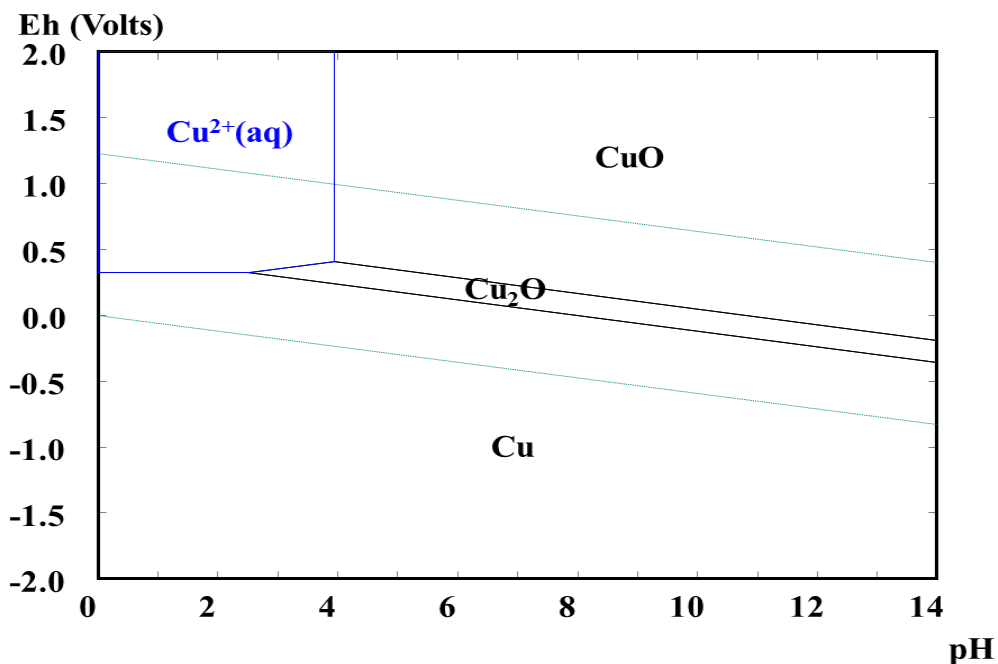


Figure 2.4. Pourbaix diagram for a copper-water system at 25°C, with 0.43 M copper.

The Pourbaix diagram for a copper-water-glycine system with glycine concentration of 1 M, is given in Figure 2.5. Of the copper-glycine complexes reported in Table 2.6, only CuL^+ and CuL_2 are available in the HSC Chemistry database. In Figure 2.5, it can be seen that with the addition of glycine as a complexing agent, under oxidising conditions, the solubility region of copper is increased as copper forms soluble complexes with glycine across a wide range of pH values. Between pH 1.8 and pH 2.4, the CuL^+ complex is the most stable. At a pH between 2.4 and 11.8, CuL_2 is the most stable. Above a pH of 11.8, CuO(s) predominates.

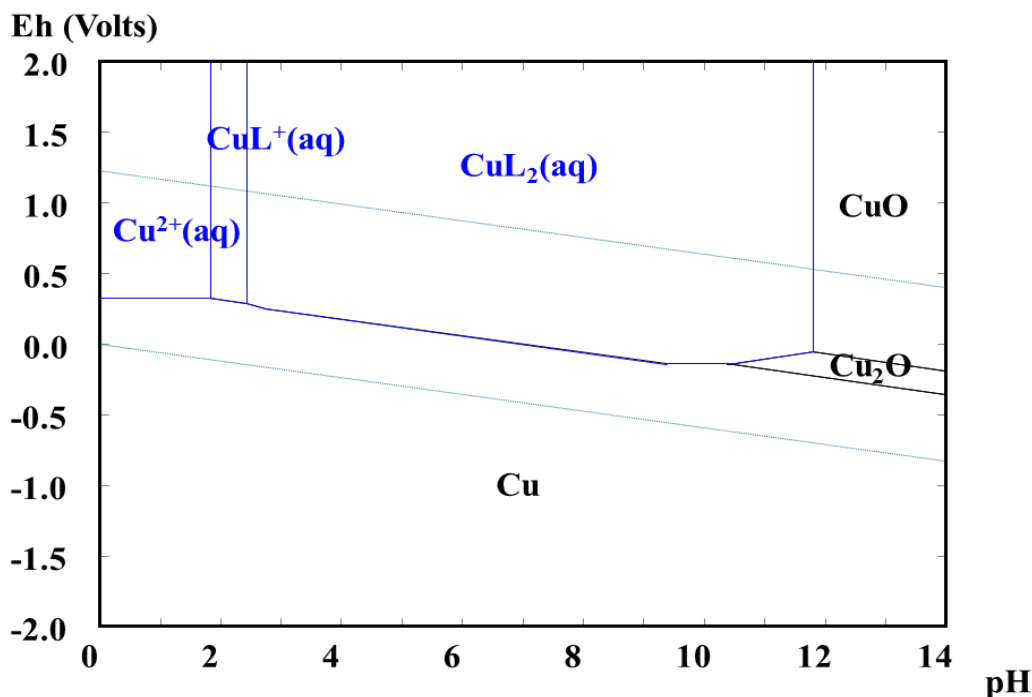


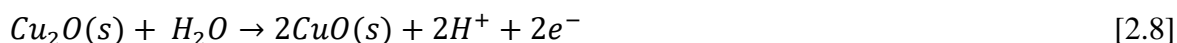
Figure 2.5. Pourbaix diagram for a copper-water-glycine system at 25°C, with 1 M glycine and 0.43 M copper.

The mechanisms proposed for the dissolution of metallic copper in oxidative glycine solutions typically consist of the following steps (Liao *et al.*, 2012; Choi, 2008; Ihnfeldt and Talbot, 2008; Du *et al.*, 2004; Luo, 2004):

- Oxidation of copper, either by dissolved oxygen in solution or by hydrogen peroxide, to form a copper oxide film as an intermediate product.
- Complexation of the intermediate copper oxide layer by glycine to form soluble copper-glycine complexes leading to the dissolution of copper.

Additionally, Hariharaputhiran *et al.* (2000) and Lu *et al.* (2004) reported that copper-glycine complexes act as catalyst to generate hydroxyl radicals (OH^{*}) from hydrogen peroxide. OH^{*} is a stronger oxidising agent than oxygen and hydrogen peroxide, leading to an increased oxidation rate. In turn, the increased rate of copper oxide formation leads to increased rates of complexation and hence the rate of formation of copper-glycine complexes increases. This cycle promotes continuous copper dissolution.

In alkaline solutions in the presence of oxygen, copper is first oxidised to form Cu_2O , followed by further oxidation of Cu_2O to CuO . The anodic oxidation reactions are presented by the following equations (Ihnfeldt and Talbot, 2008; Ganzha *et al.*, 2011):



In the presence of dissolved oxygen the cathodic reaction is the reduction of oxygen, according to Equation 2.9. If hydrogen peroxide is added to the system the cathodic reaction is described by Equation 2.10 or Equation 2.11 (Du *et al.*, 2004; Bard *et al.*, 1985):



By combining Equation 2.7, 2.8 and 2.9 the overall reaction for the oxidation of copper by oxygen can be written as:



Similarly, by combining Equation 2.7, 2.8 and 2.10 the overall reaction of copper with hydrogen peroxide is:



At alkaline pH the overall complexation reaction between CuO and glycine occurs according to Equation 2.14 (Eksteen *et al.*, 2017a; Liao *et al.*, 2012; Ihnfeldt and Talbot, 2008). Both Eksteen *et al.* (2017a) and Ihnfeldt and Talbot (2008) have demonstrated that Cu_2O is first oxidised to CuO prior to glycine complexation.



The CuL_2 complex, formed between copper and the anionic form of glycine (L^-), was shown to have the highest stability constant relative to the other copper-glycine complexes (refer to Table 2.6).

It is presumed that to form the CuL_2 complex glycine first has to dissociate into the anionic form, according to Equation 2.15. The Pourbaix diagram for a copper-water-glycine system, as seen in Figure 2.5, showed that above a pH of 2.4 the most stable copper-glycine complex is CuL_2 . However, in Figure 2.3 it was shown that between pH 2.4 and 9.78 glycine is predominantly in the zwitterionic form. Presumably, the dissociation of zwitterionic glycine, according to Equation 2.15, takes place as an intermediate step even if the zwitterion (HL) is dominant.



Subsequent complexation of $\text{CuO}(s)$ will take place, according to Equation 2.16.



The combination of Equation 2.15 and Equation 2.16, gives the overall reaction provided by Equation 2.14.

According to Equation 2.15, a higher pH favours the dissociation of HL into the anionic form (L^-). An increase in the concentration of L^- , will lead to an increase in the formation of CuL_2 by Equation 2.16. Removal of the anionic form of glycine by copper complexation will continuously alter the distribution of glycine speciation.

To summarise, operating at a higher pH favours the anionic form of glycine which leads to more stable copper complexes, CuL_2 .

The overall reaction of copper and glycine is given in Equation 2.17, for the case of oxygen as oxidant.



Equation 2.18 describes the overall equation using hydrogen peroxide as oxidant.



Halpern *et al.* (1959) reported that at low oxygen partial pressures, the rate of copper dissolution was limited by the diffusion of oxygen to the solid copper surface. At sufficiently

high oxygen partial pressures, the rate was limited by the complexation reaction between glycine and the copper-oxide film. Under these conditions, the rate of copper dissolution at 25°C was found to be independent of oxygen partial pressure and dependent on glycine concentration only.

2.4.4 Dissolution of other base metals

Of the base metals contained in PCB waste, iron, nickel, lead and zinc form soluble complexes with glycine. The stability constants for these complexes are given in Table 2.7. The mechanism of dissolution of these metals in amino acids is not available in open literature.

Table 2.7. Stability constants for complexes of glycine with base metals other than copper at 25°C and 1 atm (Martell and Smith, 1974).

Metal	Complex		Log K
Fe ²⁺	$Fe(H_2NCH_2COO)^+$	FeL^+	4.31
	$Fe(H_2NCH_2COO)_2$	FeL_2	7.65
Ni ²⁺	$Ni(H_2NCH_2COO)^+$	NiL^+	6.18
	$Ni(H_2NCH_2COO)_2$	NiL_2	11.13
Pb ²⁺	$Pb(H_2NCH_2COO)^+$	PbL^+	5.47
	$Pb(H_2NCH_2COO)_2$	PbL_2	8.86
Zn ²⁺	$Zn(H_2NCH_2COO)^+$	ZnL^+	5.38
	$Zn(H_2NCH_2COO)_2$	ZnL_2	9.81

Pourbaix diagrams for these metals in a glycine-water system are given in Figure 2.6 to Figure 2.9. Similar to copper, the complexes in the form of ML_2 (where M is the metal), have higher stability constants and are stable over a larger range of pH values than the complexes in the form of ML^+ .

For the iron-water-glycine system in Figure 2.6, it can be seen that at pH 5.5 – 10, and Eh between -0.7 V and -0.2 V, iron forms soluble complexes with glycine. At positive redox potentials, favourable for copper dissolution (refer to Figure 2.5), iron is present as $Fe_2O_3(s)$. This presents a possibility for selective iron dissolution in glycine at pH 5.5 – pH 10, at reducing conditions ($-0.7\text{ V} < Eh < -0.2\text{ V}$) prior to copper dissolution at oxidising conditions.

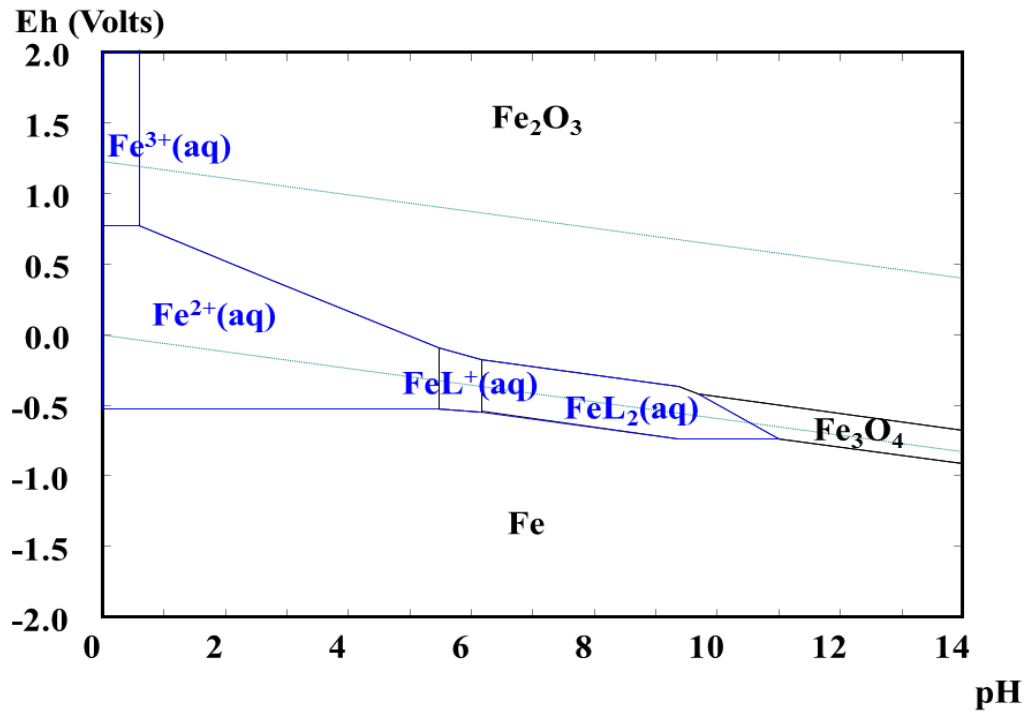


Figure 2.6. Pourbaix diagram for an iron-water-glycine system at 25°C, with 1 M glycine and 0.07 M iron.

The Pourbaix diagrams for nickel and lead in an aqueous glycine solution are shown in Figure 2.7 and Figure 2.8, respectively. Both nickel and lead show similar behaviour and are present in solution across the full range of pH values. With increasing Eh, the oxide/hydroxide form of these metals become more stable. This suggests that by increasing the Eh sufficiently, nickel and lead dissolution can be prevented.

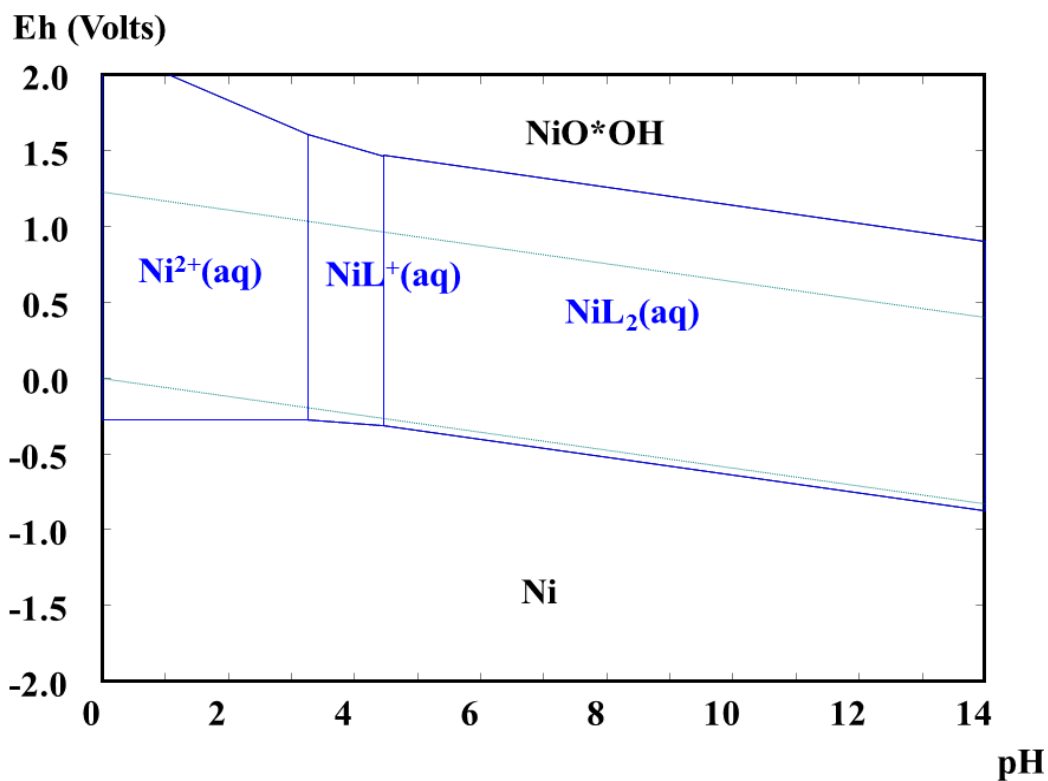


Figure 2.7. Pourbaix diagram for a nickel-water-glycine system at 25°C, with 1 M glycine and 0.01 M nickel.

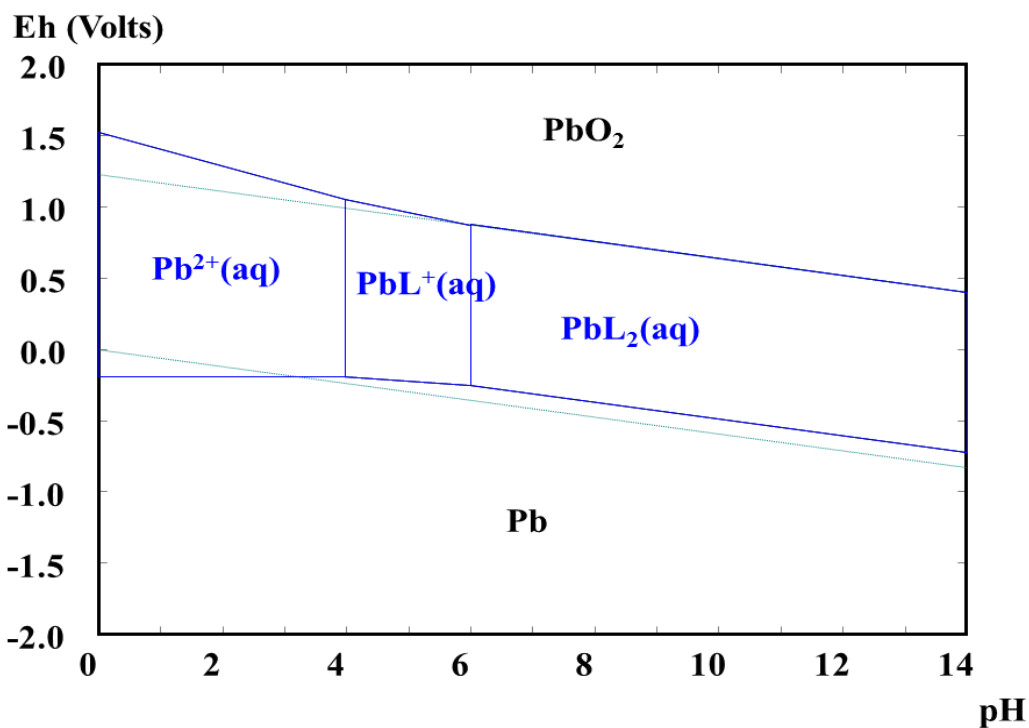


Figure 2.8. Pourbaix diagram for a lead-water-glycine system at 25°C, with 1 M glycine and 0.024 M lead.

The Pourbaix diagram for zinc in aqueous glycine solution is shown in Figure 2.9. Zinc is present in solution at a redox potential above -0.8 V and at a pH below 8.2. The ZnL_2 complex is not available in the HSC Chemistry database; however, in Table 2.7 it was seen that the ZnL_2 complex does exist, and is more stable than the ZnL^+ complex. It is possible that the ZnL_2 could expand the solubility region of zinc to higher pH values, as illustrated for copper, nickel and lead (refer to Figure 2.5, Figure 2.7 and Figure 2.8).

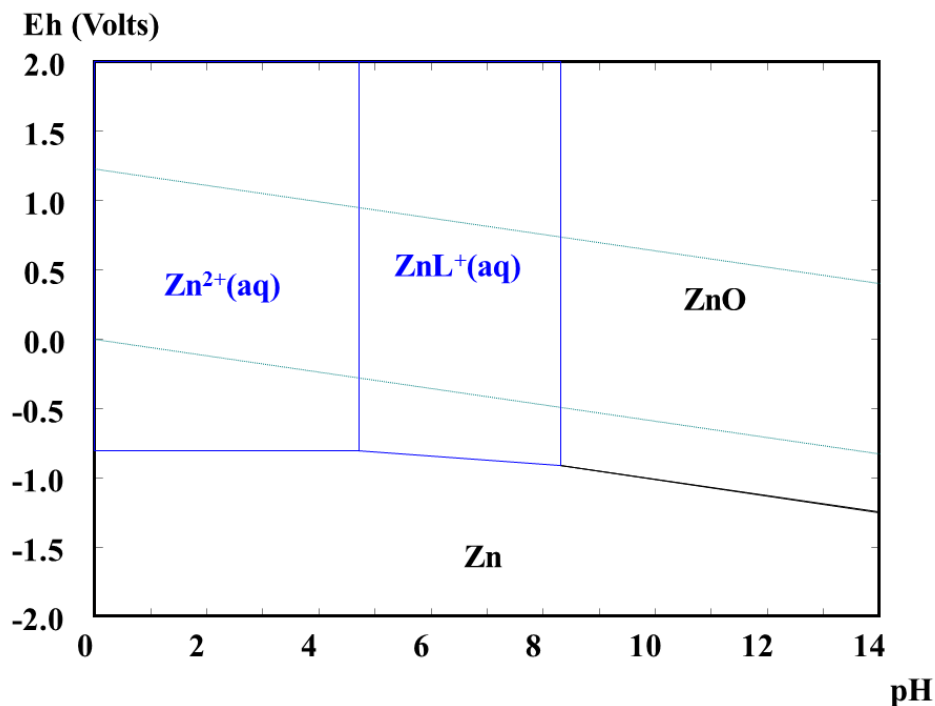


Figure 2.9. Pourbaix diagram for a zinc-water-glycine system at 25°C, with 1 M glycine and 0.057 M zinc.

It is not clear whether glycine can form complexes with aluminium and tin. These complexes are not available in the HSC Chemistry database, and neither stability constants nor thermodynamic data are available for these species in literature.

In the absence of data for a tin-glycine system, a Pourbaix diagram has been constructed for tin in water, as shown in Figure 2.10. It can be seen that under oxidative conditions tin is present as $\text{SnO}_2(\text{s})$.

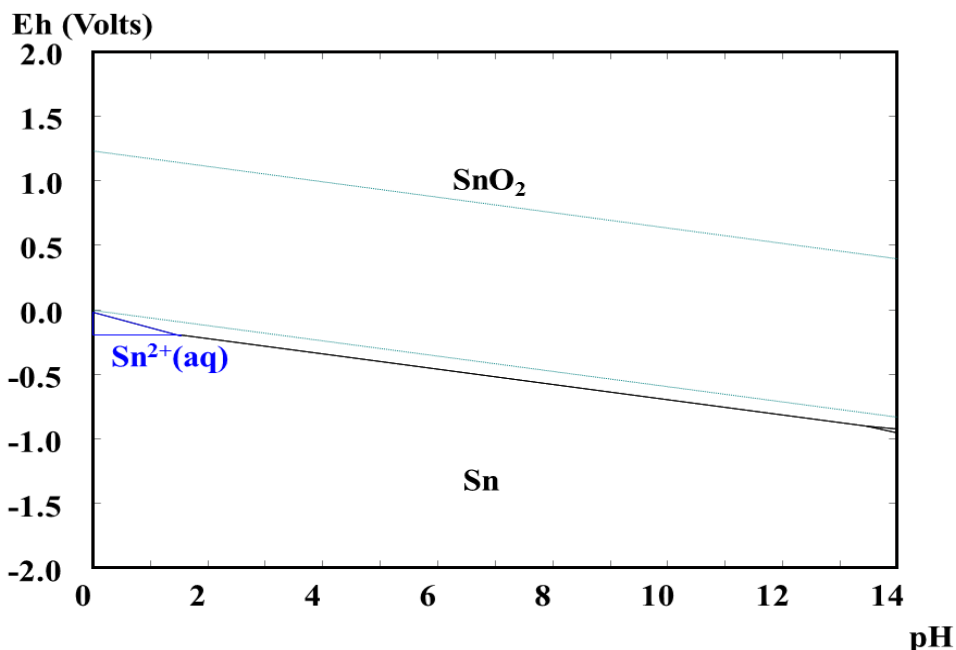


Figure 2.10. Pourbaix diagram for a tin-water system at 25°C, with 1 M glycine and 0.026 M tin.

Aluminium can dissolve in alkaline solution, without the addition of a complexing agent, such as glycine (Pyun and Moon, 2000). Dissolution takes place via reaction with water and hydroxyl ions, according to Equation 2.19.



2.4.5 Dissolution of precious metals

2.4.5.1 Glycine system

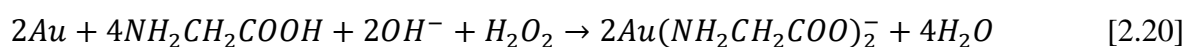
A number of studies have been performed on the solubility of gold in amino acids secreted by bacteria (Kaksonen *et al.*, 2014; Zhang *et al.*, 1997; Korobushkina *et al.*, 1983). However, besides the work of Eksteen *et al.* (2017b), Eksteen and Oraby (2015) and Oraby and Eksteen (2015a), no literature is available on the dissolution of gold and silver, with single amino acids at conditions suitable for metallurgical extraction.

Stability constants for silver and gold complexes with glycine are given in Table 2.8.

Table 2.8. Stability constants for gold and silver glycine complexes at 25°C and 1 atm.

Metal	Complex		logK	Reference
Au ⁺	$Au(NH_2CH_2COO)_2^-$	AuL_2^-	18.0	Aylmore (2005)
Ag ⁺	$Ag(H_2NCH_2COO)$	AgL	3.51	Martell and Smith (1974)
	$Ag(H_2NCH_2COO)_2^-$	AgL_2^-	6.89	

While the mechanism of gold dissolution in alkaline glycine solutions is not clear, the stoichiometry of the overall reaction is given by Equation 2.20 (Oraby and Eksteen, 2015a):



Eksteen and Oraby (2015) and Oraby and Eksteen (2015a) investigated the dissolution of gold and silver from gold and silver foils, using glycine. The leach rate at 0.5 M glycine, 1% H₂O₂, pH 11 and 60°C is given in Table 2.9. These leaching rates are reported to be 1/20th to 1/30th of the leach rates achieved with cyanide, making this system more suitable for heap leaching or in situ leaching (Eksteen and Oraby, 2015). However, these leach rates are reported for leaching in the absence of catalytic ions (such as silver and copper), and without pH control or a constant level of H₂O₂ maintained in the system. Section 2.6 discusses the effect of these parameters on leaching.

Table 2.9. Leach rate of gold from pure gold foil at 0.5 M glycine, 1% H₂O₂, pH 11, 60°C (Oraby and Eksteen, 2015a).

Leaching time (h)	Au leach rate (μmol/m ² s)
24	0.352
29	0.367
48	0.322
119	0.174
167	0.142

Neither gold nor silver glycine complexes are available in the HSC Chemistry database, and therefore Pourbaix diagrams were not generated for these metals.

2.4.5.2 Glycine-cyanide system

Oraby *et al.* (2017) and Oraby and Eksteen (2015b) used a glycine-cyanide mixture to extract gold from gold-copper ores. Oraby and Eksteen (2015b) reported that the dissolution of gold in a cuprous glycine-cyanide system is 6.5 times the rate of gold dissolution in a system using cyanide only, of the same concentration. Feasible leach rates could be obtained at very low free cyanide concentrations. It was suggested that cyanide consumption could be reduced by more than 75% by using a glycine-cyanide mixture for leaching of copper-gold ores (Eksteen *et al.*, 2017b). Oraby *et al.* (2017) reported that at a CN:Cu molar ratio of 1:1 70.1% gold dissolution could be achieved after 48 hours with the addition of glycine. In a cyanide only system, only 5% gold dissolution was achieved at the same CN:Cu molar ratio.

Additionally, it was demonstrated that the majority of copper in the final PLS is present as cupric-glycinate and not as a copper-cyanide complex. This would reduce the need for detoxification of weak acid dissociable (WAD) cyanide species (Oraby and Eksteen, 2015b). It was proposed that the main role of glycine, in this system, was to regenerate cyanide ions from copper-cyanide complexes.

2.5 Reaction kinetics

Leaching is a heterogeneous reaction between a solid and a liquid lixiviant. Using a gaseous oxidant, such as air or oxygen, introduces a third phase to the leaching system. Leaching processes typically consist of the following stages (Havlík, 2008; Levenspiel, 1999; Jackson, 1986):

1. Gaseous reactants are transported to the gas-liquid interface and dissolve in the leach solution.
2. Reactants are transported from the bulk solution, through the boundary layer, to the solid-solution interface.
3. Reactants diffuse through the porous product layer to the reaction surface.
4. Chemical, or electrochemical, reaction takes place at the reaction interface; this includes adsorption of reactants, transfer of electrons and ions, and desorption of reaction products.
5. Products diffuse through the porous product to the solid solution interface.
6. Products are transported from the solid-solution interface, through the boundary layer, into the bulk solution.

The slowest of the steps, mentioned above, controls the rate of the overall reaction. Any one or more of these steps can be rate-limiting, The rate-limiting step is dependent on the reaction conditions, and can change as the reaction progresses (Havlík, 2008; Jackson, 1986). Step 3 and 6 are only applicable if a shrinking core model is assumed.

Step 1: Dissolution of gaseous reactant

In Section 2.4.3, it was shown that in the amino-acid leaching system, dissolved oxygen in solution can act as oxidant. The rate of oxygen transfer from the gaseous phase into solution is dependent on a variety of factors. These include the reactor configuration, agitation speed, flow rate of the gas, and the solubility of oxygen in solution (Cheng, 1994).

Figure 2.11 shows the solubility of oxygen in pure water as a function of temperature, using both pure oxygen ($P_{O_2} = 1 \text{ atm}$) and air ($P_{O_2} = 0.21 \text{ atm}$) as source, where P_{O_2} is the partial pressure of oxygen in the gaseous phase. Figure 2.11 shows that the concentration of dissolved oxygen in solution increases with increasing partial pressure. At 25°C, the solubility of oxygen at a partial pressure of 1 atm is 40.9 mg/L, compared to 8.6 mg/L at a partial pressure of 0.21 atm. It is also shown that oxygen solubility decreases with increasing temperature.

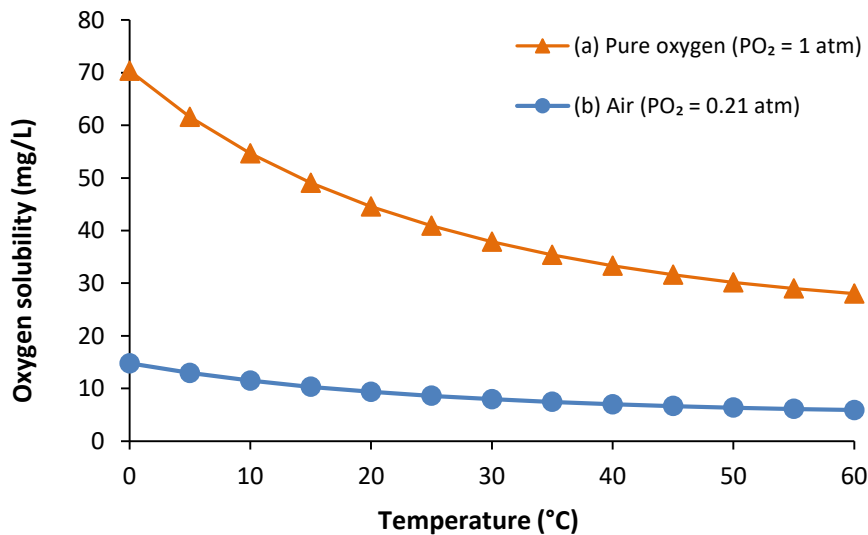


Figure 2.11. Oxygen solubility in pure water as a function of temperature at atmospheric pressure using (a) pure oxygen as source ($P_{O_2} = 1 \text{ atm}$), (b) air as source ($P_{O_2} = 0.21 \text{ atm}$) [adapted from Xing *et al.* (2014) and Jackson (1986)].

Additionally, oxygen solubility decreases with increasing solute concentrations as solutes take up a fraction of the water molecules available to interact with oxygen (Narita *et al.*, 1983).

Step 2: Diffusion of reactants through the boundary layer to the solid-solution interface

The concentration gradient of reactant in solution as a function of the distance from the solid-solution interface is shown in Figure 2.12.

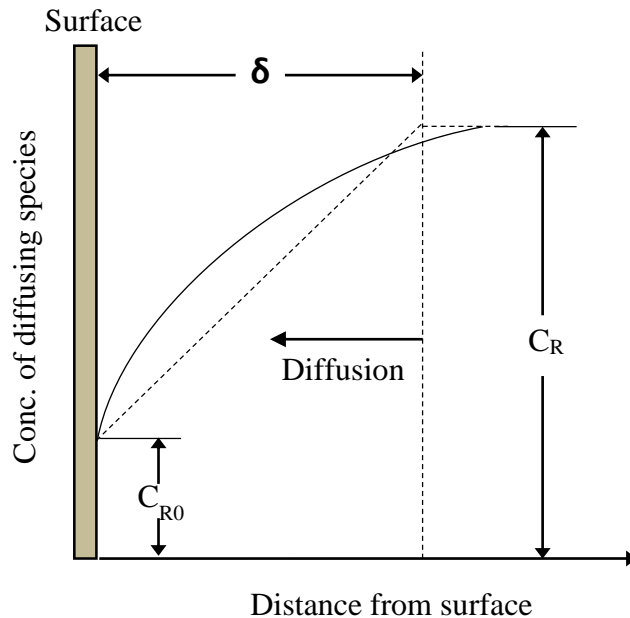


Figure 2.12. Concentration profile of reactant at solid-solution interface [Redrawn from Jackson, (1986)].

The Nernst model applies Fick's first law of diffusion and assumes a linear concentration gradient through the solid-liquid boundary layer, denoted by the broken line in Figure 2.12. The Nernst model is given by :

$$\left(\frac{dn}{dt}\right)_R = \frac{D_R A(c_R - c_{R0})}{\delta} \quad [2.21]$$

where $\left(\frac{dn}{dt}\right)_R$ is the rate of diffusion of reactant R through the boundary layer with thickness δ , diffusion coefficient D_R , and interfacial area, A . c_R and c_{R0} are the concentrations of the reactant in the bulk solution and at the surface, respectively. This difference in concentration acts as the driving force for diffusion through the boundary layer.

The diffusion coefficient, D_R , is defined by the Stokes-Einstein equation (Xing *et al.*, 2014):

$$D_R = \frac{k_B T}{6\pi r \eta} \quad [2.22]$$

where k_B is the Boltzmann constant, T is the temperature of the solution, η is the dynamic viscosity of the solution and r is the radius of the molecule. Equation 2.22 shows that D_R increases linearly with increasing temperature and is inversely proportional to the viscosity of the solution. D_R decreases with increasing electrolyte concentration due to increased solution viscosity at increasing electrolyte concentrations.

When diffusion through the boundary layer is the rate-limiting step the concentration of the reactant at the surface, c_{R0} , is equal to zero. This is due to the relatively faster surface reaction consuming all the reactant at the surface. In this case, Equation 2.21 reduces to:

$$\left(\frac{dn}{dt}\right)_R = \frac{D_R A c_R}{\delta} \quad [2.23]$$

From Equation 2.23, it can be seen that the rate of diffusion can be increased by:

- Decreasing the thickness of the boundary layer by increasing agitation
- Increasing c_R , the concentration of the reactant(s) in solution
- Increasing the interfacial area by decreasing the particle size of the solids

Diffusion controlled processes are strongly dependent on agitation rate, and largely independent of temperature (Havlík, 2008).

Step 3: Diffusion of reactants through the porous product layer

A shrinking core model, as described by Levenspiel (1999), is applicable when a porous product layer forms on the surface of the particle. The unreacted core of the particle shrinks as the reaction progresses. In this case, the reactants are required to diffuse through the product layer in order to react at the surface of the shrinking core. At the start of the reaction, diffusion through the product layer cannot be rate limiting (Prosser, 1996).

Step 4: Chemical reaction at the interface

A process controlled by chemical reaction is highly dependent on temperature, but independent of agitation speed (Havlík, 2008). Typically, the chemical reaction rate constant, k , can be defined by the Arrhenius equation:

$$k = Ae^{\left(\frac{-E}{RT}\right)} \quad [2.24]$$

where A is the pre-exponential factor, E is the activation energy for the specific reaction, R is the ideal gas constant, and T is the absolute temperature. Equation 2.24 shows that the rate constant is exponentially dependent on temperature.

Step 5: Diffusion of products through the porous product layer

Gaseous/liquid reaction products diffuse from the reaction interface, through the porous product layer, to the solid-solution interface.

Step 6: Diffusion of products from solid-solution interface into the bulk solution

Gaseous/liquid reaction products diffuse from the solid-interface, through the boundary layer, into the bulk solution.

The Nernst model, applied to the diffusion of reactants through the boundary layer in Equation 2.21, can be applied in a similar fashion to describe the diffusion of products through the boundary layer (Jackson, 1986):

$$\left(\frac{dn}{dt}\right)_P = \frac{D_P A (c_{PO} - c_P)}{\delta} \quad [2.25]$$

Where the subscript P, refers to a specific product. The driving force for diffusion, $c_{PO} - c_P$, is at a maximum when fresh solution is used i.e. the concentration of product in the bulk solution, c_P , is equal to zero.

2.6 Variables influencing rate and extent of leaching

A summary of studies performed using an amino acid as lixiviant are given in Table 2.10 and Table 2.11, for base and precious metals, respectively. The effects of process variables on leaching, as reported in these studies, are discussed in Section 2.6.1 to 2.6.6.

Table 2.10. Summary of publications on the alkaline amino acid leaching of base metals.

Feed material	Pulp density (g/L)	Glycine conc. (M)	Oxidant	pH	T (°C)	Optimum % dissolution (Metal concentration)	Time (h)	Reference
Copper-gold concentrate (<150 µm)	100 - 200	0.1, 0.3	1% H ₂ O ₂	11.5	23	98% Cu in two stages (4.75 g/L in 1 st stage; 1.07 g/L in 2 nd stage)	48	Oraby and Eksteen (2014)
Copper oxides (<75 µm)	10 – 20	0.25	Air	11	22	Azurite, malachite: >90% Cu (± 3.9 g/L) Cuprite: 83.8% Cu (3.3 g/L) Chrysocolla: 17.4% Cu (0.7 g/L)	24	Tanda <i>et al.</i> (2017)
Chalcopyrite (<45 µm)	10	0.1 – 0.4	25 mg/L DO	11.5	60	40.1% Cu (1 g/L)	24	Eksteen <i>et al.</i> (2017a)
PCBs (80% -106 µm)	4	0.4	Air	11	23	72.52% Cu (1.5 g/L), 76.5% Pb (338 mg/L), 80.94% Zn (165 mg/L)	24	Eksteen and Oraby (2016); Oraby and Eksteen (2016)

Table 2.11. Summary of publications on the alkaline amino acid leaching of precious metals.

Feed material	Pulp density (g/L)	Leaching agent	Oxidant	pH	T (°C)	Time (h)	Optimum % dissolution (Metal concentration)	Reference
Pure gold foil (Surface area = 20 cm ²)	20 cm ² foil in 400 mL	0.1 M glycine	1% H ₂ O ₂	12.8	60	96	70 mg/L Au	Eksteen and Oraby (2015)
50% Au-50% Ag foil (Surface area = 20 cm ²)	20 cm ² foil in 400 mL	1 M glycine	1% H ₂ O ₂	11	60	167	38 mg/L Au 55 mg/L Ag	Oraby and Eksteen (2015a)
Au-Cu concentrate (<75 µm)	500	0.5 M glycine	O ₂ sparged continuously	11	60	96	15.4% Au	Eksteen <i>et al.</i> (2017b)
Au-Cu concentrate (<75 µm)	500	10 g/L glycine, 0.8 g/L NaCN	Air	11	22	48	99.5% Au 97% Cu	Oraby <i>et al.</i> (2017)
PCBs (80% -106 µm)	4	0.5 g/L glycine + 0.5 g/L NaCN	Air	11	23	24	37.6% Au (0.4 mg/L) 8.8% Ag (0.088 mg/L) 87.7% Cu (1.62 g/L)	Eksteen and Oraby (2016)

2.6.1 Oxidising agent

As discussed in Section 2.4.3, either dissolved oxygen or hydrogen peroxide can be used as oxidant for copper leaching. In Figure 2.11 it was shown that the concentration of dissolved oxygen in solution can be increased by using pure oxygen instead of air as oxidant. Hydrogen peroxide is a stronger oxidant than oxygen or air, and not limited by its solubility in solution (Oraby and Eksteen, 2014; Yang *et al.*, 2011). However, rapid hydrogen peroxide degradation has been reported, particularly at increased temperatures and copper concentrations (Yazici and Deveci, 2010).

Glycine is stable in the presence of dilute solutions of hydrogen peroxide, and only oxidised by peroxide if exposed to ultra-violet light for prolonged periods (Eksteen and Oraby, 2016; Berger *et al.*, 1999).

Oraby and Eksteen (2014) investigated the effect oxidant type on the dissolution of copper from a Cu-Au concentrate, at 23°C, pH 11, glycine concentration of 0.3 M, and pulp density of 100 g/L. The system was vented to the atmosphere to allow air transfer from the surroundings. Without the addition of H₂O₂, 75% copper dissolution was achieved after 48 hours. Adding H₂O₂ increased the dissolution of copper slightly, with 81% and 85% dissolution achieved with the addition of 1% and 2% H₂O₂, respectively.

Aksu *et al.* (2003) used a mixture of hydrogen peroxide and glycine to dissolve exposed metallic copper during CMP. The addition of peroxide increased copper dissolution significantly; however, above a threshold concentration, further increase in peroxide was found to inhibit copper dissolution. This occurred at neutral pH values, where CuL₂, and not copper oxides, were expected to be dominant, according to the Pourbaix diagram (Figure 2.5). These observations were further investigated by Wang and Doyle (2003), who reported that above a threshold concentration of peroxide dissolution is inhibited by a protective copper film which gradually thickens. Similar observations were made by Ihnfeldt and Talbot (2008) who suggested that “there is an optimal H₂O₂ concentration that is needed to passivate the copper surface without inhibiting Cu–glycine complexing.” As described in Section 2.4.3, a copper oxide layer forms as an intermediate step prior to complexation. The difference between this copper oxide intermediate and the protective film inhibiting copper dissolution is not clear.

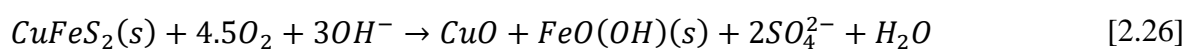
Neither Wang and Doyle (2003) nor Ihnfeldt and Talbot (2008) discussed the nature nor composition of the protective film.

In contrast to copper leaching, Eksteen and Oraby (2015) reported that hydrogen peroxide was essential for gold leaching (refer to Equation 2.20), and negligible gold dissolution was reported in the absence of peroxide. Tests were performed using pure gold foils, at 0.1 M glycine, pH 11.5, 60°C, without the addition of air or oxygen. For tests performed using 0.1 M glycine, at pH 11.5 and 60°C, increasing the concentration of peroxide from 0.1% to 2%, increased the concentration of gold in solution after 48 hours from 2.5 mg/L to 15 mg/L. However, peroxide was added to the system only at the beginning of each test. For two of the tests additional peroxide was added after 50 hours, which showed a rapid increase in leaching.

Eksteen *et al.* (2017b), however, reported 15.4% gold dissolution after 96 hours from a copper-gold ore, using oxygen sparged continuously, in the absence of hydrogen peroxide. Tests were performed at 60°C, 0.5 M glycine and pH 11.

2.6.2 Temperature

Eksteen *et al.* (2017) investigated the effect of temperature on copper dissolution from chalcopyrite at pH 11.5 with 0.2 M glycine, 10 g solids/L and DO 25 mg/L. Copper dissolution, after 24 hours, increased from 18% to 36% as temperature was increased from 23°C to 60°C. At 60°C, the pH of the solution decreased from 11.5 to 9.71 in 24 hours. The decrease in pH was attributed to the consumption of 3 moles of hydroxyl anions per mole of chalcopyrite oxidised, as shown in Equation 2.26. Subsequent glycine dissolution of oxidised copper was said to take place according to the complexation reaction given in Equation 2.14. At 23°C, the decrease in pH, from 11.5 to 10.9, was much less over the 24 hour period, reportedly due to the slower rate of oxidation at ambient temperature compared to at 60°C.



Oraby and Eksteen (2015a) reported that gold leaching from pure gold foils (1 M glycine 1% H₂O₂, pH 10, 350 rpm), was limited by chemical reaction, as opposed to being mass transfer limited, as in the case of cyanide leaching. Evidence for this was that the gold leaching was strongly dependent on temperature, and the activation energy from the experimental data was determined to be approximately 50 kJ/mol.

Eksteen and Oraby (2015) investigated the effect of temperature on gold leaching at 0.1 M glycine, 1% H₂O₂ and pH 11.5. At temperatures below 60°C, negligible dissolution was achieved after 48 hours. Increasing the temperature from 60°C to 75°C increased the concentration of gold in solution after 48 hours, from 8 mg/L to 15 mg/L. Extending the leaching time showed that no further leaching was achieved at 75°C. However, at 60°C gold dissolution continued to increase with time, with 17 mg/L gold present in solution after 150 hours of leaching. This suggests that the leaching of gold is exothermic and that at lower temperatures a greater extent of dissolution can be achieved at equilibrium.

2.6.3 Glycine concentration

Oraby and Eksteen (2014) reported that copper leaching after 24 h increased by 10% as glycine concentration was increased from 0.1 M to 0.3 M, at 23°C, pH 11, 1% H₂O₂, and pulp density of 100 g/L.

Tanda *et al.* (2017) investigated the effect of glycine concentration on copper dissolution at 22°C, and pH 11. At a pH between 2.5 and 11.8, the Pourbaix diagram for a copper-water-glycine system (Figure 2.5) predicts that CuL₂ is the most thermodynamically stable complex; with two moles of glycine required one mole of copper. Gly:Cu molar ratios between 2:1 and 8:1, were investigated, corresponding to concentrations of 0.13 M to 0.5 M. Increasing the Gly:Cu ratio from 2:1 to 4:1, increased the copper extraction after 48 hours by 20% - 30% for azurite, malachite and cuprite. Increasing the Gly:Cu ratio, from 4:1 to 8:1, increased the copper extraction initially; however, after 48 hours, increasing the Gly:Cu ratio above 4:1 had no significant effect on leaching.

Oraby and Eksteen (2016) investigated the effect of glycine concentration on the leaching of metals from PCB waste. The feed material consisted of PCBs with a particle size of 80% passing 106 µm (Eksteen and Oraby, 2016). Tests were conducted at 23°C, pH 11, a pulp density of 4 g PCBs/L and glycine concentrations ranging from 0.09 M (7 g/L) to 0.4 M (30 g/L). The reaction vessel was vented to the atmosphere allowing air to act as oxidant. Copper dissolution was independent of glycine concentration for the first 4 hours of leaching. Leaching was slow initially, with less than 5% copper dissolution achieved after 2 hours, and approximately 20% copper dissolution achieved after 4 hours, at all glycine concentrations investigated. However, as leaching progressed, increasing glycine concentration had a

significant effect on copper dissolution. After 24 hours, copper dissolution increased from 35% to 50% as the glycine concentration was increased from 0.09 M to 0.2 M. A further increase in glycine concentration to 0.4 M, led to 72.5% copper dissolution after 24 hours. Based on the reported copper content in the feed (55.2%), the stoichiometric concentration of glycine for complete copper dissolution was calculated to be 0.07 M (assuming a stoichiometric relationship for Gly:Cu of 2:1). The stoichiometric concentration required to leach all base metals was determined to be 0.1 M. The reason for the initial independence of glycine concentration was not provided.

Similarly, Oraby and Eksteen (2015a) reported that for gold leaching, the dissolution was increased by increasing glycine concentration from 0.3 M to 1 M. Leaching tests were performed with 1% H₂O₂, at pH 10 and 60°C.

2.6.4 pH

The effect of pH on copper dissolution from copper oxides was investigated by Tanda *et al.* (2017) at 22°C and 0.25 M glycine. The initial pH values investigated ranged from 9 to 11, where the pH was not controlled during the experiment. For cuprite, azurite, and malachite, an initial pH of 9 – 10 showed high copper dissolution initially, but after about 6 hours, copper started precipitating out of solution. Precipitation was not observed at pH 11. The authors reported that precipitation was inconsistent with the Pourbaix diagram for a copper-water-glycine system (Figure 2.5), as CuL₂ is the most thermodynamically stable species between pH 2.4 and 11.8. The authors proposed that the copper precipitation could be due to the zwitterion forming a less stable complex with copper, as at a pH below 9.78 the zwitterionic form of glycine predominates. The stability constant for this complex, however, was not given by the authors. As shown in Table 2.6, the stability constant for the complex formed with the zwitterion (CuHL²⁺) is significantly lower than the stability constant for the complex formed with the anion (CuL₂). As discussed in Section 2.4.3, a decrease in copper dissolution at lower pH is expected since a higher pH favours the anionic form of glycine, which forms more stable complexes.

In contrast to azurite, malachite and cuprite, Tanda *et al.* (2017) reported that leaching with chrysocolla showed no precipitation, even at pH values as low as 8. However, in the case of chrysocolla, the rate and extent of leaching was significantly slower than that of the other

minerals, with less than 1 g/L of copper in solution. For the other copper oxides, the copper concentration in solution reached between 2.5 g/L and 3.7 g/L before precipitation started. Based on this, the authors concluded that copper precipitation was dependent on both pH and on the concentration of copper in solution.

Eksteen and Oraby (2016) investigated the effect of initial pH on the glycine leaching of metals from PCB waste, with a particle size of 80% passing 106 μm . Tests were conducted at 23°C, a pulp density of 4 g PCBs/L and 0.4 M glycine, with the reaction vessel vented to the atmosphere, allowing air to act as oxidant. Copper dissolution after 24 hours increased from 20% to 72.5% as the pH was increased from 7 to 11. The change in pH during the course of the reaction was not reported. By extending the leaching time, approximately 90% copper dissolution was achieved after 72 hours at pH 11, compared to 40% dissolution at pH 7. The authors did not provide a reason for increased copper dissolution with increasing pH. However, as discussed in Section 2.4.3, it is presumed that increasing the pH favours the anionic form of glycine, which is necessary to form the CuL_2 complex via Equation 2.16.

Eksteen and Oraby (2015) and Oraby and Eksteen (2015a) reported that gold dissolution from pure gold foils was highly dependent on pH. pH values ranging from 5.8 – 12.8 were investigated. At glycine concentrations of 0.5 M glycine, 1% H_2O_2 and 60 °C, the concentration of gold in solution after 48 hours increased from 1 mg/L to 28 mg/L as the pH was increased from 10 to 11. It was not reported whether the pH was controlled in these tests, nor if there was a change in pH during the course of reaction.

2.6.5 Catalytic ions

2.6.5.1 Copper

Eksteen and Oraby (2015) reported the catalytic effect of Cu^{2+} ions on the dissolution of gold from foils. For tests performed using 0.1 M glycine, 0.1% H_2O_2 , at pH 11 and 30°C, negligible dissolution was achieved in the first 48 hours of leaching when no copper was present in the system. With the addition of 4 mM Cu^{2+} ions, the concentration of gold in solution was 0.5 mg/L and 2.2 mg/L after 2 and 48 hours, respectively. It was not reported in which form the Cu^{2+} ions were added.

Hariharaputhiran *et al.* (2000) investigated the effect of copper-glycine complexes as catalyst in generating OH* from H₂O₂. It was reported that the addition of both Cu²⁺ and glycine was necessary for the generation of OH*. In the presence of Cu²⁺ or glycine alone, an insignificant amount of OH* was generated. It was concluded that it is the CuL₂ complex that acts as catalyst to produce OH* from H₂O₂. At 0.01 M glycine and 2 wt% H₂O₂, the amount of OH* generated from peroxide increased with increasing temperature (from 21°C to 55°C), increasing concentration of Cu²⁺ added to the system (from 90 µM to 270 µM) and increasing H₂O₂ concentration (from 0% to 15%).

However, as stated in Section 2.2, metallic copper can provide a reducing surface for the cementation of gold. Nguyen *et al.* (1997) reported that the rate of gold cementation in the cyanide solution was a function of temperature, and initial cyanide and copper concentrations. The rate of cementation increased with increasing temperature and increasing initial copper concentrations.

2.6.5.2 Silver

Oraby and Eksteen (2015) reported that the presence of silver enhances the rate of gold dissolution. Tests were performed using 1 M glycine, 1% H₂O₂, pH 10, 60°C. Leaching of gold from gold-silver alloys (50% Au, 50% Ag) caused the rate of gold dissolution to be 6 times higher than the rate of dissolution achieved with leaching of gold from pure gold foils. These leach rates are given in Table 2.12. A similar effect was reported for silver and gold leaching with a cyanide system (Wadsworth and Zhu, 2003) and thiosulphate system (Chandra and Jeffrey, 2004).

Table 2.12. Precious metal leach rates from gold and gold-silver foils after 168 hours at 60°C, 1 M glycine, 1% H₂O₂, pH 10 (Oraby & Eksteen, 2015a).

Metal	Source	Leach rate (µmol/m ² /s)
Au	Pure Au sheet	0.031
Au	50% Au-50% Ag	0.185
Ag	50% Au-50% Ag	0.247

2.6.5.3 Cyanide

Oraby and Eksteen (2016) used a glycine-cyanide mixture to leach gold from PCBs. The feed material consisted of PCBs with a particle size of 80% passing 106 μm . Tests were conducted at 23°C, 0.4 M (30 g/L) glycine, pH 11 and a pulp density of 4 g PCBs/L. The reaction vessel was vented to the atmosphere allowing air to act as oxidant. The concentration of copper in solution after 24 hours was 1490 mg/L, corresponding to an extraction of 72.52%. Co-extraction of gold and silver was low, with extractions of 0.34% and 1.3%, respectively. By adding 0.5 g/L NaCN to the leach solution, copper extraction after 24 hours increased to 87.65%. The extraction of gold and silver achieved with the addition of cyanide were 37.61% and 8.84%, respectively. Further tests were performed to investigate the effect of copper content in gold leaching. Decreasing the copper content in the feed from 55% to 15% increased gold extraction after 24 hours from 37.6% to 92.1%. The reason for improved leaching at a reduced copper content, was not provided by the authors. As discussed in Section 2.6.5.1, metallic copper can act as a reducing surface for gold cementation. Increased copper content is also expected to increase reagent consumption, thereby reducing the amount of reagent available for gold dissolution.

Oraby *et al.* (2017) optimised the glycine-cyanide mixture for the leaching of a gold-copper concentrate, with particle size $<75\mu\text{m}$. Tests were conducted at 22°C, 500 g solids/L and pH 11. At the optimum CN:Cu molar ratio of 1.4:1 (0.8 g/L NaCN) and Gly:Cu molar ratio of 2.2:1 (2 g/L glycine), 99.4% Au and 88.2% Cu was extracted.

2.6.6 Pulp density

Oraby and Eksteen (2014) investigated the effect of pulp density on copper dissolution at 23°C, 0.3 M glycine, 1% H_2O_2 and pH 11. Copper dissolution achieved after 48 hours decreased by 10% as pulp density was increased from 10% to 20%. This was attributed to decreased oxygen transfer at increased pulp densities.

Similarly, Huang *et al.* (2014) observed a decrease in copper dissolution from PCBs with increasing pulp density. This was reportedly also due to decreased mass transfer at increased pulp densities. A bronsted acidic ionic liquid was used as lixiviant.

3. Experimental

3.1 Experimental planning

As discussed in Section 1.4, bench-scale base metal leach tests were performed to identify conditions at which the greatest extent of copper dissolution could be achieved, with minimal gold dissolution. The extent of extraction of the other base metals were also determined to quantify the impurities present in the PLS. At the optimal conditions identified from the bench-scale leach tests, small pilot-scale leach tests were performed to prepare the required feed material for precious metal leach tests.

The experimental planning of the base and precious metal leaching experiments are given in Section 3.1.1 and Section 3.1.2, respectively. Process conditions for the preliminary experiments in each section are based on the literature study and practical considerations. Subsequent tests were performed based on the outcome of the preliminary tests. While a brief overview of subsequent tests are also given in these sections, the motivation for these tests, together with the process conditions, are discussed in more detail in Section 4 (results and discussion).

Crushed PCBs with particle size smaller than 2 mm were used for both bench-scale base metal leach tests and small pilot-scale leach tests. Results from previous studies suggested that high metal recoveries could be achieved at these particles sizes (refer to Table 2.3 and Table 2.5).

3.1.1 Base metal leaching

Preliminary base metal leach tests were conducted to identify the conditions at which further base metal leach tests should be conducted, specifically to:

- Determine a suitable range of temperature and glycine concentration
- Determine if an oxidant stronger than air is required
- Get an indication of the leaching kinetics

Only temperature and glycine concentration were varied in these tests. The values for these parameters are given in Table 3.1, with the fixed parameters for these tests discussed in Table 3.2.

In Table 3.1, it can be seen that 3 different glycine concentrations were used for the 4 preliminary tests. Glycine concentrations were based on the metals content of 3 feed samples digested in aqua regia, which is discussed in Section 4.1. The stoichiometric concentration of glycine required for complete dissolution of the base metals, was determined to be 1.3 M (refer to Table A.1, Appendix A). A low value for glycine concentration was chosen as 1.5 M, which is just above the stoichiometric concentration of 1.3 M. For the high glycine concentration, it was desired to have a concentration 3 times the low concentration i.e. 4.5 M. However, at 25°C the solubility of glycine is only 250 g/L (± 3.3 M), compared to a solubility of 454 g/L (± 6 M) at 60°C (Araki and Ozeki, 2003). Consequently, a concentration of 2.5 M was chosen for 25°C.

Table 3.1. Temperature and glycine concentration values for preliminary base metal leach tests.

Test	Temperature (°C)	Glycine concentration (M)
1a	25	1.5
1b	25	2.5
1c	60	1.5
1d	60	4.5

Table 3.2. Fixed parameters for preliminary base metal leach tests.

Parameter	Fixed setpoint	Motivation
Initial pH	11 (monitored but not controlled)	pH sufficiently high to avoid copper precipitation (refer to Section 2.6.4).
Pulp density	100 g PCBs/L (complete dissolution would give approximately 25 g/L Cu)	As no solubility data was available for copper in glycine solutions, initial tests were performed using pulp densities similar to those used in mineral-acid leaching of base metals (Table 2.3), to see if similar copper concentrations could be achieved in the glycine system.
Agitation speed	700 rpm	Minimum speed required to keep particles in suspension.
Oxidant	Air sparged continuously at 300 mL/min	Previous studies suggested air was sufficient to leach copper; air was sparged continuously to increase mass transfer in the system. While H ₂ O ₂ is a more effective oxidant, the selectivity of the base metal leach could be compromised.

Parameters for further base metal leach tests are provided in the remainder of this section. The motivation for these tests, together with the results and discussion of the base metal leach tests, are given in Section 4.2.

Results from the preliminary tests suggested the presence of a solubility limit at 11.5 g/L Cu, which is discussed further in Section 4.2.1. Consequently, further base metal leach tests were performed at a reduced pulp density of 25 g PCBs in 1 litre of solution, compared to 100 g PCBs/L in the preliminary tests. Complete copper extraction at a pulp density of 25 g PCBs/L would correspond to a solution concentration of 6.25 g/L Cu. Due to the reduced solids loading the agitation speed was decreased to 500 rpm. These tests were performed at the same initial pH of the preliminary tests, pH 11, without pH control.

12 tests were conducted according to a full factorial experimental design with the factors and respective levels as shown in Table 3.3. Pure oxygen was investigated as oxidant, in addition to air, using a flowrate of 300 mL/min.

Table 3.3. Experimental design to determine effect of temperature, glycine concentration and oxidant type on base metal leaching.

Variable	Levels	Setpoints		
Temperature	3	25°C	40°C	60°C
Glycine concentration	2	1 M	2 M	
Oxidant	2	Air	O ₂	

Results from the experimental design tests, discussed in Section 4.2.2.2, showed that increasing the glycine concentration in the presence of pure oxygen had no significant effect on copper dissolution. An additional test was performed at a decreased glycine concentration of 0.5 M and temperature of 60°C, using pure oxygen as oxidant. The experimental conditions for each test, including the test at a reduced glycine concentration, is given in Table 3.4.

Table 3.4. Experimental conditions for base metal leach tests according to the experimental design in Table 3.3, and additional test at a reduced glycine concentration.

Test	Temperature (°C)	Glycine concentration (M)	Oxidant type
2a	25	1	Air
2b	40	1	Air
2c	60	1	Air
2d	25	2	Air
2e	40	2	Air
2f	60	2	Air
2g	25	1	O ₂
2h	40	1	O ₂
2i	60	1	O ₂
2j	25	2	O ₂
2k	40	2	O ₂
2l	60	2	O ₂
2m	60	0.5	O ₂

At the optimal temperature and glycine concentration, identified from the tests above, a third oxidant type was investigated. 30 wt% hydrogen peroxide was fed continuously, at varying flowrates, specified in Table 3.5. The duration of each test was 12 hours. These tests were

conducted at an initial pulp density of 25 g/L. To allow for the volume of peroxide fed, 12.5 g of PCBs were added to 500 mL of leach solution.

Table 3.5. Hydrogen peroxide flowrates for tests performed at 60°C, 1 M glycine.

Test	H₂O₂ flowrate (mL/min)
3a	0.15
3b	0.3
3c	0.5
3d	1

Small pilot-scale leach tests were performed at the optimum conditions identified from the bench-scale leach tests. These conditions were determined to be 60°C, 1 M glycine, using pure oxygen as oxidant, as discussed in Section 4.2.4. Results from the small pilot-scale leach tests, provided in Section 4.2.6, showed poor leaching performance compared to bench-scale leach tests. This was attributed to better oxygen mass transfer achieved in bench-scale tests. The residue from the first set of small pilot-scale leach tests were re-leached at identical conditions to reduce the copper content in the precious metal feed. The feed material for each of the small pilot-scale leach tests are specified in Table 3.6.

Table 3.6. Feed material for each of the small pilot-scale leach tests – performed at 60°C, 1 M glycine, using pure oxygen as oxidant.

Test	Feed material
4a(i)	Fresh feed
4b(i)	Fresh feed
4a(ii)	Solid residue from test 4a(i)
4b(ii)	Solid residue from test 4b(i)

3.1.2 Precious metal leaching

The solid residue from small pilot-scale tests 4a(ii) and 4b(ii) were combined using a rotary sample splitter and used as feed in the precious metal leach tests. The full factorial experimental design for the first set of precious metal leach tests are given in Table 3.7, while the fixed parameters and experimental conditions for each test are given in Table 3.8 and Table 3.9 respectively.

Table 3.7. Experimental design for preliminary tests to determine the effect of temperature, glycine concentration and pH on precious metal leaching.

Variable	Levels	Setpoints	
Temperature	2	60°C	75°C
Glycine concentration	2	0.1 M	0.5 M
pH	2	11.5 (controlled above pH 11)	12.5 (controlled above pH 12)

Table 3.8. Fixed parameters for the precious metal leach tests outlined in Table 3.7.

Parameter	Fixed setpoint	Motivation
Pulp density	40 g PCBs/L	It was estimated that 40 g of the solid residue contained approximately 10 mg Au. Literature for Au dissolution suggested that concentrations of 10 mg/L Au could be attained (Table 2.11). 20 g PCBs was added to an initial volume of 500 mL. The final volume would be approximately 690 mL (not including volume removed during sampling and added during pH control), based on the H ₂ O ₂ flowrate.
Agitation speed	550 rpm	Minimum speed required to keep particles in suspension.
Oxidant	H ₂ O ₂ fed continuously at 4 mL/hr	Due to H ₂ O ₂ degradation, particularly at increased temperatures, H ₂ O ₂ was fed continuously.

Table 3.9. Experimental conditions for precious metal leach tests according to the experimental design given in Table 3.7.

Test	Temperature (°C)	Initial pH	Glycine concentration (M)
5a	60	11.5	0.1
5b	75	11.5	0.1
5c	60	12.5	0.1
5d	75	12.5	0.1
5e	60	11.5	0.5
5f	75	11.5	0.5
5g	60	12.5	0.5
5h	75	12.5	0.5

The results from these tests, discussed in Section 4.3.1, showed low gold dissolution after 48 hours at all conditions investigated. It was therefore decided to perform an additional test for an increased duration of 96 hours, at the most aggressive conditions from the experimental design, which correspond to the highest temperature, pH and glycine concentration. This aimed to determine if gold dissolution would increase over time. An additional test would also be performed at a higher temperature, of 90°C, and increased peroxide flowrate.

A further test was performed to determine whether gold could be leached from PCBs by adding cyanide to the glycine solution. This aimed to determine whether the low dissolution of gold observed in the previous tests was due to gold being physically entrapped in the PCBs.

Parameters for additional tests are given in Table 3.10. Each test was performed for a duration of 96 hours, using the same feed material as used in the experimental design tests. Due to peroxide fed continuously over an extended period (compared to the 48 h tests), the final volume of test 6a and 6b were expected to be larger than the final volume of the 48 h tests. For test 6a and 6b, 40 g of PCBs was added to an initial volume of 500 mL. The expected final volume (not including volume removed during sampling and volume added during pH control), would be 884 mL for test 6a and 1268 mL for test 6b. For test 6c, air was used as oxidant, and therefore the only volume addition would be due to pH control. Consequently, 20 g of PCBs was added to an initial volume of 500 mL.

Table 3.10. Parameters for additional precious metal leach tests.

Test	Lixiviant	Temperature	pH	Oxidant
6a	0.5 M glycine	75°C	12.5 (controlled above 12)	H ₂ O ₂ (4 mL/hr)
6b	0.5 M glycine	90°C	12.5 (controlled above 12)	H ₂ O ₂ (8 mL/hr)
6c	0.13 M glycine + 2 0.04 M NaCN	25°C	11.5 (controlled above 11)	Air

2 additional tests were performed using pure gold foil as feed. Parameters for these tests are given in Table 3.11. 75 mg of gold foil was added to a leach solution with an initial volume of 500 mL.

Table 3.11. Parameters for precious metal leach tests performed using gold foil.

Test	Glycine conc.	Temp	pH	Oxidant
7a	0.5 M	60°C	12.5 (controlled above 12)	4 mL/hr H ₂ O ₂ (fed continuously)
7b	0.5 M	60°C	12.5 (not controlled)	2 wt% H ₂ O ₂ (fed only at the beginning)

3.2 Materials

3.2.1 Feed preparation

Motherboards from discarded computers were used as feed in this study. The waste PCBs were partially disassembled by manually removing large, valueless components, such as stainless steel heat sinks, which could not easily be crushed. Some components, expected to have a high precious metal content, such as connectors for peripheral devices (e.g. USB ports and parallel port connectors) also had to be excluded from the feed material, as these could not be crushed using the equipment available.

The partially dismantled PCBs were cut into pieces of approximately 20 mm x 20 mm using a band saw, followed by shredding in a Retsch Cutting Mill. To reduce the PCB pieces to particles smaller than 2 mm, progressively smaller sieve sizes were used on the mill - with the largest sieve size of 20 mm, and the smallest being 2 mm. After each pass through the mill, the material was classified in a sieve shaker using 2 mm sieves. Oversized material was returned

to the mill, while particles smaller than 2 mm were removed, to prevent the generation of ultrafine particles. Ultrafine particles consist of predominantly non-metallic material (Das *et al.*, 2009) and can hinder filtration. Oversized material was recycled to the mill until the entire charge passed 2mm. A rotary sample splitter was used to divide the crushed PCBs into representative samples of the required mass for each leach test.

Two precious metal leach tests were performed using 99.99% gold foil, with thickness of 0.05 mm. Each test was performed using a 6 mm x 13 mm piece of foil, with a mass of approximately 75 mg.

3.2.2 PCB characterisation

The metal content of PCBs was determined by digesting representative samples of feed in aqua regia, followed by analysis of metals in solution, discussed in Section 3.4.2. Additionally, the solid residue remaining after each bench-scale base metal leach test, excluding the preliminary tests, and precious metal leach test was also subjected to aqua regia digestion. From a mass balance, the feed composition of each test could be determined, and the variation in feed composition could be quantified.

Three different methods of acid digestion, illustrated in Figure 3.1, were tested on representative samples of feed. For each method a total of 3 samples, each with a mass of 20 g, were digested. These tests also aimed to compare the extent of silver dissolution achieved using nitric acid digestion prior to aqua regia digestion, against the silver dissolution achieved using aqua regia digestion alone. As discussed in Section 2.3.3, complete silver dissolution in aqua regia can be hindered by the formation of insoluble AgCl. It is therefore proposed that nitric acid digestion can be used to dissolve silver, and the majority of the base metals, prior to dissolution of gold using aqua regia.

As shown in Figure 3.1, two different concentrations of nitric acid were tested, 55 wt% (11.7 M) and 30 wt% (5.6 M). As discussed in Section 2.3.3 highly concentrated nitric acid has been reported to retard silver dissolution (Ozmetin *et al.*, 1998). All acid digestion tests were performed in a 500 mL Erlenmeyer flask on a hot plate with magnetic stirrer. The stirring speed was set such that all solids remained in suspension.

Solid characterisation of the feed material is discussed in Section 3.5.

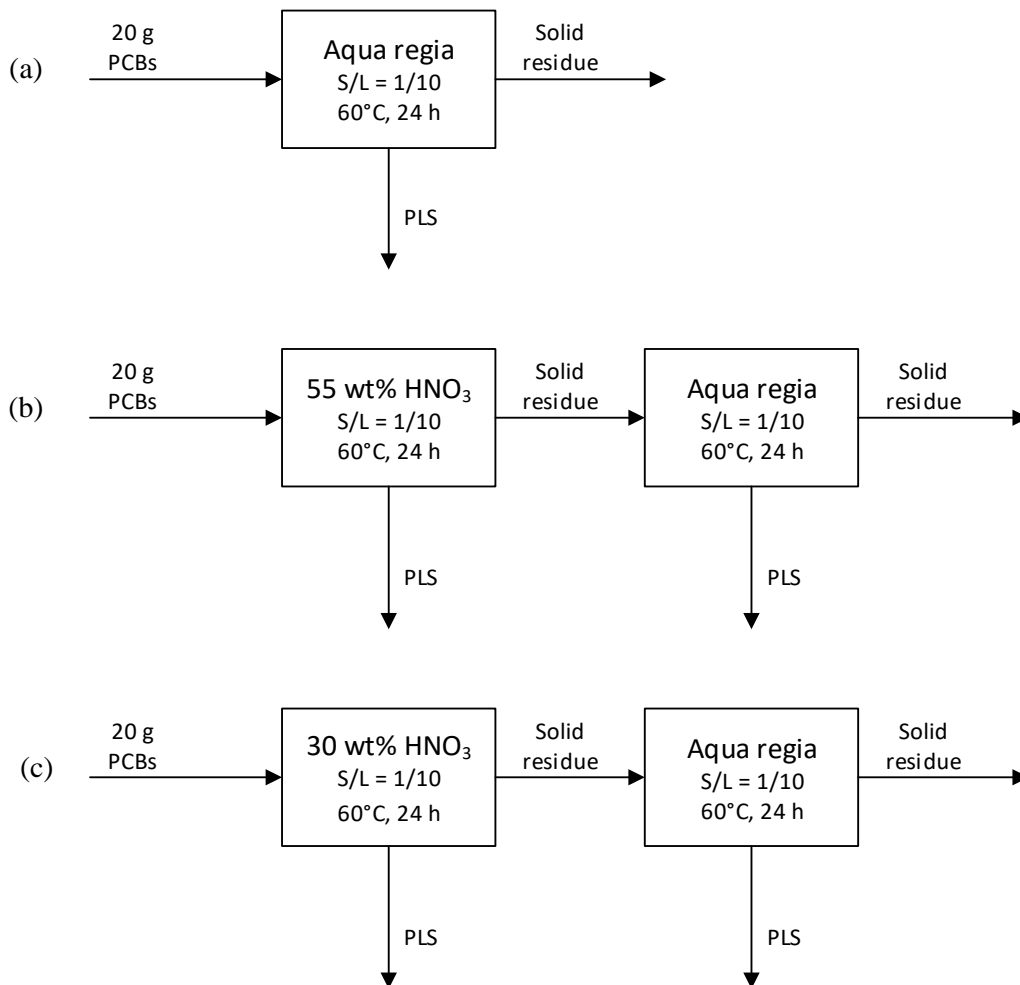


Figure 3.1. Schematic representation of the three different material characterisation methods investigated: (a) Aqua regia only, (b) 55 wt% (11.7 M) HNO₃ followed by aqua regia, (c) 30 wt% (5.6 M) HNO₃ followed by aqua regia.

3.2.3 Leaching reagents

The purity of the reagents used are given in Table 3.12. Solutions for base and precious metals were prepared by dissolving glycine in demineralised water, using sodium hydroxide to adjust the initial pH of the solution.

For pH control in the precious metal leach tests, undiluted sodium hydroxide, 50 wt%, was used in the pH controller. For base and precious metal leach tests in which hydrogen peroxide was fed continuously, undiluted hydrogen peroxide, 30 wt%, was used. Nitric acid and hydrochloric acid were used for material characterisation of the feed.

Table 3.12. Reagents used for leaching and material characterisation.

Form of reagent	Substance	Wt%
Solid (powder)	Glycine	99
	Sodium cyanide	97
Aqueous solution	Sodium hydroxide	50
	Hydrogen peroxide	30
	Nitric acid	55
	Hydrochloric acid	32

3.3 Equipment

3.3.1 Bench-scale leach tests

Leaching tests were performed using a 1.7 L jacketed glass reaction vessel, which is illustrated in Figure 3.2. The reaction vessel had a working volume of approximately 1.2 L, and an inner diameter of 105 mm. The overhead stirrer was fitted with a 4-bladed Teflon impeller, which was placed approximately 20 mm above the bottom of the vessel. The vessel was fitted with 4 Teflon baffles which promoted mixing and suppressed vortex formation.

A MS-H-Pro Plus hotplate and PT 1000 temperature sensor provided feedback control, and kept the temperature of the leaching solution within 1°C of the setpoint temperature. The temperature was measured with an accuracy of $\pm 0.1^\circ\text{C}$. When necessary, cooling was achieved by circulating water at $\pm 16^\circ\text{C}$ through the jacket of the vessel. A condenser was fitted to the lid of the vessel to prevent vapour losses. The sample port on the lid was also used for loading the solids into the vessel and sealed, along with other ports not in use, with a stopper.

For tests performed using gaseous oxidants, air or pure oxygen were sparged into solution with the outlet of the tube positioned below the impeller. The gas flowrate was measured using a rotameter. Hydrogen peroxide was fed continuously using a peristaltic pump.

For the precious metal leach tests, the pH was controlled by on-off control using a Eutech alpha 560 pH controller. A pH probe, connected to the controller, was inserted into an additional port on the lid, not shown in Figure 3.2. The feed line for sodium hydroxide, used to control the pH, was also inserted into this port. Additionally, the pH controller was used to measure the pH during the base metal leach tests.

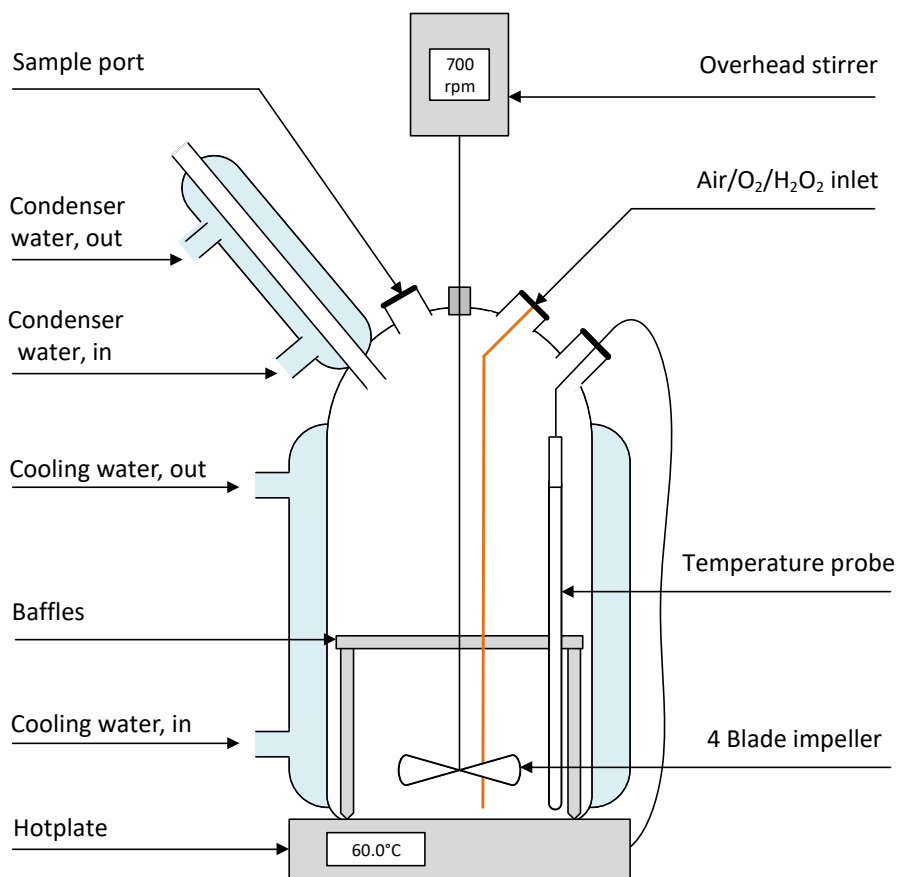


Figure 3.2. Diagram of experimental setup for bench-scale leach tests.

3.3.2 Small pilot-scale leach tests

Small pilot-scale leach tests were performed using a 20 L ball flask immersed in a water bath. The ball flask had an inner diameter of 34 cm, and working volume of 17 L. The water bath had a heating element which kept the temperature of the bath within 1°C of the required setpoint. Agitation was provided by an overhead stirrer with a 2-bladed Teflon impeller, with a length of 17 cm.

A lid, similar to the one used for the bench-scale leach tests, was fitted to the ball flask. The lid contained a condenser and a number of ports, which were sealed when not in use. Pure oxygen was sparged into solution through two separate tubes, each with a flowrate of 300 mL/min. The outlet of each sparging tube was positioned below the impeller. The pH was measured using a Eutech alpha 560 pH controller.

3.4 Experimental procedure

3.4.1 Bench-scale leach tests

A glycine solution of the required concentration and volume was prepared and the pH was adjusted using NaOH. The leach solution was added to the vessel and the lid with condenser was fastened to the vessel. The leach solution was heated to the desired temperature and the overhead stirrer set to a low stirring speed to facilitate heat transfer. Once the desired temperature was achieved, the pH probe was immersed in solution. When necessary, the pH of the solution was adjusted, and the extra volume taken into account in calculations. The required amount of crushed PCBs were added to the leach solution through one of the sample ports, and the overhead stirrer was set to the desired agitation speed. This time instance signified the start of the test, $t = 0$ minutes.

For tests in which gaseous oxidants were used, the air/oxygen valve was opened and adjusted to the required flowrate (300 mL/min) approximately 10 minutes before the start of each test. For the case of hydrogen peroxide as oxidant, the pump was started at $t = 0$.

4 mL samples were taken at predetermined time intervals. Samples were filtered immediately using 0.22 micron syringe filters to prevent further leaching from occurring. The pH of the leach solution was recorded when each sample was taken. Where applicable, the volumes of peroxide and NaOH added during the tests was recorded.

At the end of each test, the solution was allowed to cool to room temperature prior to filtration. The contents of the leach reactor was filtered using a vacuum pump and Buchner funnel with qualitative filter paper, with a pore size of 8 μm . The solid residue was air dried, weighed and digested in aqua regia at a solid to liquid ratio of 1:10, at 60°C for 24 hours.

3.4.2 Small pilot-scale leach tests

The ball flask, with lid and condenser, was immersed in the water bath, and secured with a clamp. The water bath was then set to the desired temperature.

Leach solutions of the required concentration and volume were prepared in 5 L batches. The pH was adjusted using NaOH. The 5 L batches were preheated to the desired temperature using a hotplate. Once the hot water bath had reached the required temperature, the pre-heated

solution was added to the ball flask through a port in the vessel lid. A pH probe was immersed in solution and the pH adjusted when necessary. The oxygen valve was opened and set to the required flowrate (300 mL/min) 10 minutes before the start of the test. The required amount of crushed PCB feed was added to the leach solution through a sample port, and the overhead stirrer set to the desired agitation. This time instance signified the start of the test, $t = 0$ minutes. 10 mL samples, taken at predetermined time intervals, were filtered immediately using 0.22 micron syringe filters.

At the end of the test, the hot water in the bath was replaced with cooling water and the PLS solution was allowed to cool prior to filtration. The contents of the leach reactor was filtered using a vacuum pump and Buchner funnel with qualitative filter paper, with a pore size of 8 μm . The solid residue was air dried and split into representative samples of the required mass for precious metal leach tests.

3.5 Analytical techniques and data interpretation

Inductively coupled plasma atomic emission spectrometry (ICP-AES) was used to determine the concentration of base metals (Al, Cu, Fe, Ni, Pb, Sn and Zn) in solution. ICP-AES was performed at the Department of Process Engineering at Stellenbosch University.

Ag and Au concentrations in solution were below the detection limits for ICP-AES. As a result of this, the concentration of these metals in solution were determined using inductively coupled plasma mass spectrometry (ICP-MS). For ICP-AES, the detection limits for Au and Ag, assuming no spectral interferences, are 50 $\mu\text{g/L}$ and 5 $\mu\text{g/L}$, respectively. For ICP-MS, detection limits for Au and Ag are significantly lower, at 0.1 $\mu\text{g/L}$ (EAG Laboratories, 2017). ICP-MS was performed by Stellenbosch University Central Analytical Facility. Samples were diluted prior to ICP-AES and ICP-MS, such that all elements in solution had a concentration of less than 500 mg/L.

The mass of metal in solution at a given time could be determined as a percentage of the total mass of that metal contained in the feed:

$$\% \text{ Metal dissolution} = \frac{\text{mass of metal in solution}}{\text{mass of metal in feed}} \times 100\% \quad [3.1]$$

Appendix D provides sample calculations for determining the mass of metal in solution, and in the feed.

Scanning electron microscopy (SEM) was used for characterisation of the solid feed material. Sample preparation consisted of mounting the samples in epoxy resin, polishing, and coating the surface with a conductive carbon layer. SEM was conducted by Stellenbosch University Central Analytical Facility, using a Zeiss MERLIN Field Emission Scanning Electron Microscope, with semi-quantitative Energy Dispersive X-Ray Spectrometry (EDS). Beam conditions were 20 kV accelerating voltage, beam current of 11 nA, and a working distance of 9.5 mm. A counting time of 10 seconds live-time was used.

4. Results and discussion

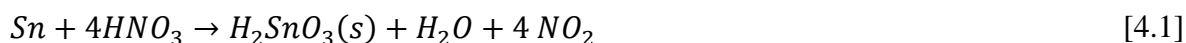
4.1 PCB Characterisation

As discussed in Section 3.2.2, three different acid digestion methods were investigated to quantify the metal composition in the feed. Experimental conditions for these tests were provided in Figure 3.1. Recall that these tests also aimed to compare the extent of silver dissolution achieved in each of the methods. As discussed in Section 2.3.3, Petter *et al.* (2014) suggested that nitric acid is more suitable for complete silver dissolution, as silver leaching in aqua regia can be inhibited by the formation of insoluble AgCl.

The average metal content, with standard deviation, for the different digestion methods are provided in Table 4.1. For each method, three 20 g samples were digested. Results for each individual sample are given in Appendix B.

In Table 4.1 it can be seen that nitric acid digestion prior to aqua regia digestion (method B and C), did not increase the mass of silver extracted compared to using aqua regia only (method A). It was expected that the majority of the silver would be leached out in the nitric acid step for method B and C. It was observed in most cases, however, that silver did not dissolve during nitric acid digestion, but did dissolve in aqua regia, refer to Figure B.1, Appendix B.

It is possible that an insoluble precipitate of tin, formed by reaction with nitric acid, could inhibit silver dissolution during nitric acid leaching. Mecucci and Scott (2002) and Yang *et al.* (2011) reported that the reaction of tin and nitric acid led to the formation of insoluble metastannic acid, given in Equation 4.1. At nitric acid concentrations of 4 M and higher a SnO₂ layer is formed, passivating the surface. This passivating layer inhibits tin dissolution and can cause the formation of metastannic acid (Mecucci and Scott, 2002).



It was observed that the mass of tin extracted in the nitric acid step, for both method B and C was significantly lower than the mass extracted in the aqua regia step, refer to Figure B.8, Appendix B. This suggests that tin was passivated during nitric acid digestion.

Table 4.1. Average composition of three 20 g PCB samples with standard deviation, for each of the three different acid digestion methods, at 60°C with S/L = 1/10: (A) Aqua regia only, (B) 55 wt% (11.7 M) HNO₃ followed by aqua regia, (C) 30 wt% (5.6 M) HNO₃ followed by aqua regia.

Digestion Method	PCB composition (wt%)								
	Ag	Al	Au	Cu	Fe	Ni	Pb	Sn	Zn
A	0.010 ±	3.57 ±	0.021 ±	23.27 ±	2.44 ±	0.47 ±	1.42 ±	4.48 ±	2.43 ±
	0.012	0.21	0.001	0.81	0.34	0.03	0.11	0.09	0.05
B	0.005 ±	3.75 ±	0.018 ±	21.66 ±	2.93 ±	0.44 ±	0.96 ±	3.28 ±	2.37 ±
	0.001	0.16	0.001	0.55	0.15	0.05	0.06	0.68	0.11
C	0.009 ±	4.08 ±	0.014 ±	23.86 ±	3.76 ±	0.85 ±	1.46 ±	2.75 ±	2.58 ±
	0.006	0.68	0.001	1.66	1.85	0.67	0.1	0.68	0.44

SEM images for characterisation of the feed are given in Figure B.10 and Figure B.11, in Appendix B. The images show that some of the copper in the feed was only partially liberated from the non-metallic material of the circuit boards (predominantly shown as Al, O and Si). It also appears that some of the copper was alloyed with other metals. The composition of these alloys were, however, not determined. The presence of gold in the PCBs was not clear from the images.

4.2 Base metal leaching

Base metal leach tests were conducted according to the experimental conditions discussed in Section 3.1.1. Recall that the base metal leach tests aimed to determine the conditions at which the greatest extent of copper dissolution could be achieved, with minimal gold dissolution. At these conditions small pilot-scale leach tests were performed to prepare the feed required for the precious metal leach tests. The concentration of base and precious metals leached as a function of time, are tabulated in Appendix C.

4.2.1 Preliminary tests

Preliminary tests were performed at the conditions given in Table 3.1 and Table 3.2. The mass of copper in the feed for each of the preliminary tests was not quantified. However, based on the aqua regia digestion results, given in Table 4.1, it was expected that each 100 g feed sample contained approximately 23 g of copper.

Figure 4.1 shows the mass of copper extracted as a function of time for the preliminary tests. For the first 3 hours, no copper dissolution was observed under any of the conditions investigated. This initial lag was possibly due to the formation of the copper oxide intermediate, as discussed in Section 2.4.3, and will be discussed further in Section 4.2.2.3. At a glycine concentration of 1.5 M, increasing the temperature from 25°C to 60°C had a significant effect on leaching as the reaction progressed. At 60°C, 8.72 g copper had dissolved after 24 hours; at 25°C, however, it took 80 hours for approximately the same mass of copper, 8.69 g, to dissolve. Increasing the glycine concentration from 1.5 to 4.5 M, at 60°C, decreased the mass of copper extracted after 8 hours from 5.63 g to 1.55 g. By extending the leaching time, however, copper extraction increased with increasing concentration, with 8.72 g and 11.51 g of copper extracted after 24 hours at 1.5 M and 4.5 M glycine, respectively. The initial decrease in leaching with increasing glycine concentration could have been due to the reduced solubility of dissolved oxygen at increased solute concentrations (Narita *et al.*, 1983).

In Figure 4.1 it can be seen that at 60°C and 4.5 M, a maximum of 11.5 g of copper was extracted after 24 hours, after which the mass of copper in solution decreased as copper precipitated out of solution. 11.5 g of copper in solution is equivalent to approximately 50% copper dissolution (based on 23% copper in the feed), with a concentration of approximately 11.5 g/L Cu. It appears that a solubility limit is reached at this concentration.

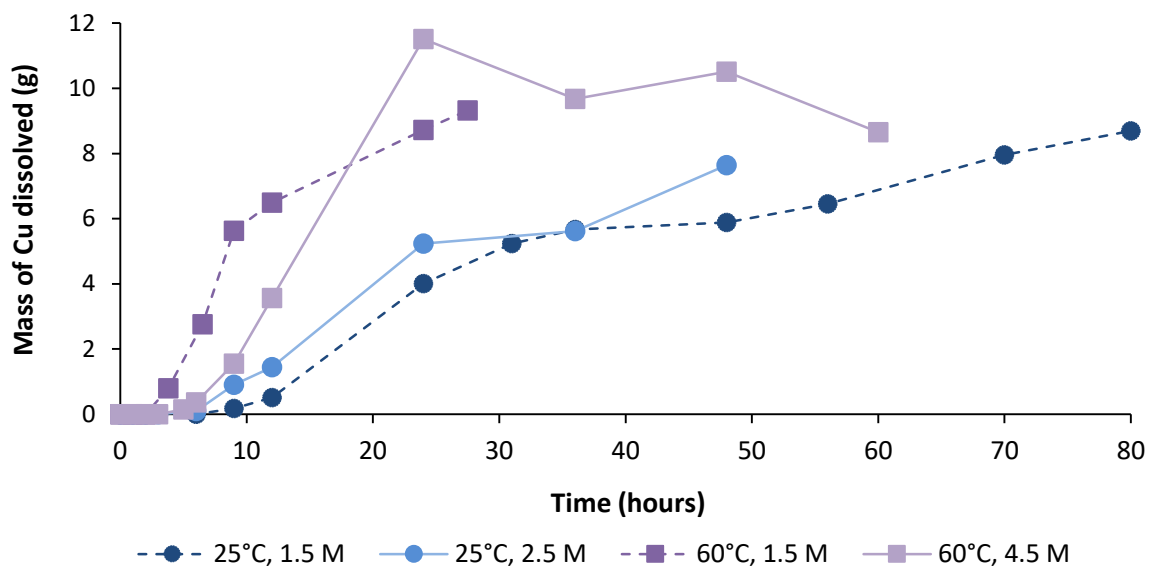


Figure 4.1. Mass of copper extracted as a function of leaching time, temperature and glycine concentration for tests performed using air as oxidant, initial pH of 11, with a pulp density of 100 g PCBs/L (approximately 23 g Cu in the feed).

No data is available on the solubility of copper in glycine solutions; however, from the optimal conditions for base metal leaching using glycine reported in literature (refer to Table 2.10) the maximum concentration of copper in solution was reported to be 4.8 g/L. While Oraby and Eksteen (2014) conducted glycine leach experiments at pulp densities ranging from 100 g/L to 200 g/L, the copper content of the concentrate was only 3.8%, which is significantly lower than the copper content of PCBs used in this work, approximately 23%. Complete copper dissolution of the concentrate used by Oraby and Eksteen (2014) would yield copper concentrations between 3.75 g/L – 7.5 g/L. Based on these findings, it was decided that further base metal leach tests would be performed at a reduced pulp density of 25 g PCBs/L. Complete copper extraction, assuming 23% copper in the feed, would correspond to a concentration of 5.8 g/L Cu. Additionally, decreasing the pulp density could increase oxygen transfer, as discussed in Section 2.6.6.

Glycine concentrations for further tests were adjusted based on the reduced pulp density of 25 g/L. The stoichiometric glycine concentration required to leach base metals was calculated to be 0.32 M, assuming the metal content reported in Table 4.1 for aqua regia digestion. This is discussed further in Table A.1, Appendix A. It was decided that glycine concentrations of 1 M and 2 M would be investigated in further tests. As discussed in Section 2.6.3, Oraby and Eksteen (2016) reported a 20% increase in copper dissolution from PCBs by increasing the

glycine concentration from 2 to 4 times the stoichiometric concentration required to leach all base metals. It was also decided that an intermediate temperature of 40°C would be investigated in subsequent tests, in addition to 25°C and 60°C.

Further tests would investigate pure oxygen as oxidant, in addition to air. As discussed in Section 2.5, using pure oxygen instead of air increases the partial pressure of oxygen in the gaseous phase, which increases the availability of oxygen in solution. This would presumably increase the rate of copper oxide formation. Oraby and Eksteen (2016) reported that air was sufficient to leach copper from PCBs during glycine leaching. However, the particle size used by the authors, 80% passing 106 µm, is significantly smaller than the particle size used in this work, which was smaller than 2 mm. A smaller particle size is expected to increase liberation of the copper, and to increase the surface area exposed to the leaching agent. As shown in Equation 2.23, increasing the surface area increases the rate of oxygen diffusion through the solid-liquid boundary layer in a diffusion-limited system. Additionally, Oraby and Eksteen (2016) used a significantly lower pulp density (4 g PCBs/L) compared to the pulp density in the preliminary tests (100 g PCBs/L). Increased oxygen mass transfer can be achieved with decreasing pulp density.

Due to the slow kinetics of the system, it was decided to run subsequent tests for a duration of 70 – 80 hours.

4.2.2 Experimental design

As discussed in Section 4.2.1, recommendations for further base metal leach tests were made based on the results of the preliminary tests. Subsequent tests were conducted according to the experimental design given in Table 3.3. All tests were conducted at a reduced pulp density of 25 g PCBs/L and initial pH of 11. Air/pure oxygen was sparged continuously at 300 mL/min.

4.2.2.1 Effect of temperature

Figure 4.2 and Figure 4.3 compare the dissolution of copper over time as a function of temperature at glycine concentrations of 1 M and 2 M, respectively, using air as oxidant. Figure 4.2 shows that at 1 M glycine, copper dissolution was slow initially and independent of temperature, with only 2.3% and 2% copper dissolution achieved after 3 hours, at 25°C and 60°C, respectively. As time progressed, the rate of dissolution at 60°C was significantly faster than at 25°C. After 80 hours 64% dissolution was achieved at 60°C, with only 33% dissolution

at 25°C. In the first 8 hours of leaching there was little difference between copper dissolution at 40°C and 60°C. After 71 hours the copper dissolution at 60°C was approximately 10% higher than at 40°C.

Similar to the tests performed at 1 M glycine, Figure 4.3 shows that at 2 M glycine, copper dissolution was also temperature-independent in the first 3 hours. Thereafter, the rate of leaching at 60°C was significantly higher than at 40°C. At 60°C, 71% dissolution was achieved after 22 hours. At 40°C, 71% copper dissolution was only achieved after 80 hours. There was, however, only a slight increase in dissolution when the temperature was increased from 25°C to 40°C.

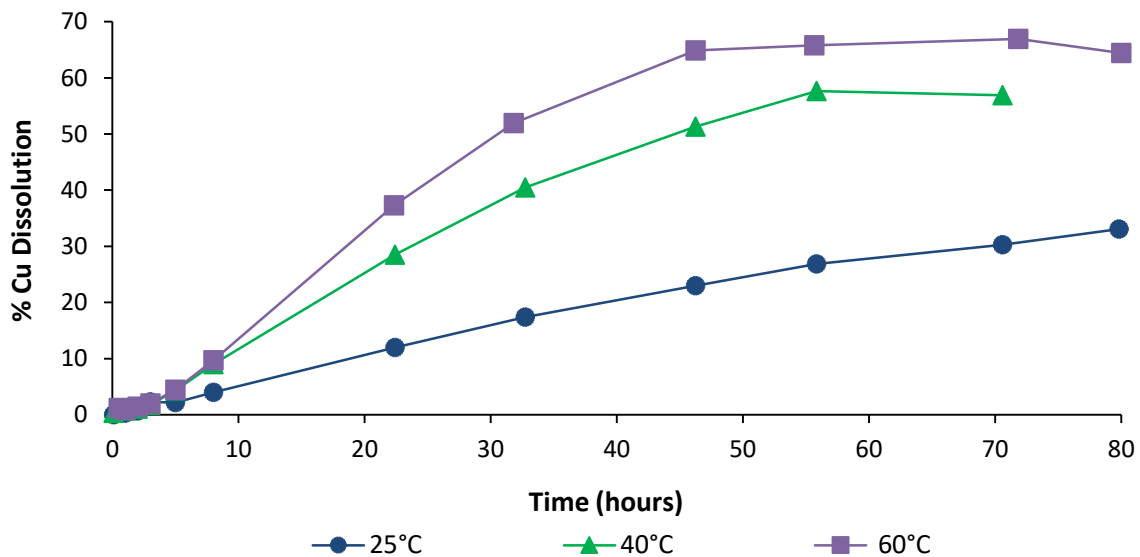


Figure 4.2. Percentage copper dissolution as a function of leaching time and temperature, using 1 M glycine, with air as oxidant.

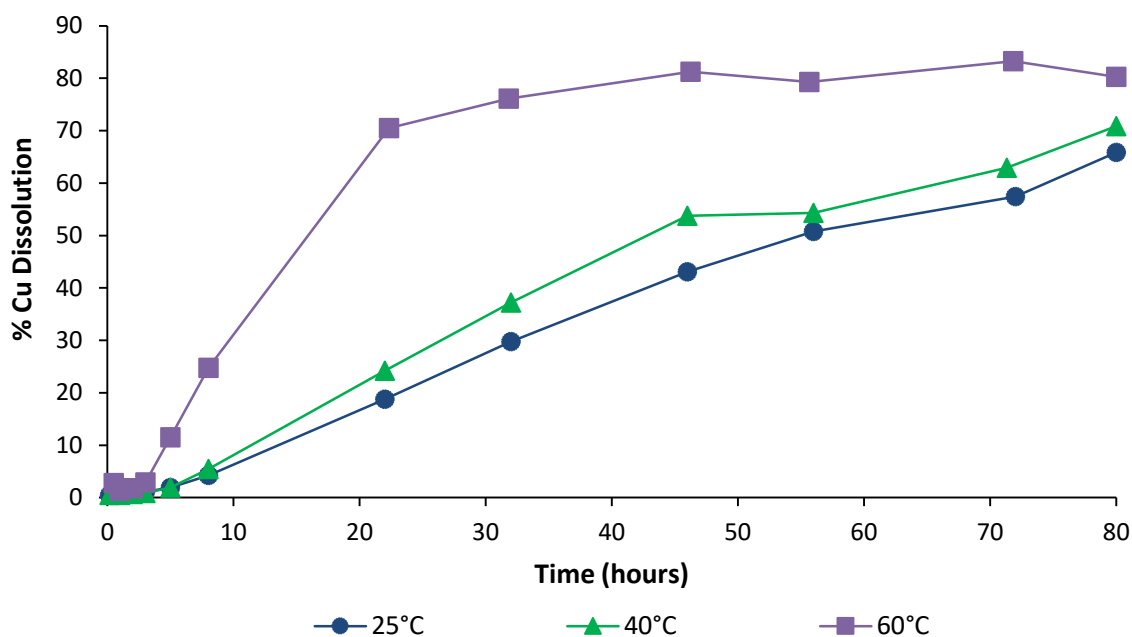


Figure 4.3. Percentage copper dissolution as a function of leaching time and temperature, using 2 M glycine, with air as oxidant.

Figure 4.4 and Figure 4.5 show the dissolution of copper over time using pure oxygen as oxidant, for glycine concentrations of 1 M and 2 M, respectively. Figure 4.4 shows that when pure oxygen was used as oxidant, with 1 M glycine, copper dissolution was strongly dependent on temperature at 3 hours.

For tests performed using air as oxidant (Figure 4.2 and Figure 4.3) there was an initial temperature-independent lag in copper dissolution for the first 3 hours of leaching. This lag in dissolution was not observed for tests at 1 M in which pure oxygen was used as oxidant (Figure 4.4). It is suggested that when air was used as oxidant, copper dissolution was controlled by oxygen diffusion through the solid-liquid boundary layer during the first 3 hours, as discussed further in Section 4.2.2.3.

In Figure 4.2 and Figure 4.3, using air as oxidant, it was seen that as the reaction progressed, copper dissolution became temperature-dependent. However, in Section 4.2.2.3 it is shown that at 1 M glycine, when pure oxygen was used instead of air, the rate of reaction also increased, even after the initial 3 hours. This suggests that oxygen diffusion is rate-limiting when using air as oxidant. As discussed in Section 2.5, diffusion controlled processes are largely

temperature-independent whereas processes controlled by chemical reaction are strongly dependent on temperature. A possible explanation for these observations are given below.

In Section 2.4.3, it was reported that the dissolution of copper in alkaline glycine solutions involves the formation of a copper-oxide intermediate, with subsequent complexation of the copper-oxide film by glycine. It is proposed that after 3 hours, when air is used as oxidant, oxygen diffusion through the copper-oxide intermediate becomes rate limiting. Increasing the temperature increases the rate of CuO dissolution via the complexation reaction (refer to Equation 2.14). This decreases the resistance to oxygen diffusion through the product layer to the reaction surface, and therefore enhances oxygen diffusion.

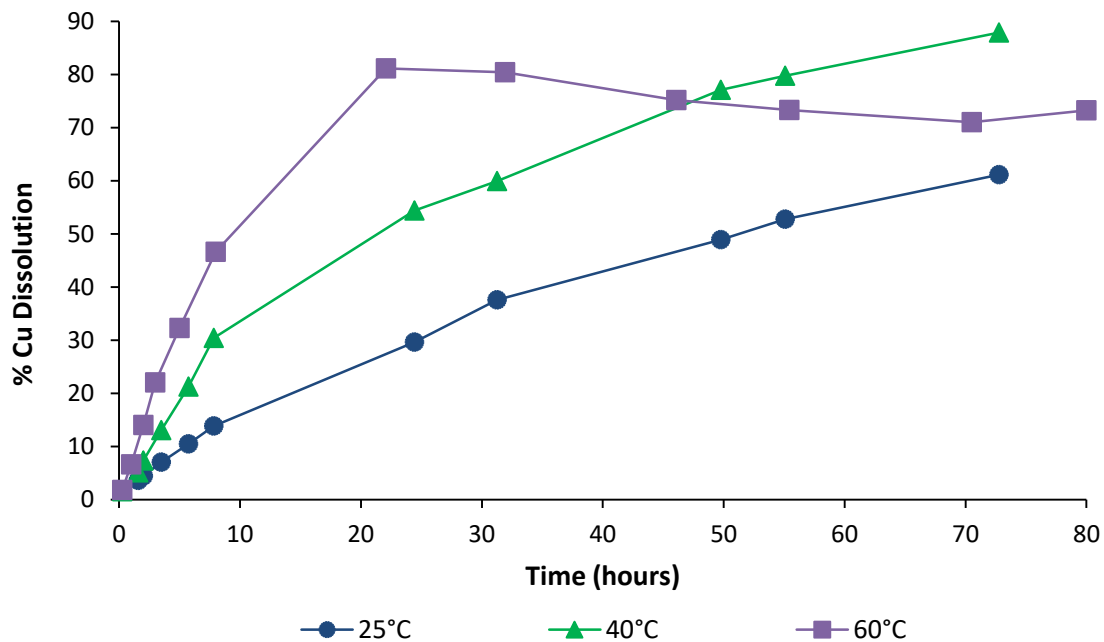


Figure 4.4. Percentage copper dissolution as a function of leaching time and temperature, using 1 M glycine, with pure oxygen as oxidant.

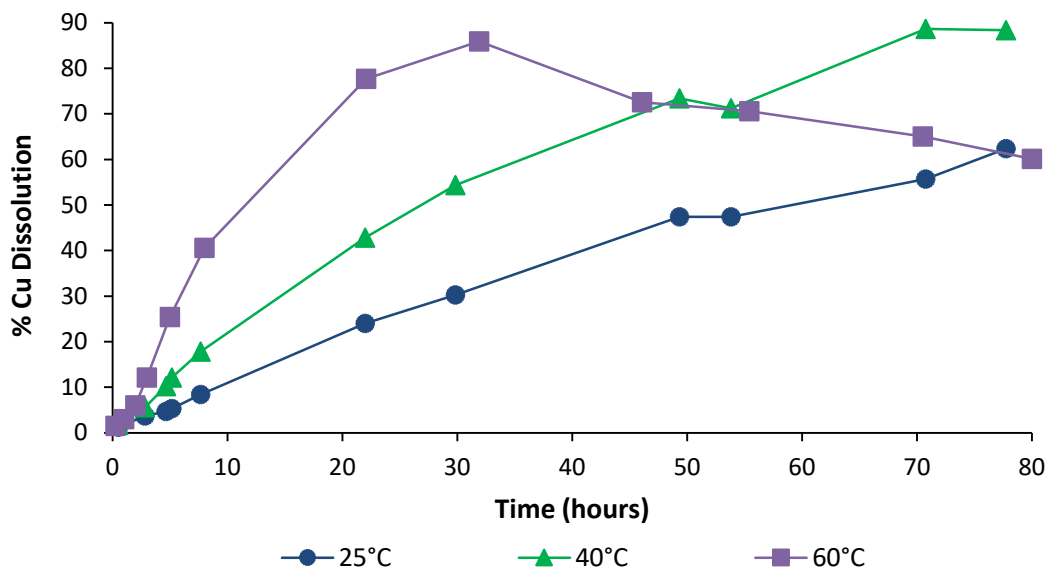
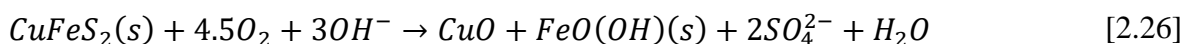


Figure 4.5. Percentage copper dissolution as a function of leaching time and temperature, using 2 M glycine, with pure oxygen as oxidant.

The change in pH over time for tests performed using air and oxygen as oxidant, is given in Figure 4.6 and Figure 4.7, respectively. For the tests performed at 60°C, using pure oxygen as oxidant, the pH dropped significantly relative to the change in pH observed in the remainder of the tests. Figure 4.7a shows that for the 60°C test at 1 M using pure oxygen as oxidant, the pH dropped from 10.48 to 8.95 between 22 and 32 hours. Figure 4.7b shows that when the glycine concentration was increased to 2 M (at 60°C, using pure oxygen as oxidant), the pH dropped from 9.9 to 8.08 between 32 and 55 hours. At these time intervals copper precipitation was observed for these tests (refer to Figure 4.4 and Figure 4.5). The remainder of the tests showed no copper precipitation.

As discussed in Section 2.6.4, Tanda *et al.* (2017) reported a significant decrease in pH after 24 hours (from 11.5 – 9.71) at 60°C relative to the decrease in pH at 23°C. Glycine leach tests were conducted on chalcopyrite in the presence of 25 mg/L DO. The decrease in pH was attributed to the consumption of hydroxyl anions in the oxidation of chalcopyrite according to Equation 2.26.



In this work, however, copper was present in metallic form, and oxidation was presumed to take place according to Equation 2.12. Consequently, copper oxidation is not expected to influence the pH.



Eksteen *et al.* (2017a) reported that iron present in chalcopyrite is oxidised to FeO(OH)(s) (refer to Equation, 2.26). The rapid decrease in pH observed at 60°C when pure oxygen was used as oxidant, as seen in Figure 4.7, could possibly be due to the oxidation of metallic iron in the PCBs to form FeO(OH)(s). It is, however, not clear why a drop in pH is not observed at 25°C and 40°C in the presence of pure oxygen.

As discussed in Section 2.6.4, Tanda *et al.* (2017) reported that precipitation was a function of both pH and copper concentration. At pH values between 9 and 10, above copper concentrations of 2.5 g/L, copper precipitated out of the glycine solution. Although these findings were inconsistent with the Pourbaix diagram for a copper-glycine system, it was proposed that copper precipitation could be due to the zwitterion forming a less stable complex with copper. As shown in Table 2.6, the stability constant for the complex formed with the zwitterion (CuHL^{2+}) is significantly lower than the stability constant for the complex formed with the anion (CuL_2). As discussed in Section 2.4.3, a decrease in copper dissolution at lower pH is expected, since a higher pH favours the anionic form of glycine, which forms more stable complexes.

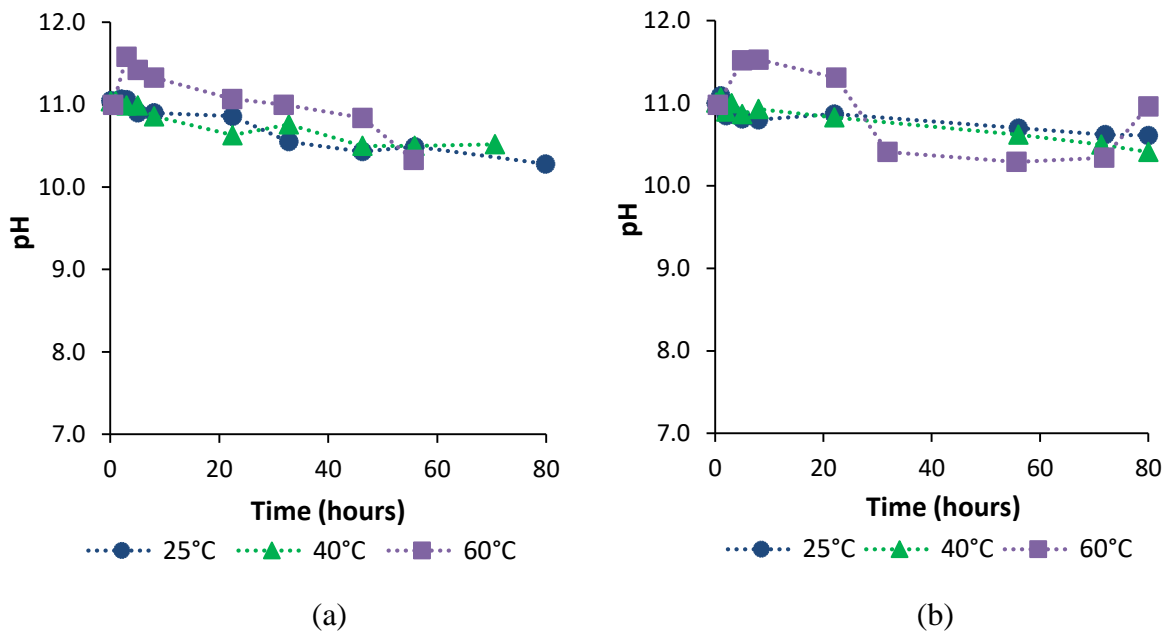


Figure 4.6. pH as a function of time and temperature with air as oxidant for glycine concentrations of (a) 1 M and (b) 2 M.

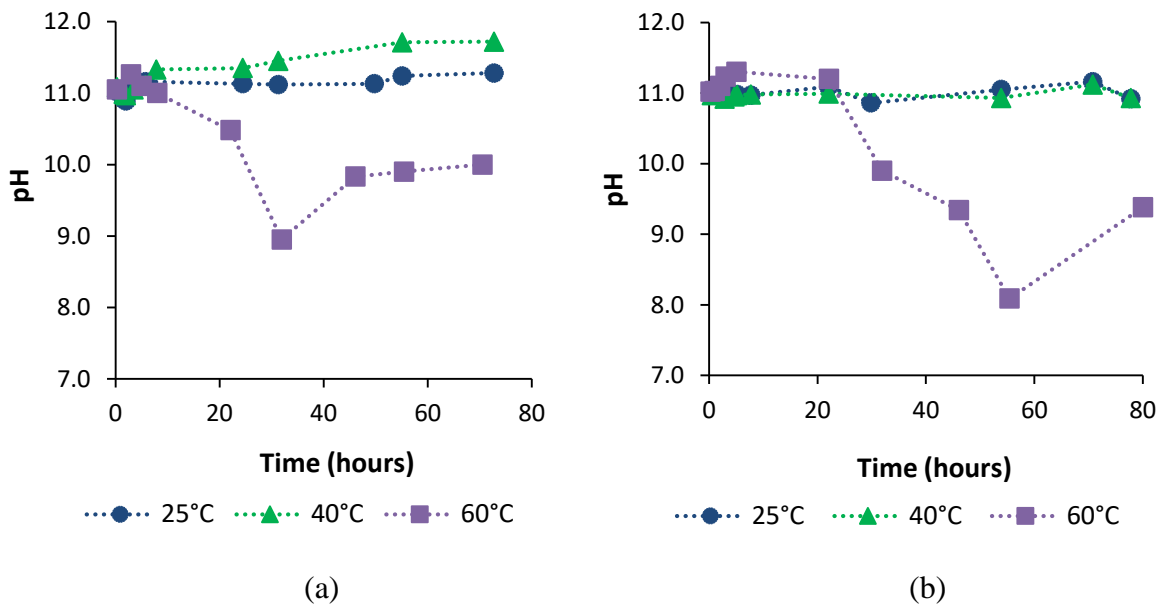


Figure 4.7. pH as a function of time and temperature with pure oxygen as oxidant for glycine concentrations of (a) 1 M and (b) 2 M.

4.2.2.2 Effect of glycine concentration

As discussed in Section 4.2.1, the stoichiometric concentration of glycine needed to dissolve all base metals, at a pulp density of 25 g/L, was approximately 0.31 M. Consequently, glycine was in excess at both the concentrations investigated (1 M and 2 M).

Figure 4.8 to Figure 4.10 compares the effect of increasing glycine concentration on copper dissolution. For tests performed using air as oxidant (Figure 4.8a, Figure 4.9a and Figure 4.10a) copper dissolution was initially independent of glycine concentration at all three temperatures investigated. As discussed in Section 2.4.3, Halpern *et al.* (1959) reported that at low oxygen partial pressures, i.e. when air was used as oxidant, the rate of copper dissolution was controlled by oxygen diffusion, and therefore independent of glycine concentration. However, at both 25°C (Figure 4.8a) and 60°C (Figure 4.10a), as time progressed, copper dissolution increased with increasing glycine concentration.

Similarly, Oraby and Eksteen (2016) reported that copper dissolution from PCB waste, was independent of glycine concentration in the first 4 hours of leaching. As leaching progressed, dissolution was reportedly strongly dependent on glycine concentration, at all concentrations investigated. As discussed in Section 2.6.3, these tests were performed at 23°C, using air as oxidant, at glycine concentrations ranging from 0.09 M to 0.4 M (the stoichiometric concentration required to leach all base metals was 0.1 M).

As in the case of increasing temperature, refer to Section 4.2.2.1, it is proposed that increasing the concentration of glycine in the air system can also enhance oxygen diffusion. Increasing the glycine concentration increases the rate of CuO dissolution through CuL_2 formation, which, in turn, decreases the resistance to oxygen diffusion through the product layer.

Contrary to the tests performed at 25°C and 60°C using air as oxidant, copper dissolution at 40°C was independent of glycine concentration for the entire duration of the leaching tests (refer to Figure 4.9a). The reason for this was not clear.

When pure oxygen was used as oxidant, increasing the glycine concentration had no significant effect on copper dissolution at all three temperatures investigated (Figure 4.8b, Figure 4.9b and Figure 4.10b). It is suggested that at increased partial pressures, i.e. when pure oxygen is used as oxidant, oxygen diffusion is no longer rate limiting. As a result of this, increasing the glycine

concentration, and hence increasing the rate of CuO removal, no longer enhances oxygen diffusion through the product layer, as in the case of air as oxidant, when oxygen diffusion is rate limiting. This suggests that the rate of dissolution in the presence of pure oxygen is limited by chemical reaction. Increasing the glycine concentration, in this case, does not increase the rate of dissolution as the complexation reaction becomes a pseudo-zero-order-reaction (i.e. independent of glycine concentration) when glycine is present in significant excess.

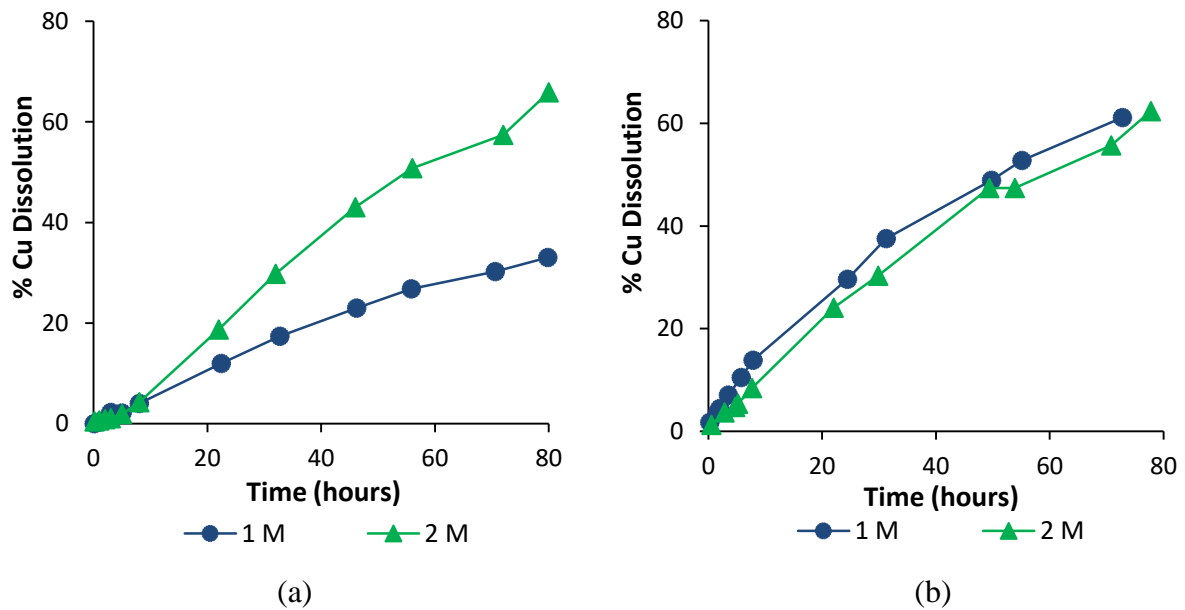


Figure 4.8. Percentage copper dissolution as a function of time and glycine concentration at 25°C for two different oxidants (a) air and (b) O₂.

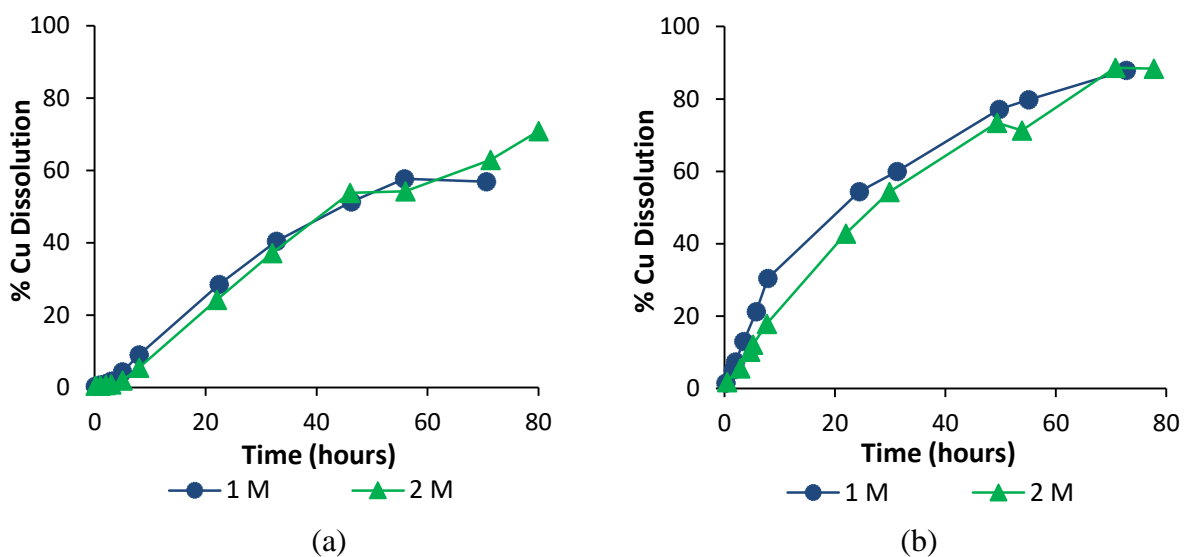


Figure 4.9. Percentage copper dissolution as a function of time and glycine concentration at 40°C for two different oxidants (a) air and (b) O_2 .

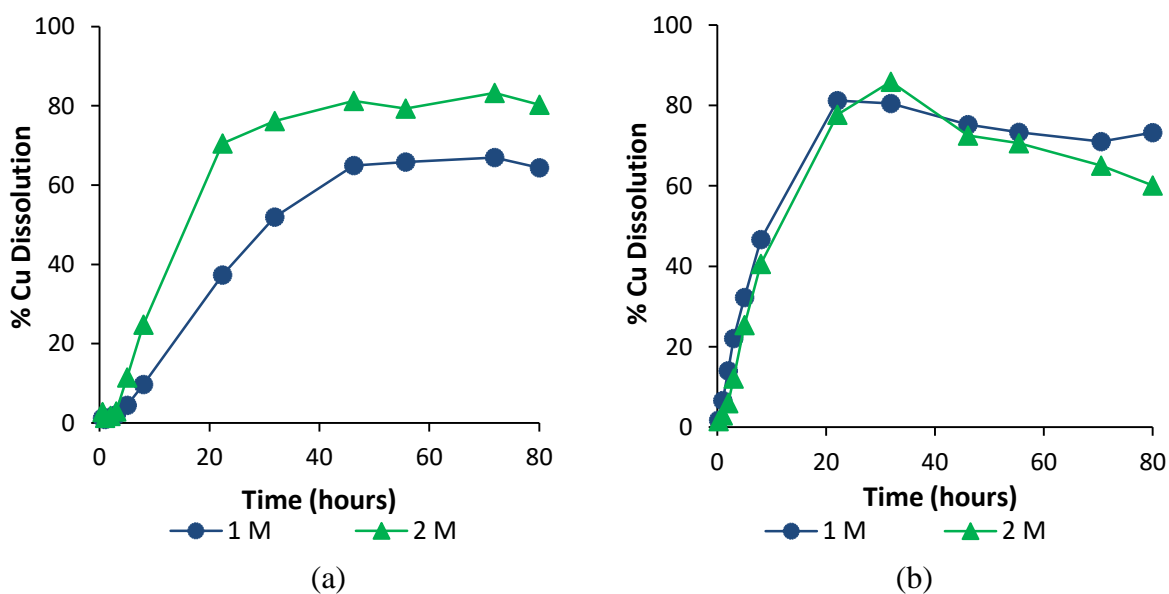


Figure 4.10. Percentage copper dissolution as a function of time and glycine concentration at 60°C for two different oxidants (a) air and (b) O_2 .

4.2.2.3 Effect of oxidant type

Figure 4.11 to Figure 4.13 compare the effect of oxidant type on copper dissolution. For tests performed with 1 M glycine, using pure oxygen as oxidant instead of air, increased the rate of copper dissolution (Figure 4.11a, Figure 4.12a and Figure 4.13a).

In Section 4.2.2.1 and 4.2.2.2, it was shown that when air was used as oxidant, copper dissolution was independent of both temperature and glycine concentration for at least the first 3 hours of leaching. During this period, there was an initial lag phase, in which copper dissolution was very low. Figure 4.11a, Figure 4.12a and Figure 4.13a, show that by using pure oxygen instead of air at 1 M glycine, this initial lag phase was decreased significantly, at all three temperatures investigated. This suggests that the initial rate of dissolution at 1 M glycine, using air as oxidant, was controlled by oxygen diffusion through the solid-liquid boundary layer, and that the initial lag in dissolution could be ascribed to the formation of the copper-oxide intermediate. At 1 M glycine, as the reaction proceeds, the rate of dissolution using pure oxygen continues to be faster than the rate achieved using air as oxidant. In Section 4.2.2.1 and 4.2.2.2 it was proposed that after the initial 3 hours, oxygen diffusion through the product layer, of CuO, becomes rate limiting.

As discussed in Section 2.5, using pure oxygen instead of air increases the partial pressure of oxygen in the gaseous phase from 0.21 atm to 1 atm. This increases the concentration of oxygen in the bulk solution c_{O_2} , refer to Figure 2.11. By increasing c_{O_2} , the rate of oxygen diffusion through both the solid-liquid boundary layer and product layer is expected to increase.

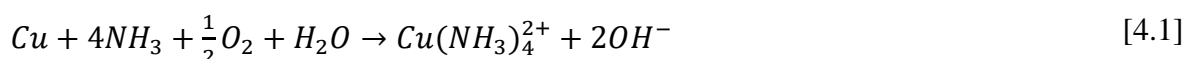
For the tests performed at a concentration of 2 M glycine there was an increase in initial copper dissolution when pure oxygen was used instead of air at 25°C and 60°C (Figure 4.11b and Figure 4.13b). However, as the reaction progressed, the difference in leaching using air versus pure oxygen (at 2 M) became less significant. As discussed in Section 4.2.2.2, increasing the glycine concentration increases the rate of CuO dissolution through CuL_2 formation. This reduces the resistance to oxygen diffusion through the product layer to the reaction surface. At lower glycine concentrations, a higher oxygen partial pressure assists in overcoming the diffusion resistance and increasing the overall reaction rate, which confirms that the air system is oxygen diffusion limited. The results suggest that at 2 M glycine (for tests at 25°C and 60°C), the system is no longer limited by oxygen diffusion, but rather chemical-reaction limited.

Another possible explanation for the lag in copper dissolution, as seen in the tests performed using air as oxidant, is that an autocatalytic mechanism contributes to copper dissolution. The 'S' shaped dissolution curves, with an induction period, is characteristic of an autocatalytic reaction i.e. the product of the reaction reacts further with the solid (Levenspiel, 1999). It could

be possible that copper is oxidised by Cu(II) to form Cu(I), followed by re-oxidation of Cu(I) to Cu(II) by oxygen. The rate of reaction is slow at the start as the concentration of Cu(II) is low initially. As Cu(II) is formed, the rate of reaction increases, as Cu(II) reacts with copper to form more product (Gupta, 2003; Levenspiel, 1999).

The autocatalytic dissolution of metallic copper in aqueous ammonia has been reported by Nicol (1975), Morioka and Shimakage (1971), Habashi (1963) and Lu and Graydon (1955). The dissolution of copper from chalcopyrite in ammonia solutions has also been reported to occur autocatalytically (Moyo *et al.*, 2015; Muzawazi, 2013).

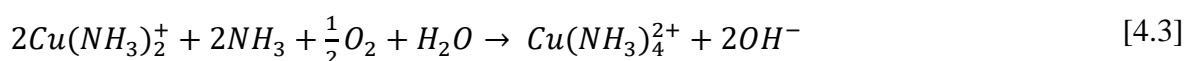
Copper dissolution in aqueous ammonia in the presence of oxygen, occurs as follows (Nicol, 1975):



The $\text{Cu}(\text{NH}_3)_4^{2+}$ formed can also act as oxidant (Cu is oxidised by Cu(II) to form Cu(I)), causing autocatalytic dissolution:



This is followed by rapid oxidation of Cu(I) to Cu(II) (Nicol, 1975; Habashi, 1963):



Morioka and Shimakage (1971) reported that the induction period during copper dissolution decreases with increasing oxygen partial pressure. This is presumably due to an increase in the rate of $\text{Cu}(\text{NH}_3)_4^{2+}$ formation via Equation 4.1, in the presence of increased oxygen concentrations. As seen in Figure 4.11 to Figure 4.13, the induction period for copper dissolution was shortened significantly when pure oxygen was used as oxidant instead of air in the glycine system.

No literature could be found on the autocatalytic dissolution of copper in the glycine system. The only Cu(I)-glycine complex reported in literature is CuL_2^- (refer to Table 2.6). Based on the reaction scheme reported for the ammonia system, it is hypothesised that in the glycine

system, CuL_2 (Cu(II) complex) could react with Cu to form CuL_2^- , followed by oxidation of CuL_2^- by oxygen back to CuL_2 .

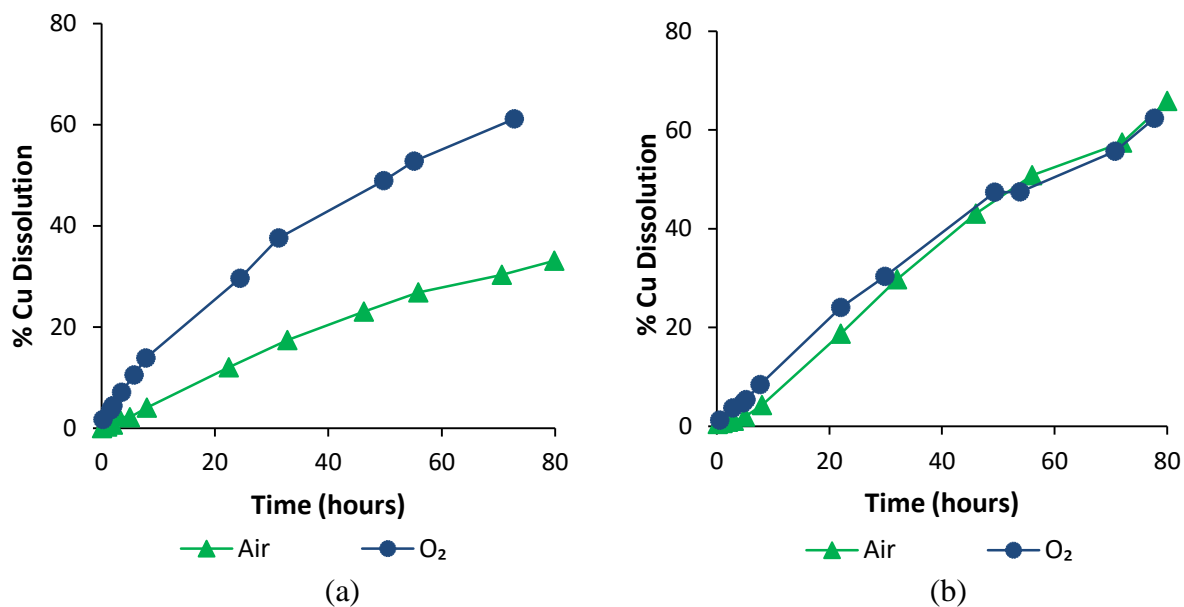


Figure 4.11. Percentage copper dissolution as a function of time and oxidant type at 25°C for glycine concentrations of (a) 1 M and (b) 2 M.

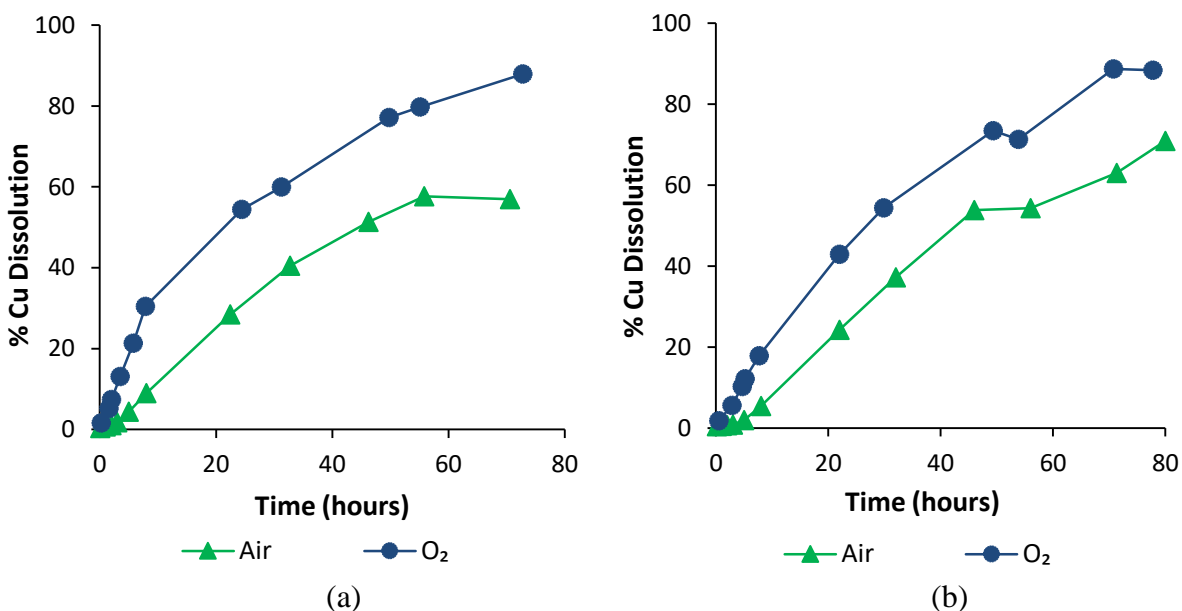


Figure 4.12. Percentage copper dissolution as a function of time and oxidant type at 40°C for glycine concentrations of (a) 1 M and (b) 2 M.

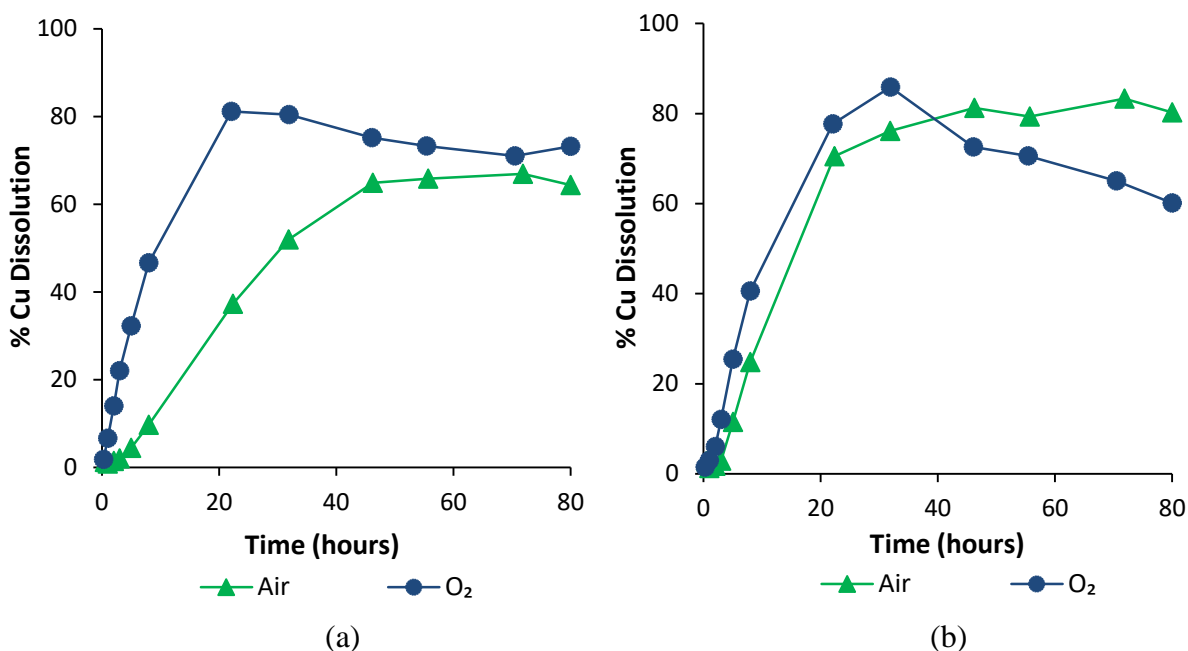


Figure 4.13. Percentage copper dissolution as a function of time and oxidant type at 60°C for glycine concentrations of (a) 1 M and (b) 2 M.

4.2.2.4 Estimation of copper dissolution rate

The rate of copper dissolution was estimated from the dissolution curves presented in Section 4.2.2.1 to 4.2.2.3, in order to quantitatively compare the dissolution rate at different conditions. Copper dissolution rates were determined from the slope of the dissolution curves i.e. the change in copper dissolution over the change in time. Dissolution rates were determined only for periods of rapid leaching, in which the slope of the curve was linear. Consequently, the initial induction period (observed mainly in the tests in which air was used as oxidant), as well as the slow leaching period after rapid leaching, were excluded from the rate analysis. Plots showing linear trendlines fitted to the rapid leaching period of the dissolution curves, for tests performed at 1 M, in the presence of air, are provided in Figure 4.14 as an example.

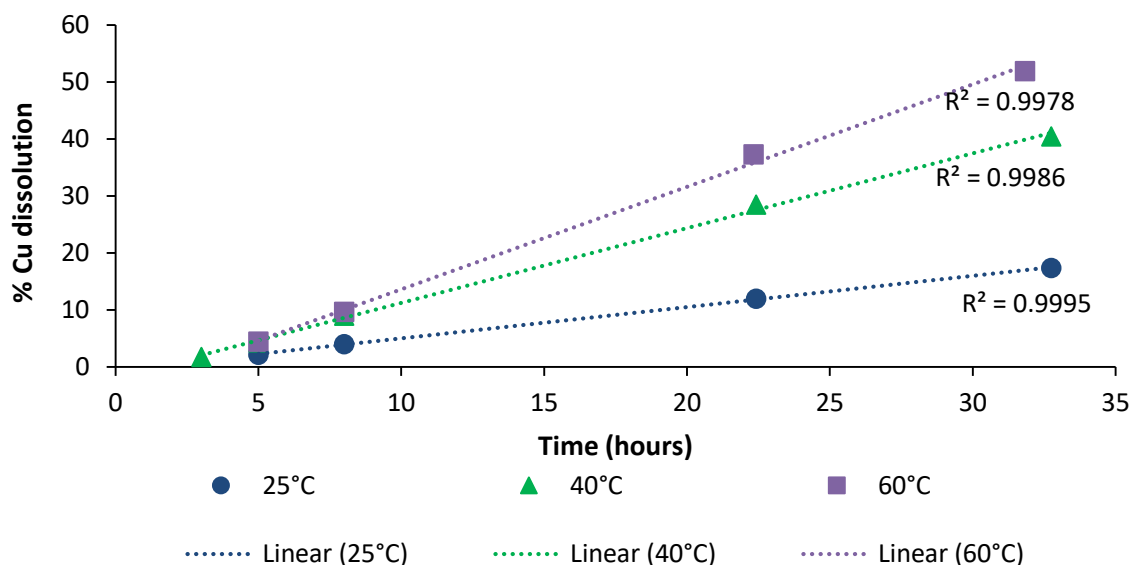


Figure 4.14. Plots for determining the rate of copper dissolution as a function of time, for tests performed at 1 M glycine, with air as oxidant. Trendlines are fitted to the period of rapid leaching, to ensure that the data used for estimating the rate of dissolution follows a linear trend.

Dissolution rates for the remaining tests conducted according to the experimental design, were determined in a similar manner. The rate of copper dissolution during rapid leaching, with corresponding R^2 values, are reported in Table 4.2 for each test.

For the tests performed using pure oxygen, the rapid leaching period typically contained two distinct linear phases, each with a different slope. As a result of this, two rapid leaching periods are reported in Table 4.2 for the majority of the tests performed in the presence of pure oxygen.

In Table 4.2 it can be seen that in the presence of air, increasing the glycine concentration from 1 M to 2 M almost doubled the rate of dissolution achieved during rapid leaching, at both 25°C and 60°C. At 40°C in the presence of air, the rate of dissolution is the same during rapid leaching $\left(1.3 \frac{\% \text{ Cu dissolution}}{h}\right)$ for both 1 M and 2 M glycine.

In the presence of pure oxygen at 25°C, the rate of leaching during the first 8 hours decreases slightly from $1.6 \frac{\% \text{ Cu dissolution}}{h}$ to $1.1 \frac{\% \text{ Cu dissolution}}{h}$ as the concentration of glycine was increased from 1 M to 2 M; however, the rate of leaching between 8 and 22 hours was nearly identical at both concentrations. At 60°C, the rate of dissolution for both rapid leaching periods was nearly identical at both 1 M and 2 M glycine. There was, however, a slight lag in initial

dissolution for the test performed using 2 M glycine, resulting in a slightly lower extent of leaching achieved within the first 22 hours at 2 M glycine compared to 1 M glycine. These findings support the qualitative observations discussed in Section 4.2.2.2.

When pure oxygen was used instead of air, at 1 M glycine, the rate of dissolution (as shown in Table 4.2) increased significantly at both 25°C and 60°C.

At 2 M glycine and 25°C, there was an initial lag in dissolution in the presence of air, which was not observed in the presence of pure oxygen. However, between 8 to 22 hours, the dissolution rate increased only slightly, from $0.97 \frac{\% \text{ Cu dissolution}}{h}$ to $1.1 \frac{\% \text{ Cu dissolution}}{h}$, with increasing oxygen partial pressure. At 60°C and 2 M glycine, the rate of dissolution in the initial rapid leaching period was significantly faster in the presence of pure oxygen ($5.8 \frac{\% \text{ Cu dissolution}}{h}$) compared to the rate achieved in the presence of air ($3.5 \frac{\% \text{ Cu dissolution}}{h}$). However, after 8 hours, the rate of leaching with pure oxygen slowed down to $2.6 \frac{\% \text{ Cu dissolution}}{h}$, while the leaching rate in the presence of air remained constant at $3.5 \frac{\% \text{ Cu dissolution}}{h}$.

Table 4.2. Estimation of the copper dissolution rate during the rapid leaching period(s).

Test	Oxidant type	Glycine conc. (M)	Temp. (°C)	Rapid leaching time period (h)	<u>%Cu dissolution</u> h	R ²
2a	Air	1	25	5 – 33	0.5	0.9995
2b	Air	1	40	3 – 33	1.3	0.9985
2c	Air	1	60	5 – 32	1.8	0.9977
2d	Air	2	25	8 – 56	0.97	0.9969
2e	Air	2	40	5 – 46	1.3	0.9992
2f	Air	2	60	3 – 22	3.5	0.9956
2g	O ₂	1	25	0.25 – 8	1.6	0.9992
				8 – 31	1.0	0.9978
2h	O ₂	1	40	0.25 – 8	3.8	0.9969
				8 – 50	1.1	0.9804
2i	O ₂	1	60	0.25 – 8	5.8	0.9886
				8 – 22	2.5	1
2j	O ₂	2	25	0.5 – 22	1.1	0.9974
				22 – 50	0.85	0.9996
2k	O ₂	2	40	0.5 – 30	1.8	0.9978
2i	O ₂	2	60	2 – 8	5.8	0.9957
				8 – 22	2.6	1

4.2.2.5 Co-extraction of precious metals

As discussed in Section 4.2.2.1, increasing the temperature had a significant effect on the rate of copper dissolution achieved in the experimental design tests. Consequently, results for co-extraction of precious metals are only presented at the highest temperature investigated, namely 60°C.

Figure 4.15 and Figure 4.16 show the co-extraction of gold and silver, respectively, during the base metal leach tests performed at 60°C. Figure 4.15 shows that gold dissolution increased when pure oxygen was used as oxidant instead of air. Increasing the glycine concentration also increased gold dissolution. After 22 hours gold dissolution increased from 1.3% to 3.8%, with increasing the glycine concentration from 1 M to 2 M.

The effect of both glycine concentration and oxidant type on silver dissolution was not clear (refer to Figure 4.16).

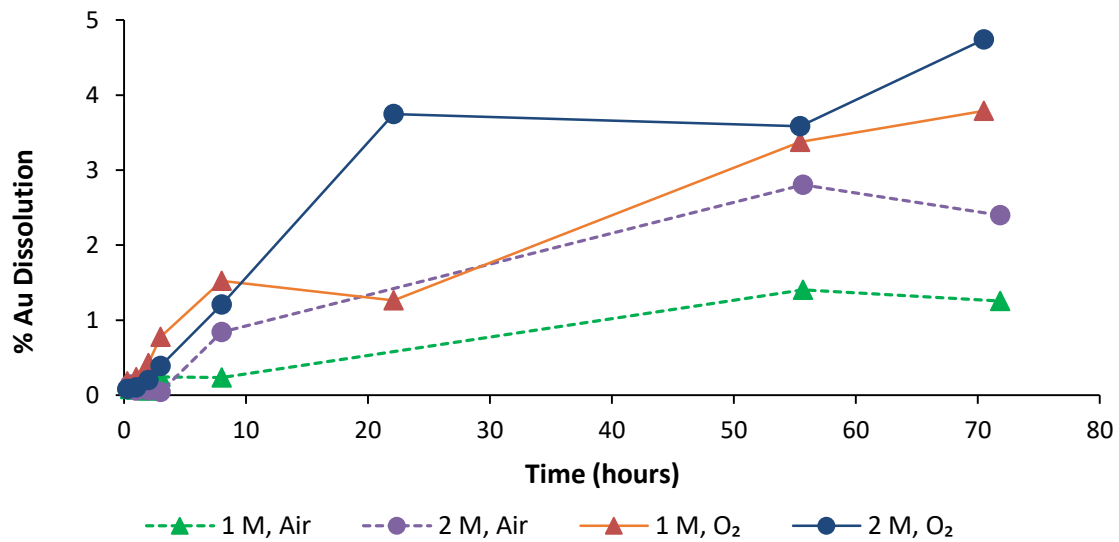


Figure 4.15. Percentage gold dissolution as a function of leaching time, glycine concentration and oxidant type for tests performed at 60°C.

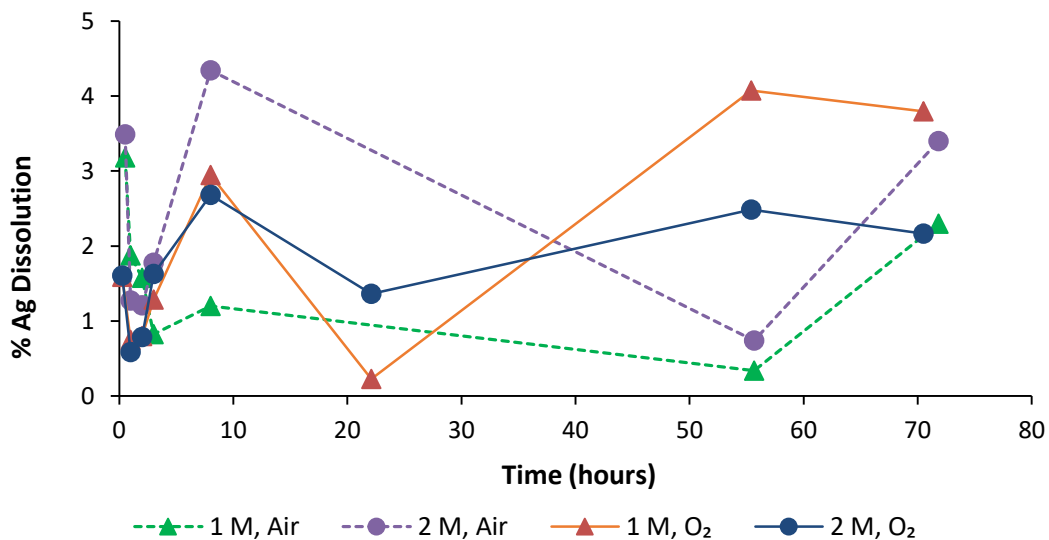


Figure 4.16. Percentage silver dissolution as a function of leaching time, glycine concentration and oxidant type for tests performed at 60°C.

4.2.2.6 Other base metals

The dissolution of other base metals is only presented for tests at which copper extraction is most favourable, with minimal gold dissolution. From the results presented in 4.2.2.1 to 4.2.2.3, and Section 4.2.2.5, these conditions are identified as 60°C, 1 M glycine, using pure oxygen as

oxidant (refer to Section 4.2.2.7 for further discussion). At these conditions 81% copper dissolution and 1.3% gold dissolution was achieved after 22 hours.

Figure 4.28 shows the percentage dissolution of the base metals as a function of time, at 60°C, 1 M glycine, using pure oxygen as oxidant. It can be seen that aluminium dissolution was significantly faster than the other base metals, with 68% dissolution after 3 hours. As discussed in Section 2.4.4, there is no literature available on the glycine dissolution of aluminium. However, aluminium can dissolve in alkaline solutions without the addition of a complexing agent according to Equation 2.19. Neither iron nor tin dissolved to a significant extent. The Pourbaix diagram for a tin-water system (Figure 2.10) shows that in an oxidative environment tin is present as $\text{SnO}_2(\text{s})$. With reference to the Pourbaix diagram for an iron-glycine-water system (Figure 2.6), it is expected that iron dissolution will be low at the conditions presented in Figure 4.28. At pH values greater than 7, in an oxidative environment, iron oxide species ($\text{Fe}_2\text{O}_3(\text{s})$ and $\text{Fe}_3\text{O}_4(\text{s})$) are the most stable. Initially, the rate of nickel and lead dissolution was similar to that of copper; however, the final extent of dissolution was low relative to copper.

93% zinc dissolution was achieved after 22 hours, with the rate of dissolution similar to that of copper throughout the experiment. As discussed in Section 2.4.4, the ZnL_2 complex was not available in the HSC Chemistry database. The Pourbaix diagram for the zinc-glycine-water system (Figure 2.9) showed that, in the absence of ZnL_2 , $\text{ZnO}(\text{s})$ is the most thermodynamically stable species above a pH of 8.2. However, the results presented in Figure 4.17 indicate that zinc dissolves to a greater extent at pH values 8.95 – 11 (refer to the change in pH over time provided in Figure 4.7a). This suggests that ZnL_2 is more stable than $\text{ZnO}(\text{s})$ up to a pH of at least 11.

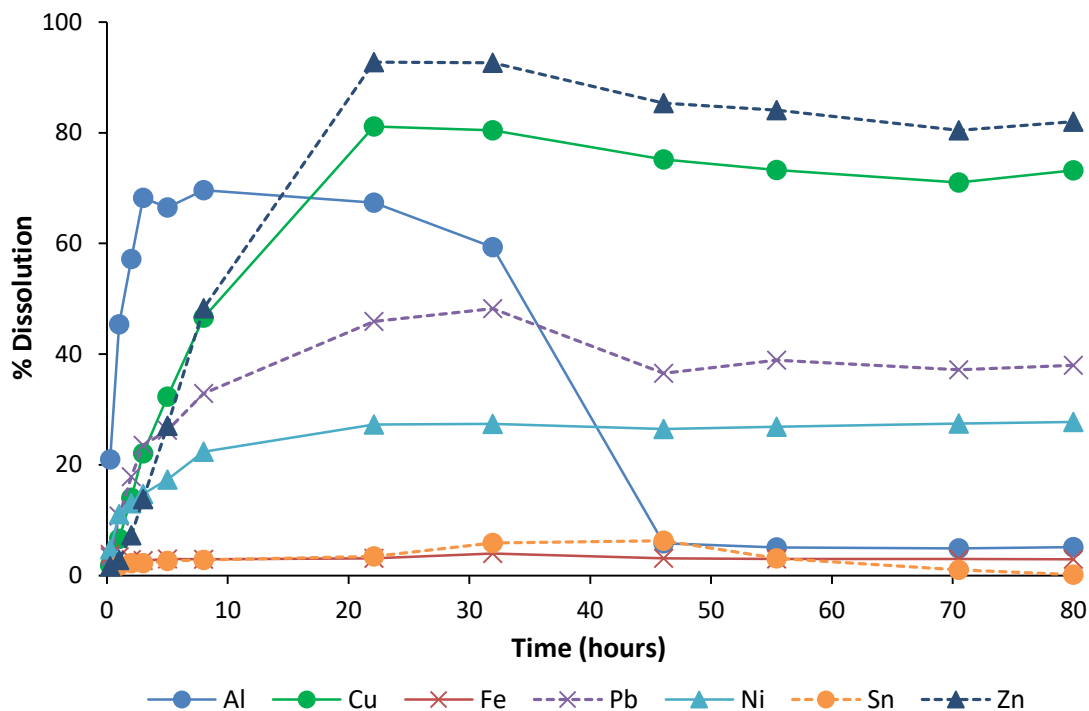


Figure 4.17. Percentage dissolution of base metals as a function of leaching time at 60°C, 1 M glycine, with pure oxygen as oxidant.

4.2.2.7 Conclusions

In Section 4.2.2.1 and Section 4.2.2.2 it was shown that for the tests performed using air as oxidant, copper dissolution was low initially, and independent of both temperature and glycine concentration. The results presented in Section 4.2.2.3 showed that the initial lag at 1 M glycine could be minimised by using pure oxygen as oxidant, instead of air. This would lead to an increase in the partial pressure of oxygen in the gaseous phase, thereby increasing the concentration of dissolved oxygen in solution.

For tests performed using air, as the reaction progressed, both temperature and glycine concentration had a significant effect on dissolution. It was suggested that increasing temperature and glycine concentration increased the rate of CuO removal by CuL_2 formation, thereby decreasing the resistance to oxygen diffusion through the product layer to the reaction surface.

In Section 4.2.2.2 it was shown that when pure oxygen was used as oxidant, increasing the glycine concentration from 1 M to 2 M had no significant effect on copper dissolution. However, this increase led to an increase in the co-extraction of gold. It was decided that an

additional test should be performed at a decreased glycine concentration, to see if there is any benefit in increasing the glycine concentration up to 1 M.

Further tests would also be performed to investigate a stronger oxidant than oxygen i.e. hydrogen peroxide. This could potentially lead to an increase in the rate of dissolution.

In Section 4.2.2.1 it was shown that the rate of copper dissolution increased significantly with increasing temperature. Consequently, additional tests were to be performed at the highest temperature investigated, namely 60°C.

4.2.3 Additional tests

These tests were performed at the same pulp density (25 g/L) and initial pH (11) as the experimental design tests, refer to Section 4.2.2. As discussed in Section 4.2.2.7, these tests were performed at 60°C.

4.2.3.1 Decreased glycine concentration

Results from Section 4.2.2 showed that when pure oxygen was used as oxidant there was no increase in copper dissolution when glycine concentration was increased from 1 M to 2 M. A further test was performed at a reduced glycine concentration to see if there was any benefit in increasing the glycine concentration up to 1 M. As discussed in Section 4.2.1, the stoichiometric concentration of glycine required to leach all base metals at a pulp density of 25 g PCBs/L, was 0.31 M. This test would be performed 0.5 M glycine, at 60°C, using pure oxygen as oxidant.

Figure 4.18 shows that after 3 hours there was little difference between copper dissolution at glycine concentrations of 0.5 M and 2 M. This could be attributed to decreased oxygen solubility at increased solute concentrations (Narita *et al.*, 1983). However, with increasing time it was seen that the rate at 0.5 M glycine was significantly slower than at 1 and 2 M. After 22 hours only 38% copper dissolution was achieved using 0.5 M glycine, compared to 81% and 78% dissolution with 1 M and 2 M glycine, respectively. This suggests that at 0.5 M, the glycine concentration is not in significant excess for the reaction to be independent of glycine concentration. It is concluded that increasing the concentration from 0.5 M to 1 M does increase copper dissolution.

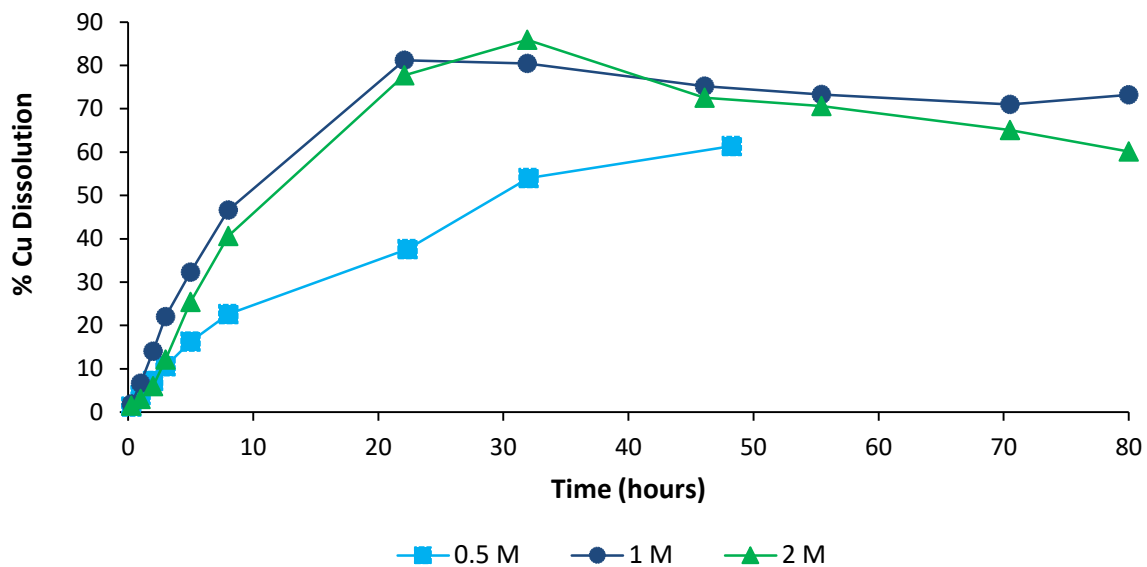


Figure 4.18. Percentage copper dissolution as a function of leaching time and glycine concentration for tests performed at 60°C, with pure oxygen as oxidant.

4.2.3.2 Hydrogen peroxide as oxidant

As discussed in Section 4.2.2.7, hydrogen peroxide was investigated to see if an oxidant more aggressive than oxygen would increase copper dissolution. In Section 4.2.3.1 it was shown that increasing the glycine concentration from 0.5 M to 1 M increased copper dissolution significantly. However, when pure oxygen was used as oxidant (i.e. when diffusion through the porous product layer was not rate-limiting), there was no benefit in increasing glycine concentration beyond 1 M. Consequently, hydrogen peroxide tests were conducted at 1 M.

A 30 wt% solution of hydrogen peroxide was fed continuously due to peroxide decomposition, particularly at high temperatures (Yazici and Devenci, 2010). 4 different flowrates were investigated and are given in Table 3.5.

Figure 4.19 shows that for the first 5 hours, increasing the peroxide flowrate from 0.15 mL/min to 0.3 mL/min had no effect on copper dissolution. After 12 hours, copper dissolution at a flowrate of 0.3 mL/min was approximately 7% higher than at 0.15 mL/min. Increasing the flowrate further to 0.5 mL/min increased copper dissolution significantly, with 44% dissolution achieved after 12 hours, compared to 27% achieved at 0.3 mL/min. However, increasing the flowrate above 0.5 mL/min, to 1 mL/min decreased copper dissolution.

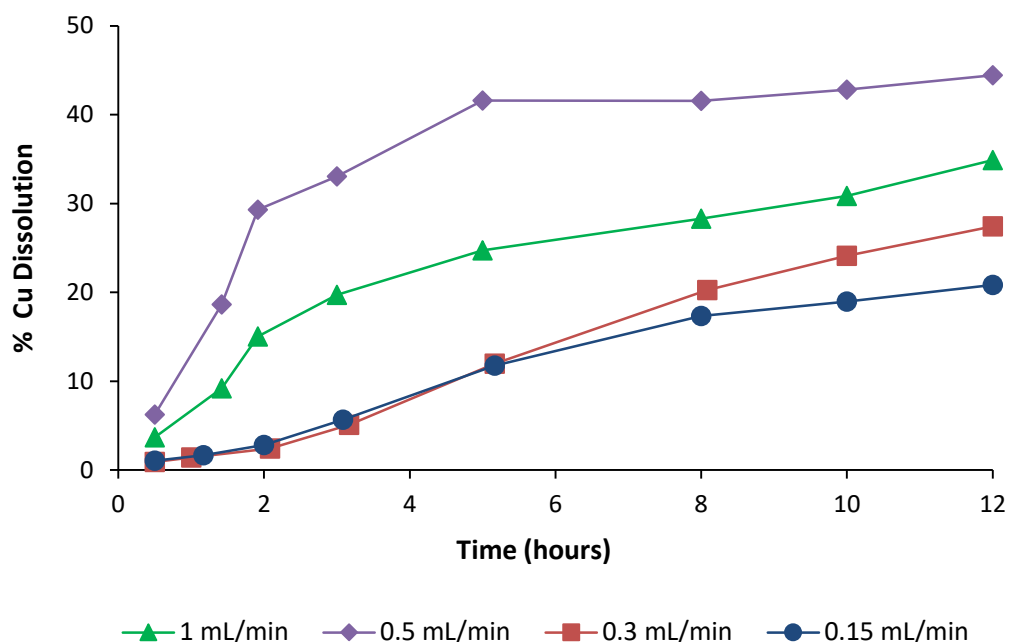


Figure 4.19. Percentage copper dissolution as a function of time and H_2O_2 flowrate for tests performed at $60^\circ C$, with 1 M glycine.

In Figure 4.20a, the peroxide flowrate which gave the greatest copper dissolution (0.5 mL/min), is compared to the tests performed with air and oxygen at the same conditions of $60^\circ C$ and 1 M glycine. Initially, the dissolution of copper achieved using peroxide was fast, with 42% dissolution after 5 hours, compared to 32% and 4% dissolution achieved in the same amount of time using pure oxygen and air, respectively. However, after 5 hours, the copper dissolution using peroxide, slowed down significantly with 42% dissolution achieved after 8 hours, and 47% achieved using pure oxygen.

A possible reason for copper dissolution slowing down significantly after 5 hours, was the formation of a protective film above a threshold concentration of peroxide, as suggested by Aksu *et al.* (2003) and Ihnfeldt and Talbot (2008). As discussed in Section 2.6.1, the nature and composition of this film was not reported by the authors. Another factor possibly contributing to the decreased leach rate is the rapid decrease in pH observed for the test performed with peroxide, relative to the test performed using air and pure oxygen as oxidant, as shown in Figure 4.20b. After 5 hours, the pH decreased to 8.75, at which point the leaching slowed down significantly. As discussed in Section 2.4.3, operating at a higher pH favours the anionic form of glycine, which forms more stable copper glycine complexes. As in the case of pure oxygen as oxidant (refer to Section 4.2.2.1), the reason for a rapid decrease in pH could

possibly be due to the oxidation of Fe to FeO(OH). This oxidation would be increased in presence of a stronger oxidant, i.e. hydrogen peroxide in this case. Another factor possibly contributing to the rapid decrease in pH, is that the 30 wt% peroxide solution fed continuously was highly acidic, having a pH of 2.2.

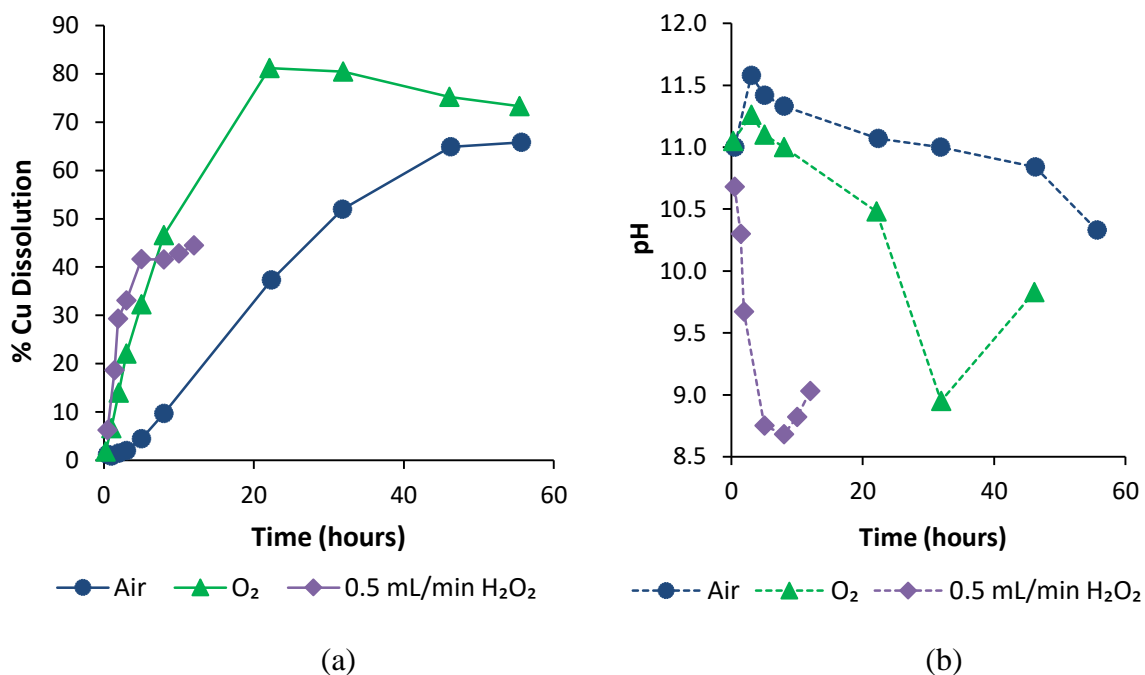


Figure 4.20. (a) Percentage copper dissolution and (b) pH, as a function of time and oxidant type for tests performed at 60°C, with 1 M glycine.

Co-extraction of precious metals for the tests performed at peroxide flowrates of 0.5 mL/min and 1 mL/min are given in Figure 4.21. Dissolution of silver increased significantly with increasing peroxide flowrate from 0.5 mL/min to 1 mL/min.

After 8 hours, 0.6% and 1.5% gold dissolution was achieved at peroxide flowrates of 0.5 mL/min and 1 mL/min, respectively. In Section 4.2.2.5 it was shown that 1.6% gold dissolution was achieved after 8 hours at the same temperature and glycine concentration (60°C and 1 M) when pure oxygen was used as oxidant (refer to Figure 4.15). It would be expected that peroxide, a stronger oxidant than oxygen, would increase gold dissolution. However, as shown in Figure 4.20b, during the test performed with peroxide, the pH decreased significantly in the first 8 hours down to pH 8.68. When pure oxygen was used as oxidant, the pH did not decrease below 11 in the first 8 hours. As discussed in Section 2.6.4, Eksteen and Oraby (2015) and Oraby and Eksteen (2015a) reported that gold dissolution increased significantly with

increasing pH from 10 to 11. This suggests the need for pH control during precious metal leach tests, when peroxide was to be fed continuously.

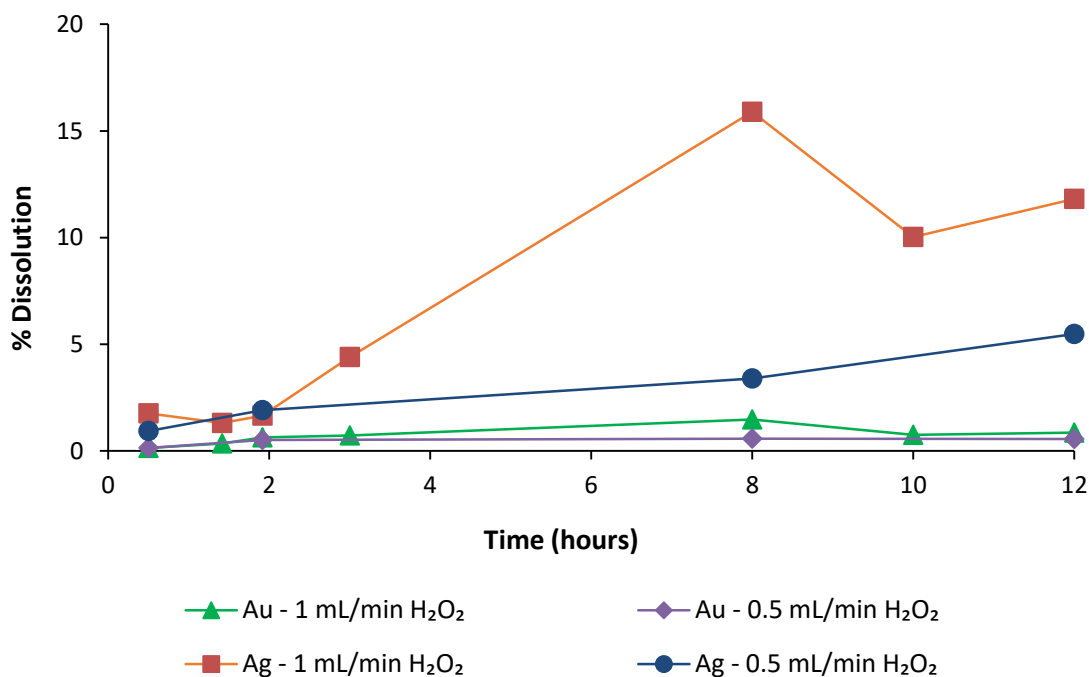


Figure 4.21. Percentage gold and silver dissolution as a function of H₂O₂ flowrate for tests performed at 60°C and 1 M glycine.

4.2.4 Bench-scale test recommendations

As discussed in Section 4.2.2.7, optimal conditions for maximum copper dissolution with minimal gold dissolution from the experimental design were determined to be 60°C, 1 M glycine, using pure oxygen as oxidant. Additional tests, discussed in Section 4.2.3, were performed to further investigate the effect of glycine concentration, and the use of hydrogen peroxide as oxidant.

An additional test was performed at a decreased glycine concentration of 0.5 M, at 60°C, using pure oxygen as oxidant. This test aimed to see if there was any benefit in increasing the glycine concentration up to 1 M. In Section 4.2.2 it was shown that when oxygen was used as oxidant, there was no increase in copper dissolution when the glycine concentration was increased from 1 M to 2 M. The co-extraction of gold, however, increased with increasing glycine concentration. The results of the 0.5 M glycine test, discussed in Section 4.2.3.1, showed that

decreasing the glycine concentration from 1 M to 0.5 M, decreased the rate of copper dissolution significantly.

The results for tests investigating hydrogen peroxide as oxidant were presented in Section 4.2.3.2. Tests were performed at 60°C and 1 M with hydrogen peroxide fed continuously at 4 different flowrates, ranging from 0.15 mL/min – 1 mL/min. Initially, copper dissolution at the optimal peroxide flowrate of 0.5 mL/min was faster than when pure oxygen was used as oxidant. However, after 5 hours, copper dissolution using peroxide slowed down considerably. Possible reasons for this included the formation of a protective film inhibiting dissolution and also a rapid decrease in pH. After 8 hours, the rate of leaching with pure oxygen as oxidant was significantly faster.

Based on the results of the additional tests, it is recommended that small pilot-scale leach tests be performed at 1 M glycine using pure oxygen as oxidant, sparged continuously through the solution. Tests were to be performed at 60°C and a pulp density of 25 g/L. Due to the adverse effect of decreased pH on copper dissolution, as discussed in Section 4.2.2.1, it was decided to control the pH of the solution above 11.

4.2.5 Variability in feed composition

As discussed in Section 3.2.2, the solid residue remaining after each of the bench-scale base metal leach tests (excluding the preliminary tests) was digested in aqua regia, for complete dissolution of the remaining metals. This allowed the feed composition of each test to be quantified by means of a mass balance, and these values are tabulated in Appendix C. The average mass of copper in 25 g PCBs was determined to be 5.8 g (23.2 wt%). This compares well to the average copper content determined by aqua regia digestion of three feed samples, reported in Table 4.1.

Based on the feed composition of each of the bench-scale base metal leach tests, a 95% confidence interval ($\alpha = 0.05$) was calculated for the mass of copper in the feed. The confidence interval, expressed as a percentage of the mean value of 5.8 g Cu (in 25 g PCBs), was determined to be 4.5%.

Figure 4.22 shows the 95% confidence interval applied to the tests performed at 60°C, using air as oxidant.

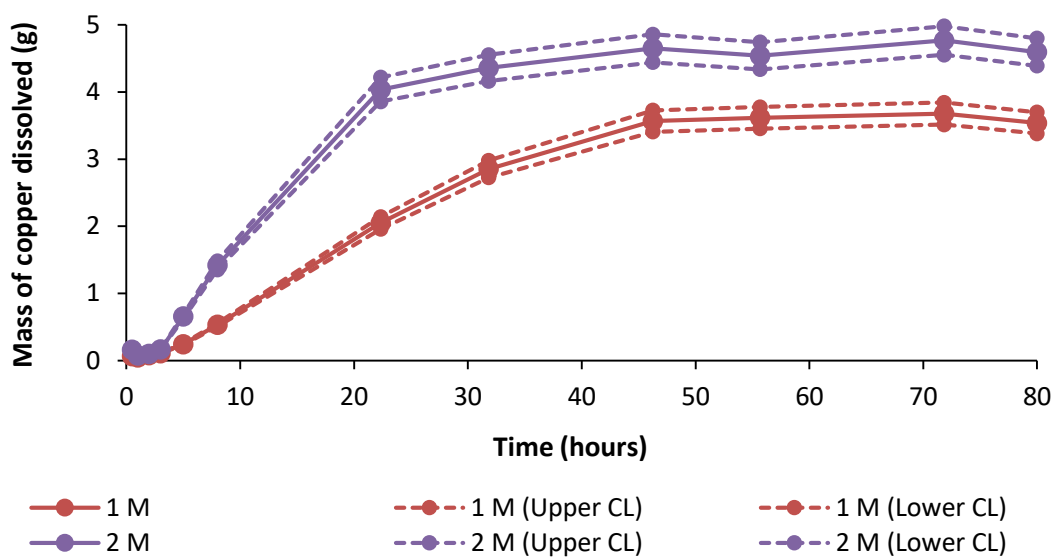


Figure 4.22. Mass of copper extracted as a function of time and glycine concentration, for tests performed at 60°C using air as oxidant. 95% Confidence intervals are shown to illustrate the variability in feed composition (CL refers to confidence limit).

4.2.6 Small pilot-scale leach tests

The aim of these tests were to prepare the necessary feed required for the precious metal leach tests. As discussed in Section 4.2.4, these tests were performed at 60°C, 1 M glycine, pH 11, using pure oxygen as oxidant sparged continuously through the solution.

PCBs were leached in a vessel with a working volume of 17 L, described in Section 3.3.2. Two batches of fresh feed were leached at identical conditions with each batch containing 425 g PCBs, yielding the desired pulp density of 25 g/L. Due to the low extent of copper dissolution achieved with the small pilot-scale leach setup, the residue from each of the tests were re-leached at the same conditions. This is discussed further, below.

Figure 4.23 compares the copper dissolution achieved in the small pilot-scale leach tests to the bench-scale leach test performed at the same conditions. A description of each of the tests are provided in Table 4.3. To determine the copper content in the feed to the small pilot-scale leach tests, the solid residue from the precious metal leach tests was digested in acid and a mass balance was performed.

Figure 4.23 shows that the copper dissolution achieved for the small pilot-scale leach tests using fresh feed, test 4a(i) and 4b(i), was significantly lower than the copper dissolution

achieved in the bench-scale leach test, test 2i. It is suggested that the mass transfer of oxygen from the gaseous phase into the solution was significantly better in the bench-scale leach tests, compared to the small pilot-scale-leach tests.

The pH was monitored throughout the course of experiment, with the intention of controlling the pH above 11. However, as shown in Figure 4.24, the pH did not drop significantly during the small pilot-scale leach tests. The reason for this is not clear, however, the poor mass transfer, and hence poor leaching, could possibly contribute to the lack of pH drop.

The solid residue of each of the small pilot-scale leach tests was re-leached at the same conditions. For test 4a(i), a maximum of 51% copper dissolution was achieved after 43 hours. In the second stage, test 4a(ii), 30% of the total copper dissolved after 41 hours. This showed that a total of 81% copper could be extracted in two stages of approximately 43 hours each. However, due to copper precipitation in test 4a(i), the final copper dissolution (achieved at the end of the test i.e. after 67 hours) was only 42%.

47% copper dissolution was achieved after 52 hours in test 4b(i), with 27% dissolution after 48 hours, in the second stage, yielding a total of 74% copper dissolution.

Table 4.3. Description of tests performed at 60°C, 1 M glycine, using pure oxygen as oxidant, at a pulp density of 25 g/L, at pH 11.

Test	Description of setup	Feed material
2i	Bench-scale test (1 L working volume)	Fresh feed
4a(i)	Small pilot-scale leach test (17 L working volume)	Fresh feed
4b(i)	Small pilot-scale leach test (17 L working volume)	Fresh feed
4a(ii)	Small pilot-scale leach test (17 L working volume)	Solid residue from test 4a(i)
4b(ii)	Small pilot-scale leach test (17 L working volume)	Solid residue from test 4b(i)

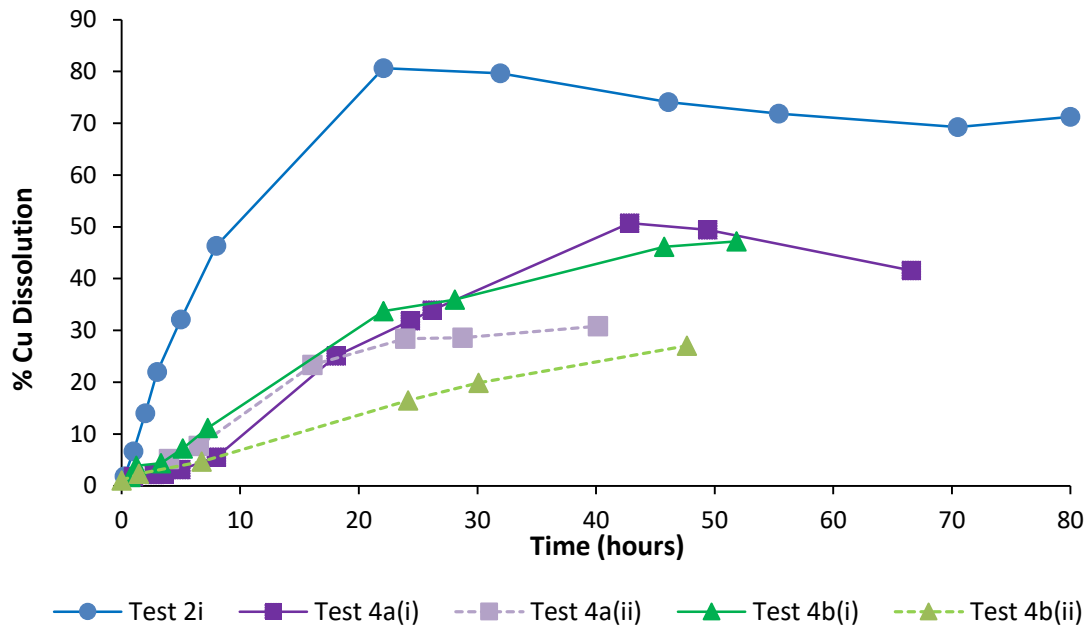


Figure 4.23. Percentage copper dissolution as a function of time for tests performed at 60°C, 1 M glycine, using O₂ as oxidant for the bench-scale test (test 2i), and two small pilot-scale leach tests, each with two stages.

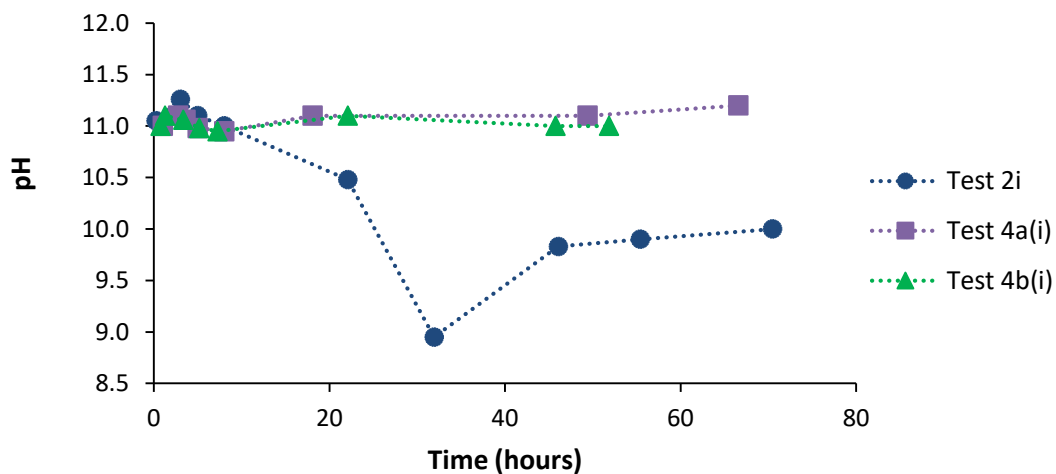


Figure 4.24. pH as a function of time for tests performed at 60°C, 1 M glycine, using O₂ as oxidant for the bench-scale test (test 2i), and the first stage of each of the two small pilot-scale leach tests.

The percentage dissolution for the rest of the base metals during the small pilot-scale leach tests are given in Table 4.4. The dissolution reported corresponds to the final extraction achieved at the end of each of the tests. The co-extraction of silver and gold during the small pilot-scale leach tests was not quantified.

Table 4.4. Final base metal extraction achieved in each of the small pilot-scale leach tests.

Test	Duration (h)	% Dissolution						
		Al	Cu	Fe	Ni	Pb	Sn	Zn
4a(i)	67	39	42	5.8	23	56	36	48
4b(i)	52	38	47	4.6	19	55	19	41
4a(ii)	40	6.1	31	2.0	9.3	4.3	10	29
4b(ii)	48	6.3	27	1.9	13	3.6	13	36

4.3 Precious metal leaching

The solid residue from the second stage of the small pilot-scale leach tests (test 4a(ii) and test 4b(ii)) were combined and split into representative samples of the required mass using a rotary sample splitter. These samples were used as feed for all precious metal leach tests, except the gold foil tests discussed in Section 4.3.4. The average metal composition of the solid residue, with standard deviation, is given in Table 4.5.

Table 4.5. Average composition of precious metal feed, with standard deviation.

	Ag	Al	Au	Cu	Fe	Ni	Pb	Sn	Zn
PCB	0.0164±	2.69±	0.0199±	8.57±	2.87±	0.41±	0.61±	2.04±	0.83±
(%)	0.0071	0.26	0.0041	0.80	0.20	0.06	0.05	1.29	0.09

The concentration of metals in solution as a function of time during the precious metal leach tests, are tabulated in Appendix C.

4.3.1 Experimental design for preliminary tests

The first set of precious metal leach tests were performed according to the experimental design given in Table 3.7. The experimental conditions for each test, originally given in Table 3.9, are repeated in Table 4.6.

Table 4.6. Experimental conditions for precious metal leach tests according to the experimental design given in Table 3.7.

Test	Temperature (°C)	Initial pH	Glycine concentration (M)
5a	60	11.5	0.1
5b	75	11.5	0.1
5c	60	12.5	0.1
5d	75	12.5	0.1
5e	60	11.5	0.5
5f	75	11.5	0.5
5g	60	12.5	0.5
5h	75	12.5	0.5

Figure 4.25 and Figure 4.26, shows the percentage dissolution of gold and silver, respectively, for each test, after 48 hours. Copper dissolution as a function of time is given in Figure 4.27.

In Figure 4.25 it can be seen that gold dissolution was low during all tests. Gold dissolution increased with increasing glycine concentration from 0.1 M to 0.5 M glycine. At 0.5 M glycine, decreasing the temperature from 75°C to 60°C increased gold dissolution at both pH 11.5 and pH 12.5. The relatively greater dissolution achieved at a lower temperature of 60°C could possibly be due to higher peroxide degradation at increased temperatures of 75°C.

Figure 4.26 shows that silver dissolution is greatest at 0.5 M glycine, pH 11.5, and 60°C. These conditions also gave the greatest gold and copper dissolution. It could be possible that increasing silver dissolution had a catalytic effect on gold dissolution, as discussed in Section 2.6.5.2. It is not clear why silver dissolution was the greatest at these specific conditions; however, the possibility of the behaviour of copper inhibiting precious metal dissolution at the remainder of the conditions, is discussed below.

Figure 4.27 shows that copper dissolution was low, with copper precipitation observed in the majority of the tests. Copper dissolution during the first 8 hours was not quantified. The Pourbaix diagram for a copper-water-glycine system (refer to Figure 2.5), showed that above pH 11.8, CuO is the most stable phase. Low copper dissolution was therefore expected at the

relatively high pH values at which the tests were conducted (11.5 to 12.5). The formation of a protective copper film in the presence of peroxide, as discussed in Section 4.2.3.2, could also suppress copper dissolution. It is possible that the formation of CuO (at increased pH), and protective film in the presence of peroxide, could inhibit gold and silver leaching. This was supported by the observation that the test in which the highest copper dissolution was achieved (test 5e), also gave the highest dissolution of gold and silver. However, the gold dissolution achieved at pH 12.5, 0.5 M glycine and 60°C (test 5g), also gave relatively high gold dissolution despite copper dissolution being low. It is also possible that cementation of gold occurred during the leach tests, contributing to the low dissolution achieved. As discussed in Section 2.6.5.1, copper can act as a reducing surface for cementation of gold. Since complete copper extraction was not achieved in the small pilot-scale leach tests, the copper content in the feed to the precious metal leach tests was high relative to the gold content (refer to Table 4.5).

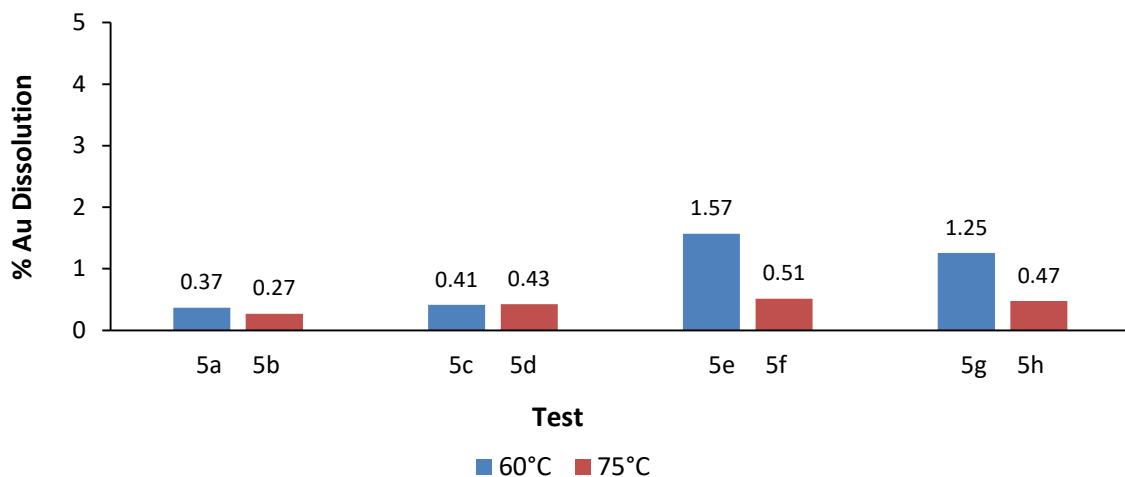


Figure 4.25. Percentage gold dissolution after 48 hours as a function of temperature, glycine concentration and pH, for precious metal tests performed using H_2O_2 as oxidant, fed continuously at 4 mL/hr.

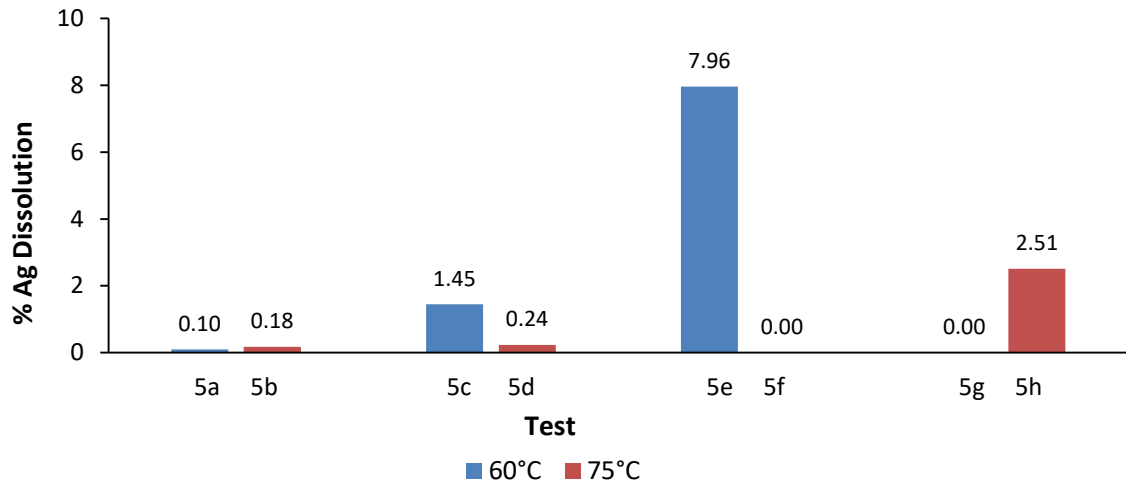


Figure 4.26. Percentage silver dissolution after 48 hours as a function of temperature, glycine concentration and pH, for precious metal tests performed using H_2O_2 as oxidant, fed continuously at 4 mL/hr.

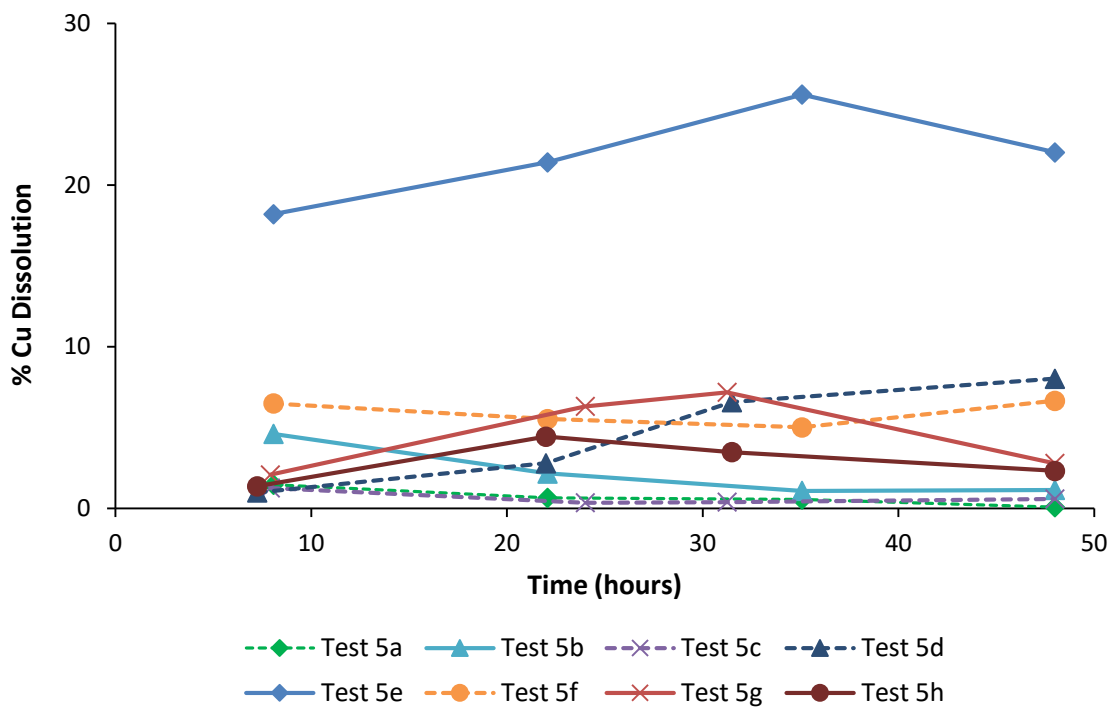


Figure 4.27. Percentage copper dissolution as a function of time and temperature for precious metal tests performed using H_2O_2 as oxidant, fed continuously at 4 mL/hr.

It was expected that the gold dissolution achieved during the precious metal leach tests, with hydrogen peroxide fed continuously, would be greater than the dissolution achieved in the base metal leach tests using air/oxygen as oxidant. As discussed in Section 2.6.1, hydrogen peroxide

is reported to increase gold dissolution significantly. However, as shown in Figure 4.25, the greatest extent of gold dissolution after 48 hours was achieved at 60°C, pH 11.5 and 0.5 M glycine, with peroxide fed continuously. At these conditions 1.6% gold dissolution was achieved, corresponding to a solution concentration of 0.08 mg/L Au and mass of 0.05 mg Au extracted. However, in the base metal leach tests, 3.8% gold dissolution was achieved after 22 hours, using pure oxygen as oxidant, at 2 M glycine, 60°C and pH 11 (refer to Section 4.2.2.5). This percentage dissolution corresponds to a solution concentration of 0.13 mg/L Au and 0.14 mg Au extracted. As discussed earlier, it is possible that the low extent of copper dissolution achieved during the precious metal leach tests inhibited gold leaching.

It could also be possible that some of the copper present in the feed was alloyed/plated with gold (Uyemura International, 2017; Le Solleu, 2010). Gold in this form could have dissolved with the copper during the small pilot-scale leach tests, and is therefore not present in the feed of the precious metal leach tests. However, as stated in Section 4.2.6, the dissolution of gold during the small pilot-scale leach tests was not quantified.

ICP-AES was initially used to determine the concentration of gold in solution for these tests. However, for all tests, gold concentrations in solution were below the detection limits for ICP-AES. As discussed in Section 3.5, ICP-MS was used to quantify gold concentrations due to the lower detection limits relative to ICP-AES. Results from ICP-MS were, however, not available prior to additional precious metal leach tests being conducted. It was determined that for gold dissolution to be below the detection limits for ICP-AES, less than 20% dissolution had to be achieved at all conditions. Since it was not known which conditions gave relatively higher gold dissolution, additional tests (in Section 4.3.2) were performed based on literature recommendations. As discussed in Section 2.6.2 to Section 2.6.4, the rate of gold dissolution was expected to increase with increasing temperature, glycine concentration and pH.

It was decided that the experimental design test conducted at the highest temperature, glycine concentration, i.e. 75°C, 0.5 M glycine and pH 12.5, should be repeated. However, the duration of the test should be extended from 48 hours to 96 hours, to see if gold dissolution would increase over time.

A further test would be conducted at an increased temperature and increased peroxide flowrate, in an attempt to increase the rate of dissolution.

4.3.2 Additional tests

Additional tests were performed based on the results and recommendations from the experimental design tests, as discussed in Section 4.3.1. Experimental conditions for these tests are given Table 3.10 (test 6a, 6b).

Figure 4.28 shows that by extending the leaching time of test 5h (75°C, 0.5 M glycine and pH 12.5) from 48 hours to 96 hours, gold dissolution was not increased.

At an increased peroxide flowrate and increased temperature of 90°C, gold dissolution was 2.2% after 30 minutes, after which gold precipitated out of solution. This could possibly be due to cementation of gold in the presence of metallic copper (as discussed in Section 2.6.5.1). Copper dissolution during the 90°C test was not quantified.

Silver behaviour for these tests are provided in Figure C.1, Appendix C.

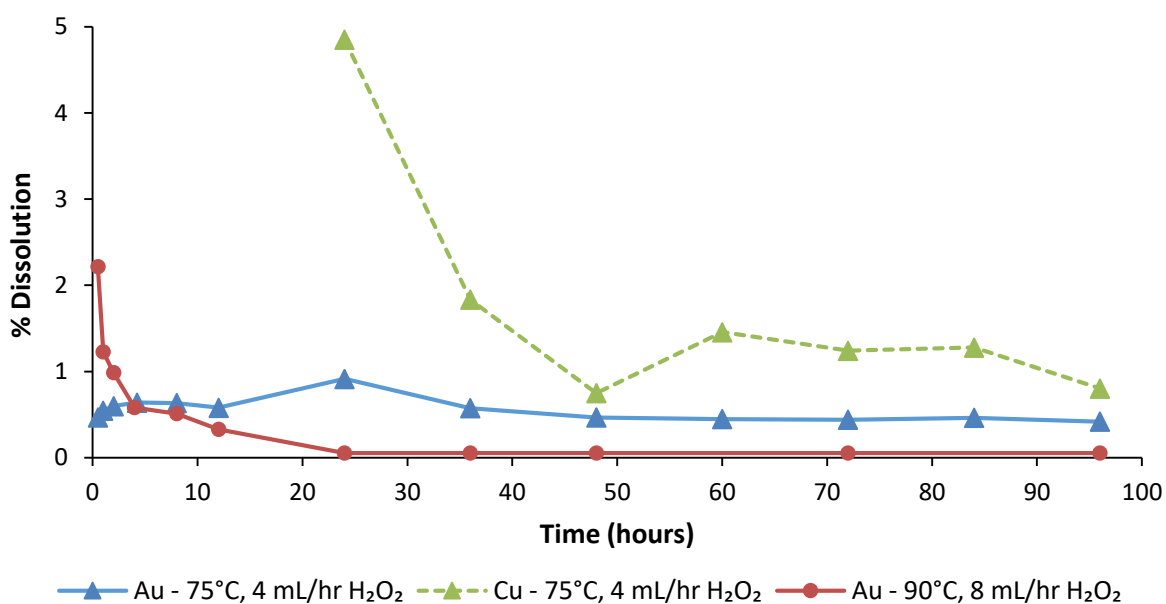


Figure 4.28. Percentage dissolution as a function of time temperature and peroxide flowrate, for the tests performed at pH 12.5 and 0.5 M glycine.

From the results of the additional tests it was clear that increasing the temperature, peroxide flowrate and residence time, did not increase gold dissolution.

It was decided that an additional test would be performed using an alternative lixiviant. This test aimed to determine whether the low dissolution of gold was due to gold being physically

entrapped in the PCBs. The parameters and results for this test are given and discussed in Section 4.3.3.

The results from Section 4.3.1 and results from the additional tests suggested the possibility of copper in the feed having a negative impact on gold dissolution. Further tests were performed using pure gold foil. These tests aimed to determine whether copper was inhibiting gold dissolution, or whether gold leaching using glycine was not feasible. Section 4.3.4 provides the discussion of the parameters and results for these tests.

4.3.3 Glycine-cyanide test

As discussed in Section 4.3.2, a further test was performed with an alternative lixiviant, to determine whether gold was physically entrapped in the PCBs. A cyanide-glycine mixture was used as lixiviant. Literature, provided in Section 2.4.5.2 and 2.6.5.3 suggested that the addition of low concentrations of cyanide increased gold dissolution significantly.

Experimental conditions for this test (test 6c) is given in Table 3.10. The same feed and pulp density (40 g/L) from the previous precious metal leach tests was used. The remainder of the experimental conditions were based on parameters used by Oraby *et al.* (2017).

The concentration of NaCN and glycine was based on the copper content of the feed given in Table 4.5, using the molar ratios reported by Oraby *et al.* (2017). At a pulp density of 40 g/L, complete copper extraction would yield a concentration of 3.4 g/L Cu. A CN:Cu molar ratio of 0.75:1 and Gly:Cu ratio of 2.5:1 was used. This corresponded to a glycine concentration of 10 g/L (0.13 M) and NaCN concentration of 2 g/L (0.04 M).

Figure 4.29 shows that after 96 hours, dissolution of gold and copper was 38% and 53%, respectively. 9.3% gold dissolution was achieved after 30 minutes and stayed approximately constant for the first 24 hours. After 24 hours, gold dissolution started to increase again. The reason for this is not clear. Table 4.7 provides the final percentage dissolution for the other metals.

Gold extraction achieved in the cyanide-glycine test was significantly higher compared to the gold extraction achieved when glycine was used alone, despite the fact that the glycine-cyanide

test was conducted at ambient temperature using only air as oxidant. It is concluded that the gold is not physically entrapped in the PCBs.

Optimisation of process variables such as temperature, oxidant type, copper content and lixiviant concentration (glycine and NaCN) are required to maximise gold dissolution in the glycine-cyanide system.

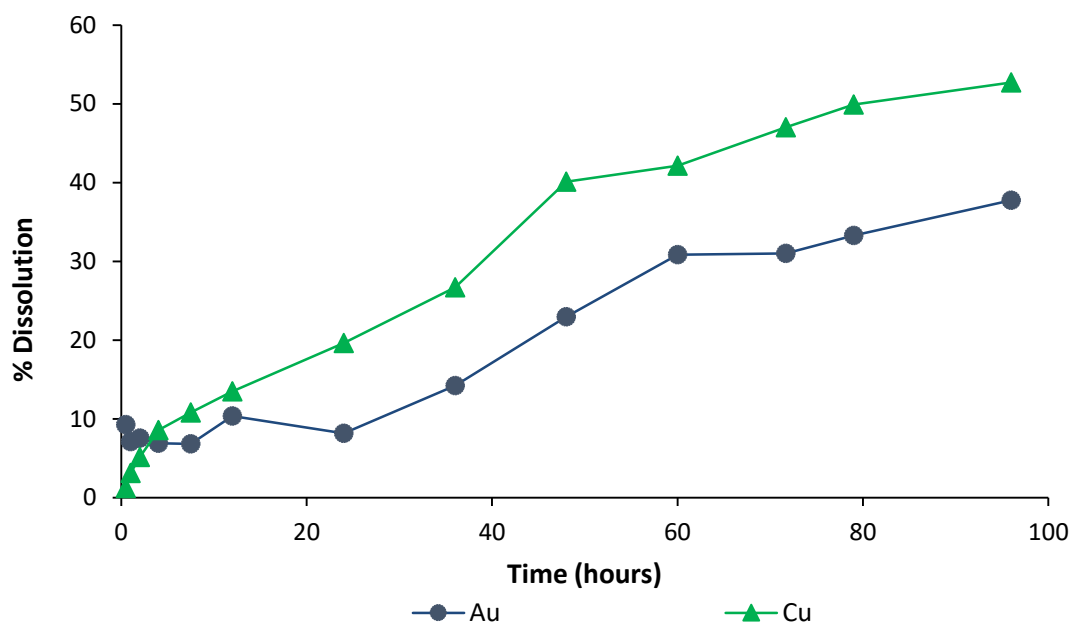


Figure 4.29. Percentage gold dissolution as a function of time for a mixture of 2 g/L NaCN, and 10 g/L glycine, at 25°C, initial pH 11.5, using air as oxidant.

Table 4.7. Percentage dissolution of metals after 96 hours for the test performed using 2 g/L NaCN and 10 g/L glycine, at 25°C, initial pH 11.5, using air as oxidant.

% Dissolution						
Ag	Al	Fe	Ni	Pb	Sn	Zn
58	38	7.7	12	0.0	0.9	16

4.3.4 Gold foil tests

As discussed in Section 4.3.2, additional tests were conducted using pure gold foils to determine whether copper was inhibiting gold dissolution, or whether gold leaching using glycine is not technically feasible.

Parameters for these tests are given in Table 3.11. 75 mg of gold foil was added to a leach solution with an initial volume of 500 mL.

The first experiment aimed to compare gold leaching from foil to gold leaching from PCBs. The test performed in Section 4.3.1 at 0.5 M glycine, 60°C, and pH 12.5, was repeated, using the gold foil as feed. Hydrogen peroxide was fed continuously and the pH was controlled.

The second experiment aimed to compare leaching from gold foil to that of the results in literature. This test was performed at the same glycine concentration, temperature and initial pH as the previous test; however, as in the gold foil tests performed by Eksteen and Oraby (2015) and Oraby and Eksteen (2015a), the pH was not controlled, and peroxide was only added at the start of the test.

Figure 4.30 shows that 0.06 mg of gold dissolved for the test in which peroxide was fed continuously, and pH was controlled. For the test where peroxide was only added at the start of the test, 0.03 mg of gold dissolved.

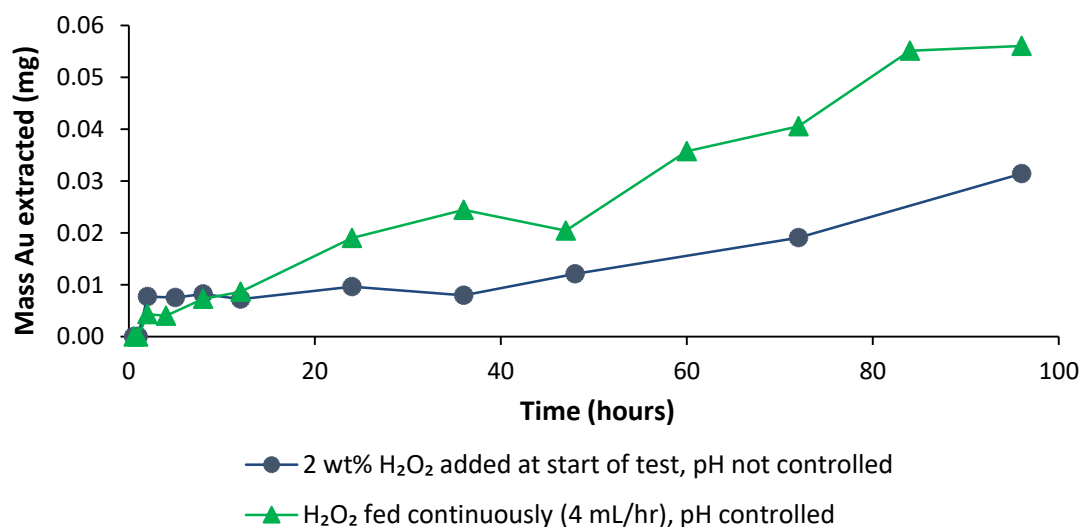


Figure 4.30. Mass of gold extracted as a function of time for tests using gold foil, at 60°C, 0.5 M glycine and initial pH 12.5.

The gold foils used in this work each had a surface area of 1.56 cm² (approximately 75mg of gold). The gold foil tests performed by Eksteen and Oraby (2015) and Oraby and Eksteen (2015a), had a surface area of 20 cm², which is approximately 12.8 times the surface area of the foil used in this work.

The leach rates reported by Oraby and Eksteen (2015a) provided in Table 2.9, were used to calculate the theoretical amount of gold that should have dissolved in this work, based on the surface of the foil. The leach rates, in $\mu\text{mol}/\text{m}^2\text{s}$, were reported at the following conditions: at 60°C , 0.5 M glycine, 1% H_2O_2 , pH 11.

Table 4.8 compares the gold dissolution reported by Oraby and Eksteen (2015a), to the theoretical amount of gold that should have dissolved in this work. Sample calculations are provided in Appendix D. Table 4.8 shows that approximately 2.31 mg of gold should have dissolved in the gold leach tests in this work. However, as shown in Figure 4.30, only 0.03 mg dissolved in the test performed at similar conditions to the test performed by Oraby and Eksteen (2015a). The only difference between these tests was the increased pH and peroxide concentration used in this work. It is not clear why the gold extraction achieved is significantly lower than the theoretical extraction.

The expected dissolution of 2.31 mg of gold after 96 hours, however, is low, considering that 75 mg gold is present in the feed. The relatively high concentrations of gold in solution reported by Oraby and Eksteen (2015a) can be attributed to the large surface area of gold foils used in their work.

Table 4.8. Gold dissolution expected based on leach rates reported in literature.

	Oraby and Eksteen (2015a)	This work (theoretical)
Surface area (cm^2)	20	1.56
Au dissolved after 48 h (mg)	23.6 (59 mg/L Au)	1.84 (3.68 mg/L Au)
Au dissolved after 96 h (mg)	29.3 (73.3 mg/L Au)	2.31 (4.62 mg/L)

4.3.5 Conclusions

As discussed in Section 2.4.5.1, Eksteen and Oraby (2015) reported that the glycine system, without the addition of cyanide, was more suitable for heap leaching due to the slow kinetics. However, these leach rates were reported for leaching in the absence of catalytic ions (such as silver and copper), and without pH control or a constant level of hydrogen peroxide maintained in the system. It was expected that leach rates could be increased by making the above-mentioned changes to the system. Results from Section 4.3.1 and 4.3.2, showed, however, that this was not the case.

It was shown that gold was not physically entrapped in the PCBs, as addition of cyanide to the glycine system showed 38% gold dissolution after 96 hours, at ambient temperature, with only air as oxidant.

It was suggested that copper behaviour during precious metal leach tests could possibly inhibit gold dissolution. However, as shown in Section 4.3.4, leaching with gold foil alone (even with controlling pH, and feeding peroxide continuously), did not improve gold dissolution.

It is therefore concluded that leaching of gold from PCBs, using glycine alone, is not technically feasible.

4.4 Hydrometallurgical flowsheet

Figure 4.31 provides a suggested flowsheet for PCB leaching. This flowsheet is based on the experimental results for base and precious metal leaching, discussed in Section 4.2 and Section 4.3, respectively.

A two-stage base metal leach at identical conditions is suggested in Figure 4.31. The percentage extraction of base metals during each stage was provided in Table 4.4. Results from the bench-scale base metal leach tests showed that at a pH of 11 and pulp density of 25 g/L, 81% copper dissolution could be achieved after 22 hours, at 60°C, 1 M glycine, using pure oxygen as oxidant. However, in the small pilot-scale leach tests performed at the same conditions, two stages (each with a duration of 41 – 52 hours) were required to reach a similar extent of copper dissolution achieved in the bench-scale leach tests (74% – 81%). This suggests that the rate and extent of copper dissolution is highly dependent on the efficiency of oxygen mass transfer from the gaseous phase to the liquid phase. Optimisation of reactor configuration, agitation speed and flow rate of the gas is required to maximise the mass transfer efficiency of oxygen from the gaseous phase to the liquid phase. Additionally, the pH for each of the base metal leach stages should be controlled above 11, to avoid copper precipitation.

It was shown that gold leaching with glycine alone was not technically feasible. The addition of cyanide to glycine, could leach 38% of the gold in 96 hours, with 53% copper dissolution. Extraction of the other metals was provided in Table 4.7. Further optimisation of process variables such as temperature, oxidant type, copper content in the feed and lixiviant (NaCN and glycine) concentrations are required to maximise gold leaching.

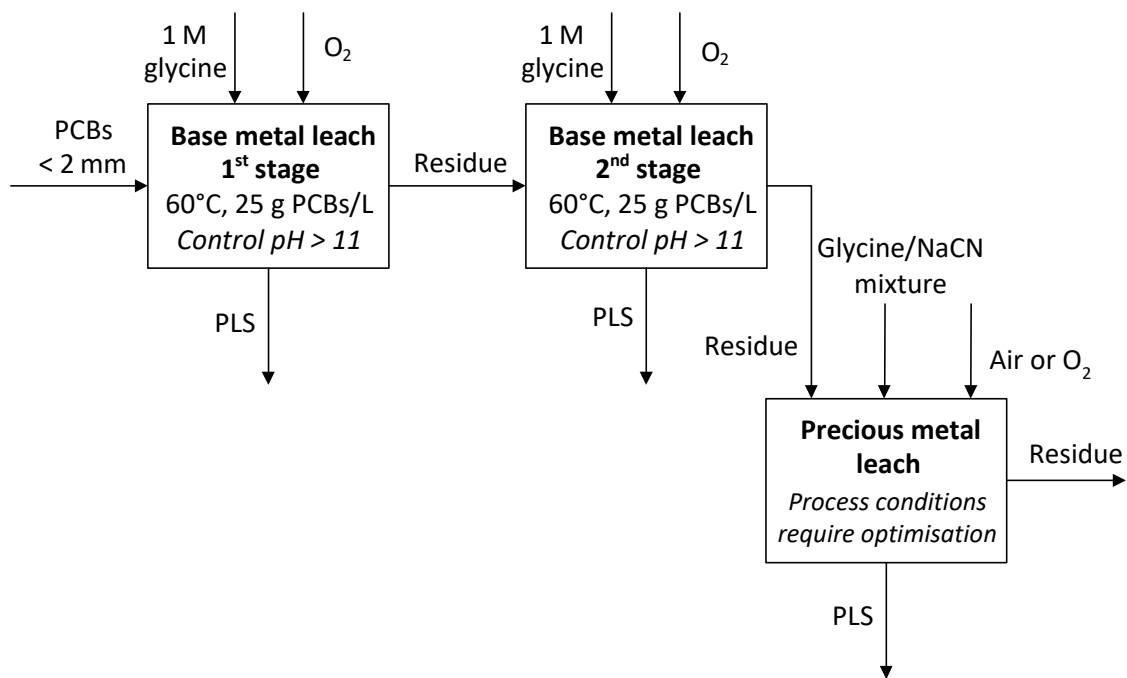


Figure 4.31. Flowsheet for base and precious metal leaching of PCB waste.

5. Conclusions and Recommendations

Conclusions are given according to the objectives provided in Section 1.3.

5.1 Base metal leaching

Results from preliminary base metal leach tests, performed at a pulp density of 100 g PCBs/L, suggested the presence of a solubility limit at copper concentrations of approximately 11.5 g/L, at 60°C and 4.5 M glycine. Further tests were conducted at a reduced pulp density of 25 g/L, such that complete copper extraction yields concentrations of approximately 5.8 g/L Cu.

Tests conducted according to an experimental design investigated the effect of temperature, glycine concentration and oxidant type on copper dissolution, at an initial pH of 11. For the tests performed using air as oxidant, copper dissolution was low initially, and independent of both temperature and glycine concentration during this period. It was shown that the initial lag in copper dissolution, at 1 M glycine, could be minimised by using pure oxygen as oxidant, instead of air. This suggested that the initial rate of copper dissolution in the air system was limited by oxygen diffusion through the solid-liquid boundary layer. As the reaction progressed, increasing both temperature (from 25°C to 60°C) and glycine concentration (from 1 M to 2 M), increased copper dissolution significantly in the presence of air. It was suggested that increasing temperature and glycine concentration increased the rate of CuO removal by CuL_2 formation, thereby decreasing the resistance to oxygen diffusion through the product layer to the reaction surface.

When pure oxygen was used as oxidant, increasing the temperature from 25°C to 60°C increased copper dissolution by approximately 50% at both glycine concentrations investigated. Increasing the glycine concentration above 1 M, in the presence of pure oxygen, had no effect on copper dissolution at all temperatures investigated. However, co-extraction of gold increased with increasing glycine concentration. Using hydrogen peroxide as oxidant, did not improve copper leaching relative to using pure oxygen.

Based on the experimental results, optimal conditions for maximum copper dissolution and minimum gold dissolution were determined to be 60°C, 1 M glycine, using O_2 as oxidant, at a pH of 11, and pulp density of 25 g/L. At these conditions, 81% copper dissolution was achieved

after 22 hours, with 1.3% co-extraction of gold. Small pilot-scale leach tests were performed at these optimal conditions to prepare the required feed for the precious metal leach tests.

5.2 Precious metal leaching

Precious metal leach tests conducted according to an experimental design showed less than 2% gold dissolution after 48 hours at all temperatures (60°C, 75°C), glycine concentrations (0.1 M, 0.5 M) and pH values (11.5, 12.5) investigated. Further tests showed extending the leaching time to 96 hours, increasing the temperature to 90°C and increasing the flowrate of hydrogen peroxide did not improve gold dissolution.

38% gold dissolution was achieved after 96 hours by adding cyanide to the glycine solution, at ambient temperature, with air as oxidant. It was concluded that gold was not physically entrapped in the PCBs.

Additional tests were performed on pure gold foil using glycine in the absence of cyanide. These tests aimed to determine whether copper behaviour during the glycine tests inhibited gold dissolution. Results from these tests showed negligible gold extraction after 96 hours, at 60°C, pH 12.5, 0.5 M glycine, with hydrogen peroxide as oxidant.

It was concluded that gold leaching with glycine alone is not technically feasible.

5.3 Suggested flowsheet

Based on the experimental results, a flowsheet was proposed for selective copper dissolution, followed by gold dissolution in a subsequent stage.

Results from the bench-scale base metal leach tests showed that at 81% copper dissolution could be achieved after 22 hours, at 60°C, 1 M glycine, using pure oxygen as oxidant, at an initial pH of 11 and pulp density of 25 g/L. However, in the small pilot-scale leach tests performed at the same conditions, two stages (each with a duration of 41 – 52 hours) were required to reach a similar extent of copper dissolution achieved in the bench-scale leach tests (74% – 81%). This large difference in leaching performance was attributed to better mass transfer of oxygen into solution in the bench-scale leach tests (working volume of 1 L), compared to the small pilot-scale leach tests (working volume of 17 L). Optimisation of reactor configuration, agitation speed and flow rate of the gas is required to maximise the mass transfer

efficiency of oxygen from the gaseous phase to the liquid phase. Additionally, it is recommended that the pH in the base metal leach stage be controlled above 11, in order to prevent copper precipitation.

In a subsequent leaching stage, 38% gold dissolution could be achieved after 96 hours, by adding 10 g/L glycine to 2 g/L NaCN. This could be achieved at ambient temperature, pH 11.5, using air as oxidant.

5.4 Recommendations

The solubility limit of copper in glycine solutions is not available in literature. A pulp density of 25 g PCBs/L was chosen for the base metal leach tests based on relatively limited information. This pulp density was low compared to pulp densities used in mineral acid leaching systems for metal recovery from PCBs. Further tests should be performed to experimentally determine the solubility limit at different conditions. This will aid in maximising the pulp density; therefore increasing the amount of feed material that can be leached at a given time.

Further investigation is required to determine the cause of the rapid decrease in pH at elevated temperatures, in the presence of pure oxygen. While it is suggested that the oxidation of metallic iron could contribute to the decrease in pH, the reason for the rapid decrease in pH observed in the presence of pure oxygen at 60°C, but not at 25°C or 40°C, is not well understood.

Experimental results showed that increasing the partial pressure of oxygen, and hence the oxygen concentration in the bulk solution, increased copper dissolution significantly. It is recommended that tests be performed to determine the optimal concentration of dissolved oxygen required to maximise copper leaching. Subsequent leaching tests should be performed by controlling the concentration of dissolved oxygen at the optimal level. Further leach tests are also required in order to gain a better understanding of the lag period observed in the presence of air, to investigate the autocatalytic reaction scheme, and to quantify oxygen mass transfer rates.

The behaviour of base metals, other than copper, is not well understood in the glycine system. The Pourbaix diagram generated for iron in a glycine system suggested that iron could

selectively be leached at reducing conditions, prior to copper dissolution. The Pourbaix diagrams also indicated that nickel and lead dissolution could be avoided during copper extraction, by increasing the Eh sufficiently. Further study is required to develop and optimise a process for selective recovery of these other base metals from PCBs.

The leaching of gold from PCBs using glycine alone has proven to be technically infeasible. However, it has been illustrated that a glycine-cyanide mixture shows potential for gold extraction. Decreasing the copper content in the feed to the precious metal leach stage is expected to lower the concentration of cyanide required (Oraby *et al.*, 2017). A reduced copper content can be achieved by improving the copper dissolution during the base metal leach stage. Further study is required to optimise process variables including temperature, glycine and cyanide concentration, copper content in the feed and oxidant type, in order to maximise glycine-cyanide leaching of gold from PCBs.

6. References

- Akcil, A., Erust, C., Gahan, C.S., Ozgun, M., Sahin, M. & Tuncuk, A., 2015. Precious metal recovery from waste printed circuit boards using cyanide and non-cyanide lixivants - A review. *Waste Management*, 45:258–271.
- Aksu, S. & Doyle, F.M., 2001. Electrochemistry of copper in aqueous glycine solutions. *Journal of The Electrochemical Society*, 148(1):51–57.
- Aksu, S., Wang, L. & Doyle, F.M., 2003. Effect of hydrogen peroxide on oxidation of copper in CMP slurries containing glycine. *Journal of The Electrochemical Society*, 150(11):718–723.
- Albertyn, P.W., 2017. *Ammonium thiosulphate leaching of gold from printed circuit board waste. MEng Thesis*. Stellenbosch University, South Africa.
- Araki, K. & Ozeki, T., 2003. Amino Acids. *Kirk-Othmer Encyclopedia of Chemical Technology*, 2:554–618.
- Aylmore, M.G., 2005. Alternative lixivants to cyanide for leaching gold ores. *Developments in Mineral Processing*, 15:501–539.
- Bard, A.J., Parsons, R. & Jordan, J., 1985. *Standard potentials in aqueous solution*. New York: Marcel Dekker, Inc.
- Bas, A.D., Deveci, H. & Yazici, E.Y., 2013. Bioleaching of copper from low grade scrap TV circuit boards using mesophilic bacteria. *Hydrometallurgy*, 138:65–70.
- Bas, A.D., Deveci, H. & Yazici, E.Y., 2014. Treatment of manufacturing scrap TV boards by nitric acid leaching. *Separation and Purification Technology*, 130(2):151–159.
- Behnamfard, A., Salarirad, M.M. & Veglio, F., 2013. Process development for recovery of copper and precious metals from waste printed circuit boards with emphasize on palladium and gold leaching and precipitation. *Waste Management*, 33(11):2354–2363.

- Berger, P., Karpel Vel Leitner, N., Doré, M. & Legube, B., 1999. Ozone and hydroxyl radicals induced oxidation of glycine. *Water Research*, 33(2):433–441.
- Birloaga, I., Coman, V., Kopacek, B. & Veglio, F., 2014. An advanced study on the hydrometallurgical processing of waste computer printed circuit boards to extract their valuable content of metals. *Waste Management*, 34(12):2581–2586.
- Birloaga, I., De Michelis, I., Ferella, F., Buzatu, M. & Veglio, F., 2013. Study on the influence of various factors in the hydrometallurgical processing of waste printed circuit boards for copper and gold recovery. *Waste Management*, 33(4):935–941.
- Brandl, H., Bosshard, R. & Wegmann, M., 2001. Computer-munching microbes: Metal leaching from electronic scrap by bacteria and fungi. *Hydrometallurgy*, 59:319–326.
- Camelino, S., Rao, J., López, R. & Lucci, R., 2015. Initial studies about gold leaching from printed circuit boards of waste cell phones. *Procedia Materials Science*, 9:105–112.
- Chandra, I. & Jeffrey, M.I., 2004. An electrochemical study of the effect of additives and electrolyte on the dissolution of gold in thiosulfate solutions. *Hydrometallurgy*, 73:305–312.
- Chatterjee, S. & Kumar, K., 2009. Effective electronic waste management and recycling process involving formal and non-formal sectors. *International Journal of Physical Sciences*, 4(13):893–905.
- Choi, C., 2008. *Kinetic study of copper chemistry in chemical mechanical polishing (CMP) by an in-situ real time measurement technique*. PhD Diss. Iowa State University, USA.
- Cui, H. & Anderson, C.G., 2016. Literature Review of Hydrometallurgical Recycling of Printed Circuit Boards (PCBs). *Journal of Advanced Chemical Engineering*, 6(1):1–11.
- Cui, J. & Forssberg, E., 2003. Mechanical recycling of waste electric and electronic equipment: a review. *Journal of Hazardous Materials*, 99(3):243–263.
- Cui, J. & Zhang, L., 2008. Metallurgical recovery of metals from electronic waste: A review. *Journal of Hazardous Materials*, 158:228–256.

- Das, A., Vidyadhar, A. & Mehrotra, S.P., 2009. A novel flowsheet for the recovery of metal values from waste printed circuit boards. *Resources, Conservation and Recycling*, 53(8):464–469.
- Deveci, H., Yazici, E.Y., Aydin, U., Yazici, R. & Akcil, A., 2010. Extraction of copper from scrap tv boards by sulphuric acid leaching under oxidising conditions. In: *Going Green - Care Innovation*. 2010, 8–11.
- Du, T., Luo, Y. & Desai, V., 2004a. The combinatorial effect of complexing agent and inhibitor on chemical-mechanical planarization of copper. *Microelectronic Engineering*, 71(1):90–97.
- Du, T., Vijayakumar, A. & Desai, V., 2004b. Effect of hydrogen peroxide on oxidation of copper in CMP slurries containing glycine and Cu ions. *Electrochimica Acta*, 49(25):4505–4512.
- EAG Laboratories, 2017. *EAG Laboratories*. [Online]. 2017. Available from: <http://www.eag.com/icp-oes-and-icp-ms-detection-limit-guidance/>. [Accessed: 1 April 2017].
- Eksteen, J.J. & Oraby, E.A., 2014. *A process for copper and/or precious metal recovery, Patent No. WO2015/031943A1*.
- Eksteen, J.J. & Oraby, E.A., 2015. The leaching and adsorption of gold using low concentration amino acids and hydrogen peroxide: Effect of catalytic ions, sulphide minerals and amino acid type. *Minerals Engineering*, 70:36–42.
- Eksteen, J.J. & Oraby, E.A., 2016. *Process for selective recovery of chalcophile group elements, Patent No. WO2016/141438 A1*.
- Eksteen, J.J., Oraby, E.A. & Tanda, B.C., 2017a. A conceptual process for copper extraction from chalcopyrite in alkaline glycinate solutions. *Minerals Engineering*, 108:53–66.
- Eksteen, J.J., Oraby, E.A., Tanda, B.C., Tauetsile, P.J., Bezuidenhout, G.A., Newton, T., Trask, F. & Bryan, I., 2017b. Towards industrial implementation of glycine based leach adsorption technologies for gold-copper ores. In: *7th International World Gold*

- Conference*. 2017, Vancouver, Canada.
- Eswaraiyah, C., Kavitha, T., Vidyasagar, S. & Narayanan, S.S., 2008. Classification of metals and plastics from printed circuit boards (PCB) using air classifier. *Chemical Engineering and Processing: Process Intensification*, 47(4):565–576.
- Ficeriova, J., Balaz, P. & Gock, E., 2011. Leaching of gold, silver and accompanying metals from circuit boards (PCBs) waste. *Acta Montanistica Slovaca*, 16(2):128–131.
- Ganzha, S. V., Maksimova, S.N., Grushevskaya, S.N. & Vvedenskii, A. V., 2011. Formation of oxides on copper in alkaline solution and their photoelectrochemical properties. *Protection of Metals and Physical Chemistry of Surfaces*, 47(2):191–202.
- Garret, R.H. & Grisham, C.M., 2012. *Biochemistry*. 5th Ed. Canada: Cengage Learning.
- Ghosh, B., Ghosh, M.K., Parhi, P., Mukherjee, P.S. & Mishra, B.K., 2015. Waste Printed Circuit Boards recycling: An extensive assessment of current status. *Journal of Cleaner Production*, 94:5–19.
- Gorantla, V.R.K., Matijevic, E. & Babu, S.V., 2005. Amino acids as complexing agents in chemical - mechanical planarization of copper. *Chemistry of Materials*, 17(8):2076–2080.
- Guo, C., Wang, H., Liang, W., Fu, J. & Yi, X., 2011. Liberation characteristic and physical separation of printed circuit board (PCB). *Waste Management*, 31(9–10):2161–2166.
- Gupta, C.K., 2003. *Chemical Metallurgy: Principles and Practice*. Weinheim, Germany: Wiley-VCH.
- Habashi, F., 1963. Kinetics and mechanism of copper dissolution in aqueous ammonia. *Journal of the German Bunsen Society for Physical Chemistry*, 67(4):402–406.
- Hagelucken, C., 2006. Improving metal returns and eco-efficiency in electronics recycling. In: *Proceedings of the 2006 IEEE International Symposium on Electronics and the Environment*. 2006, 218–223.
- Halpern, J., Milants, H. & Wiles, D.R., 1959. Kinetics of the dissolution of copper in oxygen-

- containing solutions of various chelating agents. *Journal of The Electrochemical Society*, 106(8):647–650.
- Hariharaputhiran, M., Zhang, J., Ramarajan, S., Keleher, J.J., Li, Y. & Babu, S.V., 2000. Hydroxyl radical formation in H₂O₂ -amino acid mixtures and chemical mechanical polishing of copper. *Journal of The Electrochemical Society*, 147(10):3820–3826.
- Havlík, T., 2008. *Hydrometallurgy: principles and applications*. Cambridge, England: Woodhead Publishing Limited.
- He, W., Li, G., Ma, X., Wang, H., Huang, J., Xu, M. & Huang, C., 2006. WEEE recovery strategies and the WEEE treatment status in China. *Journal of Hazardous Materials*, 136(3):502–512.
- Hilson, G. & Monhemius, A.J., 2006. Alternatives to cyanide in the gold mining industry: what prospects for the future? *Journal of Cleaner Production*, 14:1158–1167.
- Huang, J., Chen, M., Chen, H., Chen, S. & Sun, Q., 2014. Leaching behavior of copper from waste printed circuit boards with Brønsted acidic ionic liquid. *Waste Management*, 34(2):483–488.
- Ihnfeldt, R. & Talbot, J.B., 2008. Effect of CMP slurry chemistry on copper nanohardness. *Journal of The Electrochemical Society*, 155(6):412–420.
- Ilyas, S., Anwar, M.A., Niazi, S.B. & Afzal Ghauri, M., 2007. Bioleaching of metals from electronic scrap by moderately thermophilic acidophilic bacteria. *Hydrometallurgy*, 88(1–4):180–188.
- Jackson, E., 1986. *Hydrometallurgical extraction and reclamation*. West Sussex: Ellis Horwood Limited.
- Kaksonen, A.H., Mudunuru, B.M. & Hackl, R., 2014. The role of microorganisms in gold processing and recovery - A review. *Hydrometallurgy*, 142:70–83.
- Kaya, M., 2016. Recovery of metals from electronic waste by physical and chemical recycling processes. *International Journal of Chemical, Molecular, Nuclear, Materials and*

Metallurgical Engineering, 10(2):232–243.

Kemcore, 2017. *Kemcore - leaching chemicals*. [Online]. 2017. Available from: <http://www.kemcore.com/leaching-chemicals.html>. [Accessed: 26 September 2017].

Korobushkina, E.D., Karavaiko, G.I. & Korobushkin, I.M., 1983. Biochemistry of gold. *Environmental Biogeochemistry*, 35:325–333.

Kumar, M., Lee, J., Kim, M., Jeong, J. & Yoo, K., 2014. Leaching of metals from waste printed circuit boards (WPCBs) using sulfuric and nitric acids. *Environmental Engineering and Management Journal*, 13(10):2601–2607.

Lee, C., Tang, L. & Popuri, S.R., 2011. A study on the recycling of scrap integrated circuits by leaching. *Waste Management and Research*, 29(7):677–685.

Lehninger, A.L., 1988. *Principles of biochemistry*. New York: Worth Publishers, Inc.

Levenspiel, O., 1999. *Chemical reaction engineering*. 3rd Ed. New York, USA: John Wiley and Sons.

Liao, C., Guo, D., Wen, S. & Luo, J., 2012. Effects of chemical additives of CMP slurry on surface mechanical characteristics and material removal of copper. *Tribology Letters*, 45(2):309–317.

Lu, B.C.Y. & Graydon, W.F., 1955. Rates of Copper Dissolution in Aqueous Ammonium Hydroxide Solutions. *Journal of the American Chemical Society*, 77(23):6136–6139.

Lu, J., Garland, J.E., Pettit, C.M., Babu, S. V. & Roy, D., 2004. Relative roles of H₂O₂ and glycine in CMP of copper studied with impedance spectroscopy. *Journal of The Electrochemical Society*, 151(10):717–722.

Luo, Y., 2004. *Slurry chemistry effects on copper chemical mechanical planarization*. University of Central Florida, USA.

Martell, A.E. & Smith, R.M., 1974. *Critical stability constants Vol 1: Amino acids*. New York, USA: Plenum Press.

- Mecucci, A. & Scott, K., 2002. Leaching and electrochemical recovery of copper, lead and tin from scrap printed circuit boards. *Journal of Chemical Technology and Biotechnology*, 77(4):449–457.
- Morioka, S. & Shimakage, K., 1971. Studies on the ammonia pressure leaching of metallic nickel and copper powders. *Transactions of the Japan Institute of Metals*, 12(3):197–205.
- Moyo, T., Petersen, J., Franzidis, J.-P. & Nicol, M., 2015. An electrochemical study of the dissolution of chalcopyrite in ammonia–ammonium sulphate solutions. *Canadian Metallurgical Quarterly*, 54(3):269–278.
- Muzawazi, C., 2013. *Base metal heap and tank leaching of a Platreef flotation concentrate using ammonical solutions*. 40–90.
- Narita, E., Lawson, F. & Han, K.N., 1983. Solubility of oxygen in aqueous electrolyte solutions. *Hydrometallurgy*, 10:21–37.
- Nguyen, H.H., Tran, T. & Wong, P.L.M., 1997. Copper interaction during the dissolution of gold. *Minerals Engineering*, 10(5):491–505.
- Nicol, M.J., 1975. Electrochemical investigation of the dissolution of copper, nickel, and copper-nickel alloys in ammonium carbonate solutions. *Journal of The South African Institute of Mining and Metallurgy*, 75(11):291–302.
- Ogunniyi, I.O. & Vermaak, M.K.G., 2009. Froth flotation for beneficiation of printed circuit boards comminution fines: an overview. *Mineral Processing and Extractive Metallurgy Review*, 30(2):101–121.
- Ogunniyi, I.O., Vermaak, M.K.G. & Groot, D.R., 2009. Chemical composition and liberation characterization of printed circuit board comminution fines for beneficiation investigations. *Waste Management*, 29(7):2140–2146.
- Oraby, E.A. & Eksteen, J.J., 2014. The selective leaching of copper from a gold-copper concentrate in glycine solutions. *Hydrometallurgy*, 150:14–19.
- Oraby, E.A. & Eksteen, J.J., 2015a. The leaching of gold, silver and their alloys in alkaline

- glycine-peroxide solutions and their adsorption on carbon. *Hydrometallurgy*, 152:199–203.
- Oraby, E.A. & Eksteen, J.J., 2015b. Gold leaching in cyanide-starved copper solutions in the presence of glycine. *Hydrometallurgy*, 156:81–88.
- Oraby, E.A. & Eksteen, J.J., 2016. The use of glycine in the recovery of precious metals from e-waste. *ALTA 2016*. Perth, Aus.
- Oraby, E.A., Eksteen, J.J. & Tanda, B.C., 2017. Gold and copper leaching from gold-copper ores and concentrates using a synergistic lixiviant mixture of glycine and cyanide. *Hydrometallurgy*, 169:339–345.
- Ozmetin, C., Copur, M., Yartasi, A. & Kocakerim, M.M., 1998. Kinetic Investigation of Reaction between Metallic Silver and Nitric Acid Solutions in the Range 7 . 22 - 14 . 44 M. *Industrial & Engineering Chemistry Research*, 37:4641–4645.
- Park, Y.J. & Fray, D.J., 2009. Recovery of high purity precious metals from printed circuit boards. *Journal of Hazardous Materials*, 164:1152–1158.
- Petter, P.M.H., Veit, H.M. & Bernardes, A.M., 2014. Evaluation of gold and silver leaching from printed circuit board of cellphones. *Waste Management*, 34(2):475–482.
- Pyun, S.-I. & Moon, S.-M., 2000. Corrosion mechanism of pure aluminium in aqueous alkaline solution. *Journal of Solid State Electrochemistry*, 4(5):267–272.
- Quan, C., Li, A. & Gao, N., 2012. Study on characteristics of printed circuit board liberation and its crushed products. *Waste Management & Research*, 30(11):1178–1186.
- Quinet, P., Proost, J. & Van Lierde, A., 2005. Recovery of precious metals from electronic scrap by hydrometallurgical processing routes. *Minerals and Metallurgical Processing*, 22(1):17–22.
- Rossouw, W.A., 2015. *Effect of mechanical pre-treatment on leaching of base metals from waste printed circuit boards*. MEng Thesis. Stellenbosch University, South Africa.

- Le Solleu, J. P., 2010. Sliding contacts on printed circuit boards and wear behavior wear behavior. *European Physical Journal: Applied Physics, EDP Sciences*, 50(1).
- Stewart, M. & Kappes, D., 2012. SART for copper control in cyanide heap leaching. *Journal of the Southern African Institute of Mining and Metallurgy*, 112(12):1037–1043.
- Tanda, B.C., Oraby, E.A. & Eksteen, J.J., 2017a. An investigation into the leaching behaviour of copper oxide minerals in aqueous alkaline glycine solutions. *Hydrometallurgy*, 167:153–162.
- Tanda, B.C., Oraby, E.A. & Eksteen, J.J., 2017b. Recovery of Copper from Alkaline Glycine Leach Solution using Solvent Extraction. *Separation and Purification Technology*,
- Tsydenova, O. & Bengtsson, M., 2011. Chemical hazards associated with treatment of waste electrical and electronic equipment. *Waste Management*, 31(1):45–58.
- Tuncuk, A., Stazi, V., Akcil, A., Yazici, E.Y. & Deveci, H., 2012. Aqueous metal recovery techniques from e-scrap: Hydrometallurgy in recycling. *Minerals Engineering*, 25(1):28–37.
- Uyemura International, 2017. *Direct immersion gold as a final finish*. [Online]. 2017. Available from: <http://www.uyemura.com/direct-immersion-gold-as-a-final-finish.htm>. [Accessed: 10 September 2017].
- Vijayaram, R., Nesakumar, D. & Chandramohan, K., 2013. Copper extraction from the discarded printed circuit boards by leaching. *Research Journal of Engineering Sciences*, 2(1):11–14.
- Wadsworth, M.E. & Zhu, X., 2003. Kinetics of enhanced gold dissolution: activation by dissolved silver. *International Journal of Mineral Processing*, 72:301–310.
- Wang, L. & Doyle, F.M., 2003. Mechanisms of passivation of copper in CMP Slurries containing peroxide and glycine. In: *Materials Research Society Symposium Proceedings*. 2003, 1–10.
- Xing, W., Yin, M., Lv, Q., Hu, Y., Liu, C. & Zhang, J., 2014. Oxygen solubility, diffusion

- coefficient, and solution viscosity. In: *Rotating Electrode Methods and Oxygen Reduction Electrocatalysts*. Oxford, UK: Elsevier, 1–31.
- Yang, H., Liu, J. & Yang, J., 2011. Leaching copper from shredded particles of waste printed circuit boards. *Journal of Hazardous Materials*, 187:393–400.
- Yazici, E. & Deveci, H., 2010. Factors affecting decomposition of hydrogen peroxide. In: *Proceedings of the 12th international mineral processing symposium*. 2010, 609–616.
- Yoo, J.M., Jeong, J., Yoo, K., Lee, J. & Kim, W., 2009. Enrichment of the metallic components from waste printed circuit boards by a mechanical separation process using a stamp mill. *Waste Management*, 29(3):1132–1137.
- Zhang, J., Lu, J., Zhai, J. & Yang, F., 1997. Simulating experiments on enrichment of gold by bacteria and their geochemical significance. *Chinese Journal of Geochemistry*, 16(4):369–373.
- Zhang, S. & Forssberg, E., 1997. Mechanical separation-oriented characterization of electronic scrap. *Resources, Conservation and Recycling*, 21(4):247–269.
- Zhang, Y., Liu, S., Xie, H., Zeng, X. & Li, J., 2012. Current status on leaching precious metals from waste printed circuit boards. *Procedia Environmental Sciences*, 16:560–568.
- Zhao, Y., Wen, X., Li, B. & Tao, D., 2004. Recovery of copper from waste printed circuit boards. *Minerals and Metallurgical Processing*, 21(2):99–102.

Appendix A: Supplementary material

The stoichiometric concentration of glycine required to leach all base metals at a specific pulp density, was based on the average metal content of 3 samples, determined by aqua regia digestion (refer to Table 4.1). The overall reaction for glycine leaching of copper in the presence of oxygen (Equation 2.17) and hydrogen peroxide (Equation 2.18), shows that 2 moles of glycine is required for every mole of copper. It is assumed that this stoichiometric relationship also applies to the other base metals – in Table 2.7 it was shown that for Fe, Ni, Pb and Zn, the ML_2 complex (i.e. 2 moles of glycine for every mole of metal, M) is the most stable. It is not known whether Al or Sn form glycine-complexes, however a 2:1 ratio of Gly:Metal was also assumed for Al and Sn.

In Table A.1 it can be seen that the stoichiometric concentration of glycine required for complete base metal dissolution, is 1.3 M and 0.32 M for pulp densities of 100 g/L and 25 g/L respectively.

Table A.1. Metal content in the feed to base metal leach tests, with corresponding stoichiometric glycine concentration, at pulp densities of 100 g/L and 25 g/L.

			100 g PCBs/L		25 g PCBs/L	
	wt% of PCB	MW	Amount of metal in feed per litre solution		Amount of metal in feed per litre solution	
		g/mol	g/L	mol/L	g/L	mol/L
Al	3.57	26.98	3.57	0.132	0.89	0.033
Cu	23.27	63.55	23.27	0.366	5.82	0.092
Fe	2.44	55.85	2.44	0.044	0.61	0.011
Ni	0.47	58.69	0.47	0.008	0.12	0.002
Pb	1.42	207.20	1.42	0.007	0.36	0.002
Sn	4.48	118.71	4.48	0.038	1.12	0.009
Zn	2.43	65.38	2.43	0.037	0.61	0.009
Total	38.08		38.08	0.632	9.519	0.158
<i>Stoichiometric glycine conc.</i>				<i>[Gly] = 1.3 M</i>		<i>[Gly] = 0.32 M</i>

Appendix B: PCB Characterisation

B.1 Acid digestion results

For each digestion method (A, B and C), 3 samples were digested, each with a mass of 20 g.

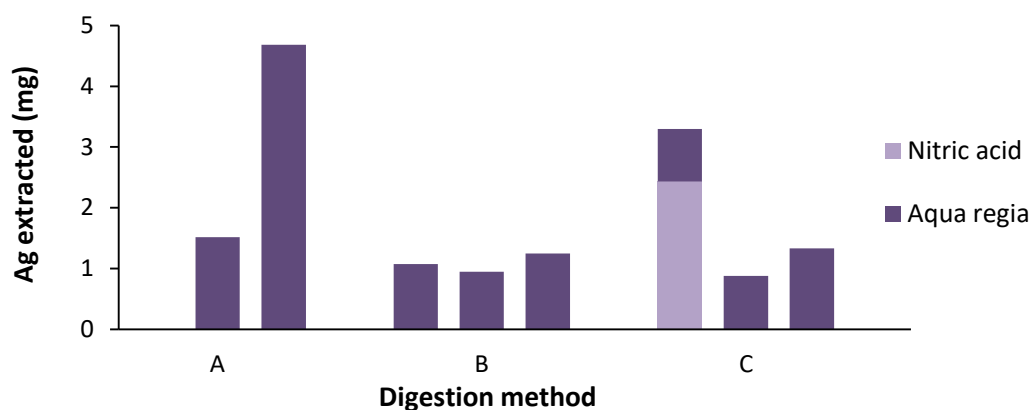


Figure B.1. Ag extraction from 20 g PCB samples, using: (A) Aqua regia only, (B) 55 wt% HNO_3 followed by aqua regia, (C) 30 wt% HNO_3 followed by aqua regia.

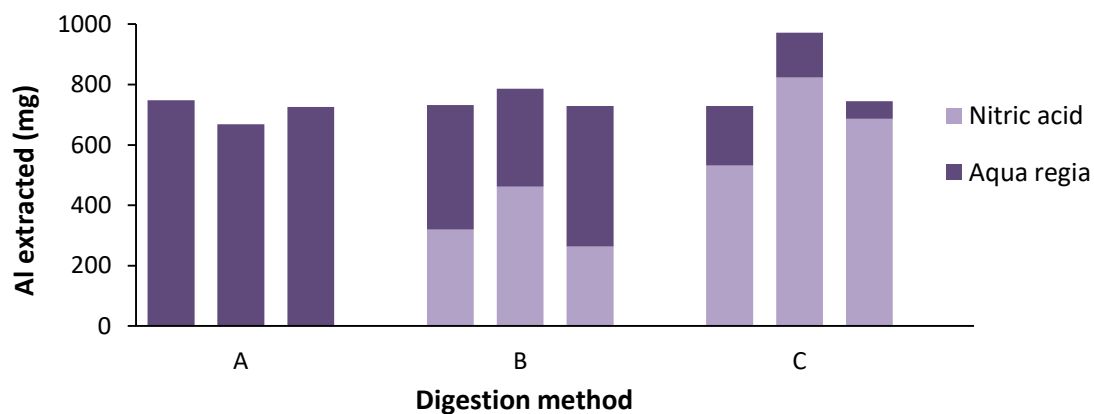


Figure B.2. Al extraction from 20 g PCB samples, using: (A) Aqua regia only, (B) 55 wt% HNO_3 followed by aqua regia, (C) 30 wt% HNO_3 followed by aqua regia.

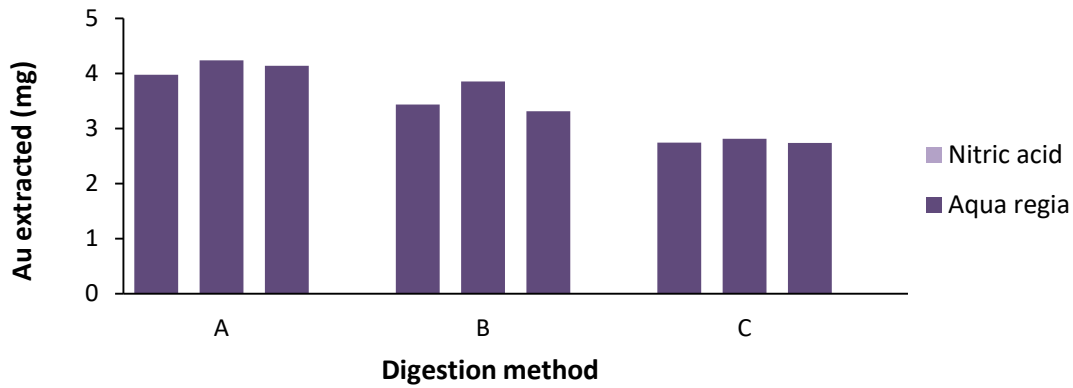


Figure B.3. Au extraction from 20 g PCB samples, using: (A) Aqua regia only, (B) 55 wt% HNO₃ followed by aqua regia, (C) 30 wt% HNO₃ followed by aqua regia.

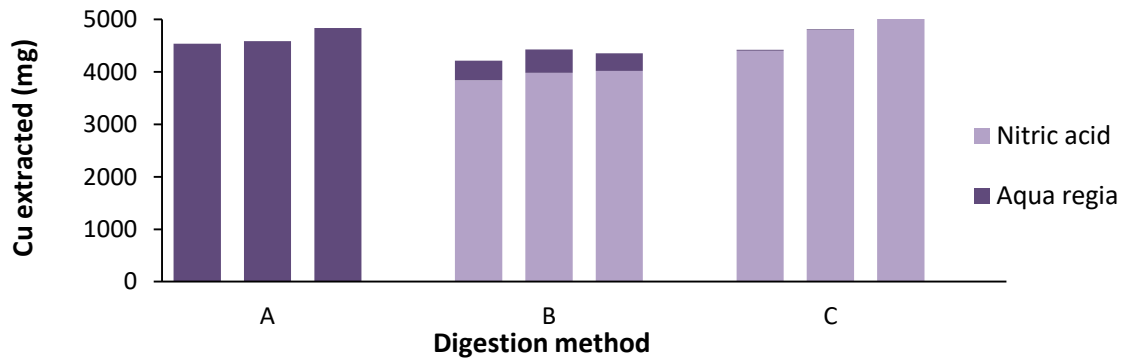


Figure B.4. Cu extraction from 20 g PCB samples, using: (A) Aqua regia only, (B) 55 wt% HNO₃ followed by aqua regia, (C) 30 wt% HNO₃ followed by aqua regia.

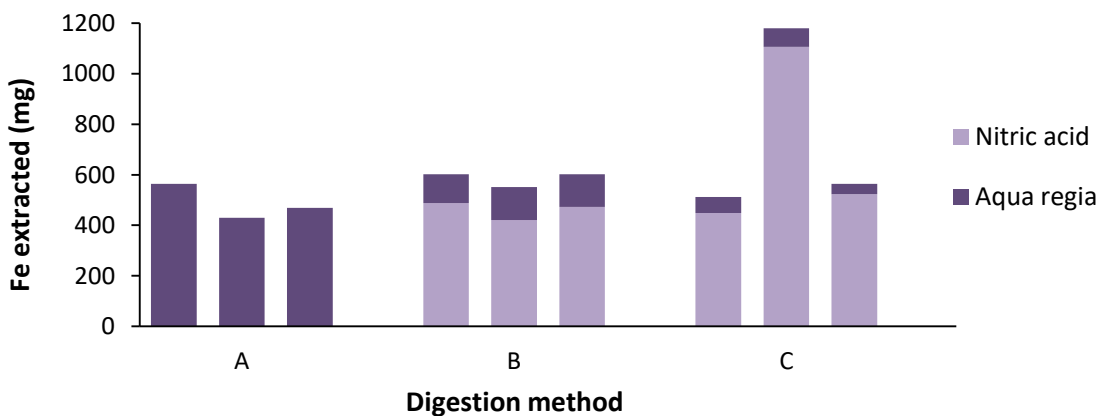


Figure B.5. Fe extraction from 20 g PCB samples, using: (A) Aqua regia only, (B) 55 wt% HNO₃ followed by aqua regia, (C) 30 wt% HNO₃ followed by aqua regia.

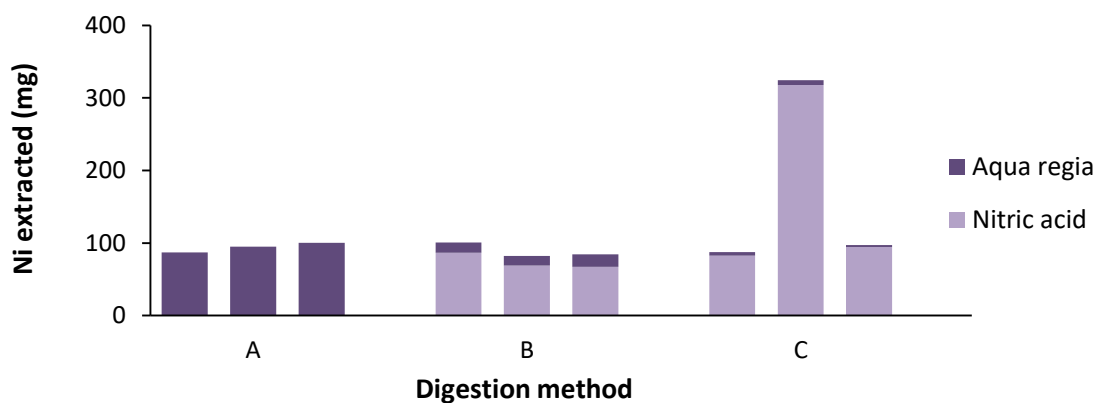


Figure B.6. Ni extraction from 20 g PCB samples, using: (A) Aqua regia only, (B) 55 wt% HNO_3 followed by aqua regia, (C) 30 wt% HNO_3 followed by aqua regia.

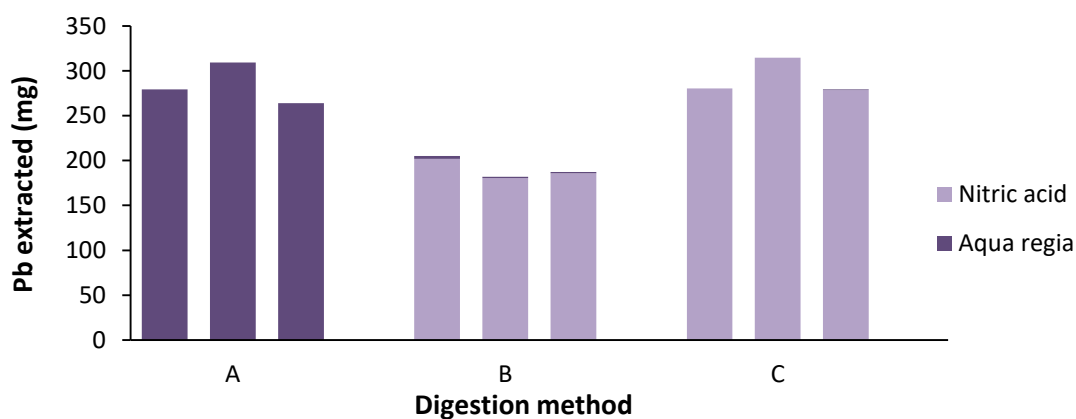


Figure B.7. Pb extraction from 20 g PCB samples, using: (A) Aqua regia only, (B) 55 wt% HNO_3 followed by aqua regia, (C) 30 wt% HNO_3 followed by aqua regia.

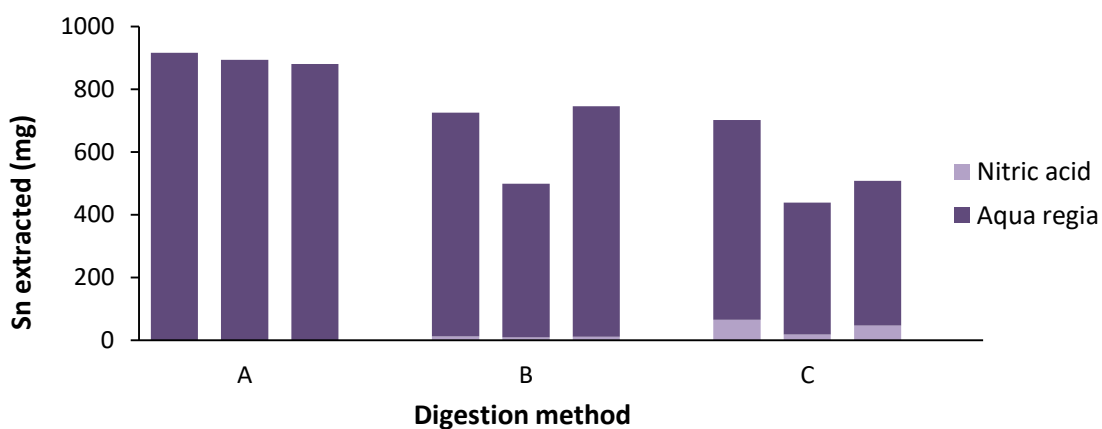


Figure B.8. Sn extraction from 20 g PCB samples, using: (A) Aqua regia only, (B) 55 wt% HNO_3 followed by aqua regia, (C) 30 wt% HNO_3 followed by aqua regia.

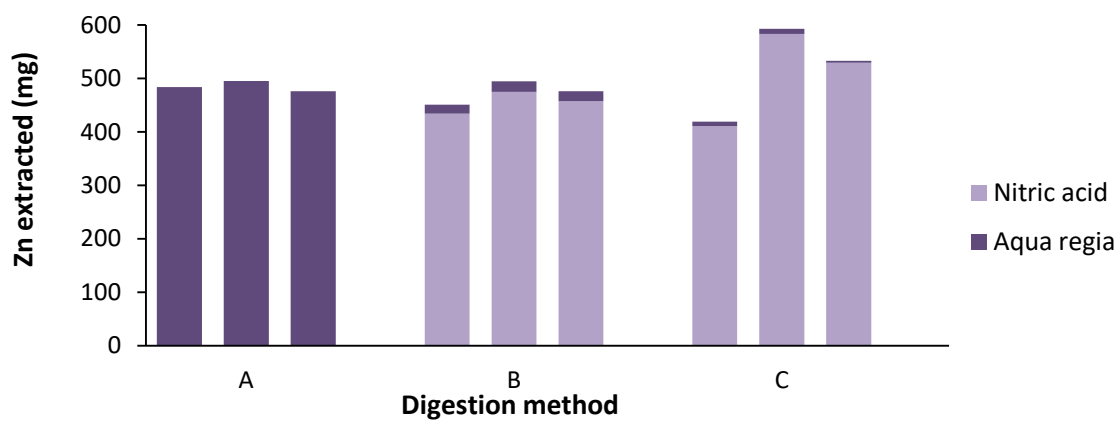
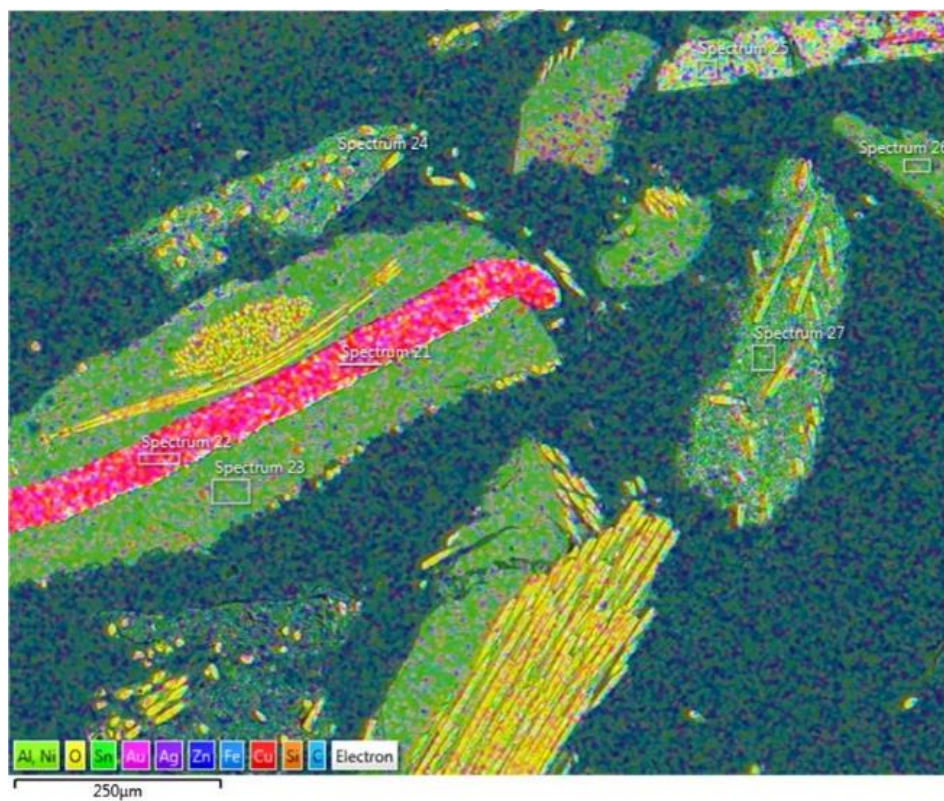
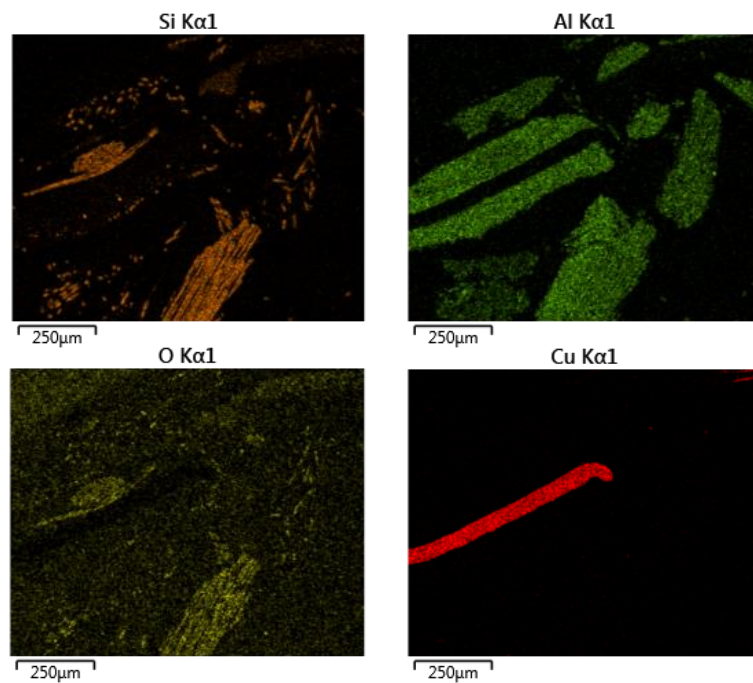


Figure B.9. Zn extraction from 20 g PCB samples, using: (A) Aqua regia only, (B) 55 wt% HNO₃ followed by aqua regia, (C) 30 wt% HNO₃ followed by aqua regia.

B.2 SEM Images



(a)



(b)

Figure B.10. SEM image of fresh feed showing incomplete liberation of copper from non-metallic material: (a) EDS layered map (b) Individual element maps for Si, Al, O and Cu.

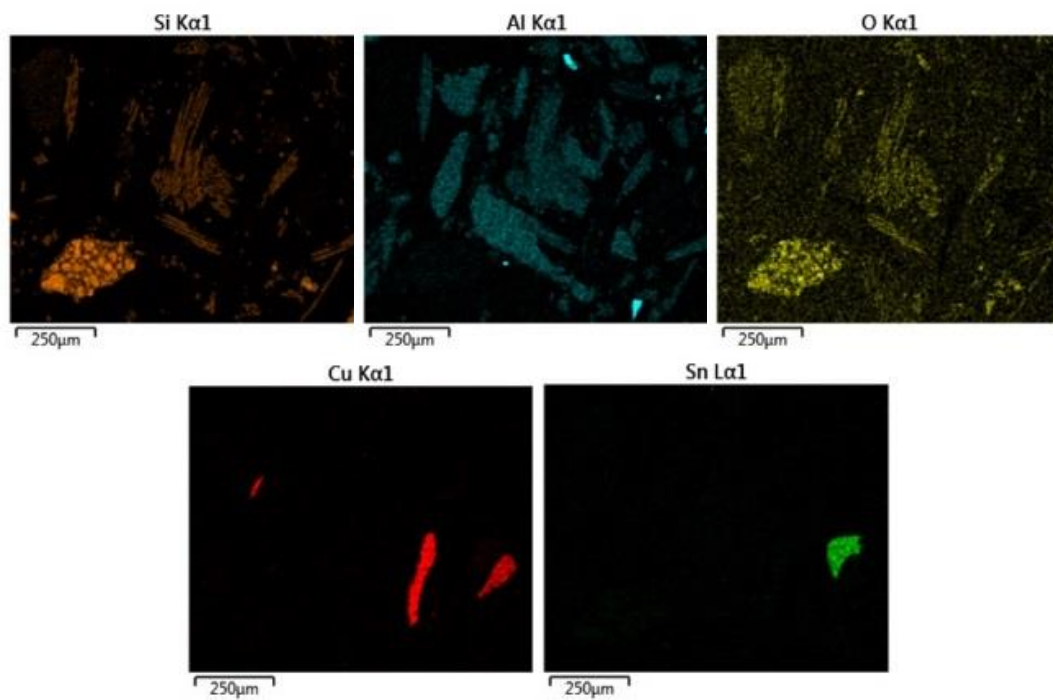
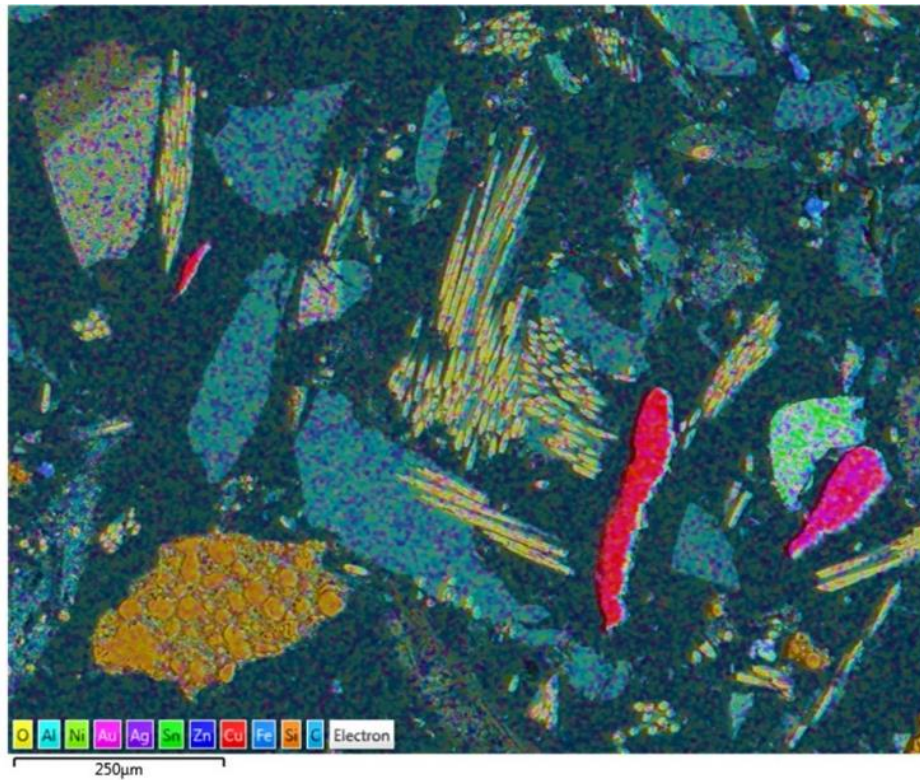


Figure B.11. SEM image of fresh feed showing almost complete liberation of copper from non-metallic material: (a) EDS layered map (b) Individual element maps for Si, Al, O, Cu and Si

Appendix C: Experimental data

C.1 Base metal leach tests

C.1.1 Preliminary tests

Table C.1. Copper concentration and mass extracted during preliminary tests at $t = 24$ hours

Test	Cu (g/L)	Volume	Cu (g)
1a	4.09	0.98	4.01
1b	7.64	1.00	7.64
1c	9.74	0.90	8.72
1d	11.87	0.97	11.51

C.1.2 Experimental design

The volume was kept constant during these tests, by adding water to the system after each sample was taken, to replace the volume removed during sampling.

Table C.2. ICP results for test 2a.

t (h)	Concentration (mg/L)							Volume (L)
	Al	Cu	Fe	Ni	Pb	Sn	Zn	
0.1	0.0	0.0	5.5	0.0	0.0	0.0	0.0	(kept constant)
1.0	6.7	17.5	6.9	0.0	3.9	0.0	0.0	
2.0	49.1	38.0	23.0	0.0	8.5	0.0	4.2	
3.0	190.9	127.8	109.7	0.0	30.0	18.0	9.6	
5.0	135.1	120.5	96.0	0.0	38.9	12.5	5.7	
8.0	166.3	226.2	110.6	5.8	65.6	14.6	8.8	
22.4	173.3	677.1	97.2	13.6	98.9	16.3	33.2	
32.8	97.2	979.2	49.4	15.6	92.1	10.9	52.4	
46.3	94.4	1294.3	66.7	17.3	104.8	14.3	81.3	
55.8	94.3	1506.4	69.0	18.8	110.6	15.8	99.2	
70.6	67.1	1695.3	56.5	20.6	107.3	18.8	121.0	
79.8	30.0	1847.1	24.4	19.5	63.4	12.6	109.6	
96.8	37.4	2051.6	31.2	21.0	67.6	12.9	146.7	
Aqua regia	3089.1	17353.4	2593.9	507.6	889.9	5024.9	1861.7	

Table C.3. ICP results for test 2b.

t (hr)	Concentration (mg/L)							Volume (L)
	Al	Cu	Fe	Ni	Pb	Sn	Zn	
0.1	16.3	21.7	7.3	0.0	5.7	0.0	0.0	1.010 (kept constant)
1.0	81.9	47.6	27.2	0.0	13.8	11.6	5.0	
2.0	129.8	71.1	62.2	0.0	33.1	19.3	5.5	
3.0	168.8	117.2	76.4	0.0	54.8	22.1	6.8	
5.0	222.9	287.7	43.4	7.7	77.0	19.1	10.8	
8.0	269.5	596.6	41.8	13.5	101.7	20.2	35.9	
22.4	194.6	1893.4	19.9	22.2	112.9	12.7	214.6	
32.8	142.7	2685.7	16.0	25.7	128.2	11.6	353.8	
46.3	100.7	3396.4	15.4	28.6	136.9	13.8	482.9	
55.8	89.9	3807.2	8.2	28.2	113.8	14.0	518.8	
70.6	91.0	3742.1	15.9	25.9	124.1	20.6	496.4	
Aqua regia	6435.8	14356.3	4241.8	753.9	1416.5	9501.3	713.6	

Table C.4. ICP results for test 2c.

t (hr)	Concentration (mg/L)							Volume (L)
	Al	Cu	Fe	Ni	Pb	Sn	Zn	
0.5	168.5	63.7	17.0	0	5.2	19.4	14.4	1.030 (kept constant)
1.0	221.6	46.9	6.1	0	0	19.2	4.7	
2.0	278.1	76.4	4.6	0	0	26.7	5.1	
3.0	292.1	106.4	3.2	0	0	27.0	5.8	
5.0	312.4	235.5	0	3.6	0	25.4	6.8	
8.0	314.7	513.7	0	6.7	0	28.0	17.4	
22.3	321.5	1986.5	0	13.5	8.1	36.8	157.3	
31.8	324.6	2759.1	0	15.6	22.2	48.6	256.9	
46.3	292.9	3440.1	3.7	18.4	34.5	63.1	319.4	
55.7	285.5	3475.5	4.2	18.3	45.7	75.3	319.2	
71.8	110.6	3522.3	4.6	18.8	33.1	12.6	193.7	
80.0	56.2	3373.2	3.6	18.4	32.2	3.3	165.4	
99.8	89.9	3264.5	4.6	18.6	44.6	10.5	187.5	
Aqua regia	1298.7	10643.7	2261.6	461.3	976.2	4472.5	1329.1	0.193

Table C.5. ICP results for test 2d.

t (hr)	Concentration (mg/L)							Volume (L)
	Al	Cu	Fe	Ni	Pb	Sn	Zn	
0.2	10.3	26.0	112.3	0	12.3	0	15.1	1.0138 (kept constant)
1.0	31.3	38.6	16.0	0	22.8	4.4	10.8	
2.0	47.8	51.6	35.0	0	16.7	7.0	12.5	
3.0	58.3	63.6	59.3	0	14.1	9.0	12.7	
5.0	152.1	110.0	151.1	0	24.5	26.1	5.7	
8.0	114.8	244.4	180.0	3.1	118.1	18.5	15.4	
22.0	126.7	1080.9	198.1	13.9	156.0	21.7	79.7	
32.0	115.8	1712.7	189.1	18.5	154.7	23.5	154.5	
46.0	121.3	2473.3	189.9	24.4	155.2	27.3	271.4	
56.0	53.0	2911.2	171.8	25.5	159.5	24.3	349.3	
72.0	148.1	3283.3	188.6	27.1	193.3	33.5	415.6	
80.0	41.6	3755.8	171.7	30.3	205.9	29.4	481.9	
96.3	34.8	3699.5	156.4	28.4	192.4	29.7	471.9	
Aqua regia	1405.5	10748.1	2177.2	393.8	584.1	5282.9	630.9	

Table C.6. ICP results for test 2e.

t (hr)	Concentration (mg/L)							Volume (L)
	Al	Cu	Fe	Ni	Pb	Sn	Zn	
0.2	14.5	27.8	6.9	0	35.7	4.0	7.6	1.020 (kept constant)
1.0	57.3	29.4	13.0	0	17.6	6.9	4.6	
2.0	66.6	37.5	21.8	0	14.6	9.1	4.4	
3.0	58.3	49.9	30.7	0	0	9.6	3.1	
5.0	85.0	109.5	117.0	0	19.2	13.2	12.1	
8.0	197.9	308.6	204.8	4.5	93.9	34.2	9.2	
22.0	176.5	1377.4	136.0	18.7	131.4	36.0	106.7	
32.0	129.6	2111.1	119.7	24.5	144.8	40.5	202.7	
46.0	115.4	3045.8	125.6	29.8	169.6	52.0	332.6	
56.0	123.5	3063.3	126.9	29.1	177.4	57.4	345.9	
71.3	110.9	3544.0	115.8	32.3	190.1	73.1	401.4	
80.0	125.7	3980.2	124.4	35.4	212.2	88.0	444.8	
95.6	138.1	4056.4	123.4	34.7	209.2	104.9	444.4	
Aqua regia	1567.6	9035.5	2157.3	394.2	302.0	5099.9	461.7	

Table C.7. ICP results for test 2f.

t (hr)	Concentration (mg/L)							Volume (L)
	Al	Cu	Fe	Ni	Pb	Sn	Zn	
0.5	171.3	155.5	3.2	0	0	16.7	78.7	1.026 (kept constant)
1.0	237.7	71.6	9.5	0	0	29.7	19.5	
2.0	288.5	97.3	13.3	0	0	44.4	15.1	
3.0	322.8	159.5	7.7	4.0	19.0	49.9	16.2	
5.0	389.5	638.8	6.2	14.2	56.5	61.6	38.4	
8.0	376.3	1378.3	5.2	21.1	42.8	66.9	120.1	
22.3	373.8	3925.7	8.4	33.8	196.5	118.6	445.7	
31.8	369.4	4223.5	10.0	33.7	208.8	204.7	447.9	
46.3	390.5	4492.0	18.6	36.1	224.5	581.7	466.9	
55.7	376.2	4366.1	17.2	34.8	212.2	610.6	437.2	
71.8	377.7	4571.4	18.5	35.1	194.7	545.4	398.2	
80.0	356.2	4385.3	17.3	33.3	190.4	433.5	332.3	
99.8	110.0	4505.8	12.0	34.3	156.7	108.1	171.8	
Aqua regia	1339.9	5649.2	1625.9	447.7	300.6	2674.2	468.8	

Table C.8. ICP results for test 2g.

t (hr)	Concentration (mg/L)							Volume (L)	
	Al	Cu	Fe	Ni	Pb	Sn	Zn		
0.3	21.3	93.3	0	0	10.0	8.4	28.1	1.031 (kept constant)	
1.6	50.9	195.1	19.3	0	25.8	5.9	14.2		
2.0	59.7	241.2	22.3	0	26.0	5.1	6.2		
3.5	80.1	382.8	25.5	3.2	40.7	4.3	13.2		
5.8	98.6	568.5	25.6	4.6	46.5	4.1	23.2		
7.8	105.6	749.4	21.8	5.8	45.8	3.5	32.4		
24.4	113.2	1609.4	27.4	9.7	68.0	4.4	84.8		
31.3	118.1	2036.5	20.9	11.0	67.9	4.9	101.2		
49.8	103.9	2648.0	21.3	12.5	76.6	4.3	214.2		
55.1	100.9	2847.9	18.6	12.9	74.3	3.7	242.6		
72.8	98.2	3294.7	18.6	14.1	84.7	3.7	305.8		
Aqua regia	1596.7	10943.0	2220.7	416.8	401.8	4489.1	1283.6		0.20

Table C.9. ICP results for test 2h.

t (hr)	Concentration (mg/L)							Volume (L)	
	Al	Cu	Fe	Ni	Pb	Sn	Zn		
0.3	42.7	100.2	12.6	0	46.8	6.5	20.0	1.002 (kept constant)	
1.6	122.1	324.6	42.0	7.1	63.2	9.9	25.0		
2.0	134.0	463.2	27.6	8.2	56.1	7.2	36.1		
3.5	128.2	824.1	13.6	11.2	52.5	3.8	65.5		
5.8	130.9	1341.0	9.4	14.5	57.3	0	117.7		
7.8	190.1	1914.4	12.7	17.4	77.9	4.6	193.9		
24.4	209.7	3424.7	5.6	25.1	104.4	5.7	452.9		
31.3	173.4	3762.5	3.4	25.3	112.8	5.6	500.8		
49.8	159.6	4835.3	0	27.4	128.0	8.5	654.9		
55.1	156.8	4982.4	0	27.9	130.2	9.6	669.0		
72.8	161.4	5478.2	0	28.9	56.5	12.7	665.7		
Aqua regia	2354.2	3896.9	2217.2	394.6	653.2	4988.9	188.9		0.197

Table C.10. ICP results for test 2i.

t (hr)	Concentration (mg/L)							Volume (L)
	Al	Cu	Fe	Ni	Pb	Sn	Zn	
0.2	116.1	84.5	20.0	5.8	7.8	14.1	8.2	1.007 (kept constant)
1.0	250.7	307.3	17.9	13.6	25.1	17.4	13.9	
2.0	314.8	647.2	14.9	15.9	41.8	17.6	35.9	
3.0	374.9	1017.3	14.0	17.9	54.9	20.4	68.0	
5.0	363.7	1487.1	15.4	21.0	61.0	21.9	133.4	
8.0	379.4	2145.1	15.1	27.1	76.5	26.6	237.9	
22.1	365.7	3736.1	16.0	33.0	106.6	45.8	457.1	
31.9	319.5	3688.2	20.5	33.0	111.6	48.7	454.7	
46.1	22.3	3430.1	15.8	31.8	83.8	23.5	416.9	
55.4	18.2	3328.4	15.1	32.1	89.0	6.9	409.0	
70.5	16.9	3209.4	15.0	32.7	84.6	0	389.2	
80.0	18.3	3300.3	14.7	32.9	86.2	0	395.4	
97.2	16.8	3158.4	14.6	32.3	82.1	0	376.7	
Aqua regia	2649.9	6889.8	2585.9	448.6	750.9	3951.8	535.0	0.20

Table C.11. ICP results for test 2j.

t (hr)	Concentration (mg/L)							Volume (L)
	Al	Cu	Fe	Ni	Pb	Sn	Zn	
0.5	39.6	66.5	25.3	0	17.0	9.0	6.9	1.051 (kept constant)
2.8	124.6	197.5	85.8	6.4	45.6	8.8	9.6	
4.7	132.0	252.1	99.2	7.3	49.5	8.4	9.7	
5.2	140.5	285.9	106.4	8.0	59.2	8.6	10.8	
7.7	159.5	448.3	128.0	11.2	95.9	10.6	19.2	
22.0	188.2	1287.1	139.1	20.5	163.1	14.7	126.0	
29.8	206.2	1618.0	128.0	23.4	169.2	16.8	179.9	
49.3	212.1	2530.4	72.9	32.1	191.1	20.0	317.3	
53.8	192.6	2521.9	64.5	31.2	179.2	19.1	311.1	
70.8	159.4	2956.1	54.0	33.4	172.9	19.4	358.6	
77.8	185.6	3302.3	83.4	39.8	200.5	26.8	398.0	
96.0	171.8	3830.1	73.7	38.6	212.2	29.6	456.7	
Aqua regia	2194.9	8608.5	2077.8	482.7	360.8	5083.2	511.9	

Table C.12. ICP results for test 2k.

t (hr)	Concentration (mg/L)							Volume (L)
	Al	Cu	Fe	Ni	Pb	Sn	Zn	
0.5	67.4	92.6	39.1	5.7	14.4	7.8	9.3	1.037 (kept constant)
2.8	167.4	292.4	128.1	7.9	98.6	16.5	11.8	
4.7	191.2	534.1	127.1	12.6	132.5	17.4	25.0	
5.2	211.8	631.8	133.3	13.9	140.1	18.7	31.2	
7.7	224.9	927.1	79.8	17.5	134.3	16.6	59.3	
22.0	239.3	2230.6	41.5	26.7	164.7	22.1	261.4	
29.8	234.6	2821.8	36.8	30.5	188.1	26.3	334.9	
49.3	172.6	3805.1	28.8	34.4	203.3	34.0	444.0	
53.8	147.9	3679.5	28.3	33.1	190.0	31.8	432.7	
70.7	140.3	4573.6	26.0	36.7	211.7	44.8	519.1	
77.7	130.5	4542.0	25.1	36.0	203.3	47.3	514.4	
96.0	117.9	4586.7	26.4	34.9	198.4	51.3	507.2	
Aqua regia	3170.8	3141.9	2572.7	474.5	688.0	5899.8	173.8	

Table C.13. ICP results for test 2l.

t (hr)	Concentration (mg/L)							Volume (L)
	Al	Cu	Fe	Ni	Pb	Sn	Zn	
0.2	119.4	77.9	25.4	9.4	9.1	14.2	8.6	1.013 (kept constant)
1.0	225.3	155.1	26.1	10.5	0	30.3	9.8	
2.0	286.3	309.7	17.7	12.0	27.5	35.3	11.3	
3.0	328.7	622.5	17.9	17.3	75.2	39.5	24.4	
5.0	333.1	1306.7	19.3	22.0	94.3	46.8	84.4	
8.0	323.4	2084.5	15.7	23.0	102.9	52.7	187.8	
22.1	312.8	3987.4	16.9	26.3	151.3	89.5	447.7	
31.9	317.5	4395.7	19.1	27.2	185.7	136.3	481.1	
46.1	322.3	3690.1	21.0	27.5	217.7	415.6	472.4	
55.4	319.7	3575.2	20.1	26.8	194.6	426.3	483.6	
70.5	48.7	3276.1	15.3	26.8	157.4	259.3	452.2	
80.0	20.2	3007.9	12.8	25.5	124.1	128.6	413.7	
97.2	17.7	3096.6	14.0	27.0	119.2	80.9	424.2	
Aqua regia	3076.5	10084.7	2332.1	404.6	865.9	4392.7	526.2	

Table C.14. ICP results for precious metal co-extraction.

t (hr)	Concentration (mg/L)							
	Test 2c		Test 2f		Test 2i		Test 2j	
	Au	Ag	Au	Ag	Au	Ag	Au	Ag
0.2	0.004	0.178	0.008	0.140	0.006	0.142	0.003	0.182
1.0	0.003	0.104	0.003	0.050	0.008	0.067	0.004	0.067
2.0	0.003	0.087	0.003	0.048	0.014	0.071	0.007	0.090
3.0	0.011	0.045	0.002	0.070	0.026	0.114	0.014	0.185
8.0	0.011	0.066	0.045	0.172	0.051	0.263	0.043	0.305
22.1	-	-	-	-	0.042	0.018	0.134	0.155
55.4	0.063	0.017	0.152	0.028	0.113	0.363	0.128	0.282
70.5	0.056	0.127	0.129	0.134	0.126	0.336	0.170	0.246
97.2	0.059	0.171	0.131	0.381	0.127	0.259	0.186	0.243
Aqua regia	23.754	28.962	21.214	31.000	43.849	16.255	55.946	17.060

C.1.3 Additional tests

Table C.15. ICP results for test 2m.

t (hr)	Concentration (mg/L)							Volume (L)
	Al	Cu	Fe	Ni	Pb	Sn	Zn	
0.3	84.8	71.7	7.5	0	12.1	7.4	9.8	1.003 (kept constant)
1.0	178.7	222.1	10.2	0	35.7	6.7	14.5	
2.0	232.3	408.6	7.3	0	46.8	5.8	22.3	
3.0	203.2	600.9	6.7	0	49.8	5.0	31.4	
5.0	226.8	925.0	6.8	0	60.4	6.1	51.0	
8.0	236.9	1281.6	6.4	0	67.8	6.7	78.7	
22.3	253.8	2130.7	12.8	7.2	112.9	14.0	195.1	
32.0	253.3	3059.2	9.0	8.1	128.4	22.6	292.6	
48.3	51.4	3471.6	8.0	8.3	52.9	7.2	235.9	
Aqua regia	2527.5	10179.8	3496.8	601.7	1311.1	5189.4	1243.4	0.217

Table C.16. ICP results for test 3a.

t (hr)	Concentration (mg/L)							Volume (L)
	Al	Cu	Fe	Ni	Pb	Sn	Zn	
0.5	115.3	215.9	28.6	0	29.1	6.5	10.7	0.530
1.4	124.3	491.2	24.8	0	35.3	6.9	32.3	0.581
1.9	51.5	766.0	21.2	0	31.7	6.4	55.8	0.607
3.0	47.3	909.8	21.3	4.3	29.6	6.1	64.6	0.668
5.0	30.1	969.4	19.7	0	22.2	4.5	65.4	0.784
8.0	21.5	903.6	13.1	0	13.3	0	54.5	0.960
10.0	37.5	876.3	11.4	0	12.7	0	48.5	1.076
12.0	60.3	893.7	8.7	0	12.3	0	45.3	1.192
Aqua regia	3884.8	19957.3	2802.7	493.2	2017.4	6014.5	2669.1	0.102

Table C.17. ICP results for test 3b.

t (hr)	Concentration (mg/L)							Volume (L)
	Al	Cu	Fe	Ni	Pb	Sn	Zn	
0.5	150.4	333.2	26.1	6.9	25.9	8.6	18.2	0.515
1.4	139.3	949.2	12.1	8.3	27.0	4.4	62.0	0.539
1.9	136.6	1456.3	12.1	9.3	27.5	7.9	116.4	0.549
3.0	110.0	1552.7	12.8	9.5	25.2	7.3	128.3	0.578
5.0	41.1	1776.4	14.4	10.0	24.6	7.0	154.7	0.634
8.0	61.3	1553.1	9.4	7.6	16.0	4.6	128.9	0.720
10.0	14.1	1477.3	8.7	6.9	15.8	0	122.9	0.776
12.0	12.3	1425.3	7.9	6.0	14.1	0	118.0	0.832
Aqua regia	2920.0	13957.1	3850.8	489.1	1177.1	4318.0	1259.3	0.109

Table C.18. ICP results for test 3c.

t (hr)	Concentration (mg/L)							Volume (L)
	Al	Cu	Fe	Ni	Pb	Sn	Zn	
0.5	151.1	60.2	19.0	0	4.9	11.0	7.1	0.509
1.0	217.2	91.2	24.4	0	0	18.7	7.9	0.514
2.1	203.8	151.9	19.8	0	4.7	16.2	7.7	0.529
3.2	196.5	309.3	15.1	0	13.9	14.9	17.6	0.545
5.2	212.6	690.1	15.5	4.6	26.3	17.5	50.7	0.577
8.1	76.5	1075.2	13.6	5.9	24.4	15.8	93.0	0.625
10.0	43.1	1214.3	10.5	6.2	20.9	13.8	109.3	0.656
12.0	34.0	1311.5	9.5	6.5	21.0	12.0	119.5	0.688
Aqua regia	2377.6	21280.8	2441.0	603.8	1437.9	5250.0	2305.9	0.114

Table C.19. ICP results for test 3d.

t (hr)	Concentration (mg/L)							Volume (L)
	Al	Cu	Fe	Ni	Pb	Sn	Zn	
0.5	122.3	60.8	26.6	0	7.0	11.1	5.2	0.509
1.2	160.2	95.4	27.6	0	8.4	16.1	5.6	0.511
2.0	167.8	159.4	24.7	0	9.9	16.7	7.2	0.514
3.1	175.7	319.6	21.2	0	19.3	17.4	16.2	0.520
5.2	108.9	643.0	18.8	10.3	24.3	17.5	37.9	0.535
8.0	47.9	908.7	15.9	6.1	23.5	15.8	56.8	0.556
10.0	35.6	963.4	14.0	6.6	17.5	13.2	57.2	0.570
12.0	29.0	1029.4	13.0	7.0	18.0	10.7	62.0	0.584
Aqua regia	2229.3	20153.7	2305.5	537.1	1309.1	4275.0	2712.3	0.116

Table C.20. ICP results for precious metal co-extraction.

t (hr)	Concentration (mg/L)			
	Test 3a		Test 3b	
	Au	Ag	Au	Ag
0.5	0.012	0.076	0.008	0.128
1.4	-	-	0.019	0.086
1.9	0.042	0.144	0.034	0.104
3.0	-	-	0.035	0.253
8.0	0.036	0.194	0.049	0.638
10.0	-	-	0.022	0.356
12.0	0.030	0.270	0.022	0.378
Aqua regia	31.010	33.610	40.680	35.710

C.1.4 Feed composition for bench-scale tests

Table C.21. Feed composition for bench-scale base metal leach tests.

Test	PCB composition (wt%)								
	Ag	Al	Au	Cu	Fe	Ni	Pb	Sn	Zn
2a	0.03	2.82	0.03	23.50	2.36	0.52	1.05	4.36	2.21
2b	0.02	5.59	0.04	26.92	3.50	0.72	1.66	7.76	2.61
2c	0.02	1.42	0.02	21.98	1.77	0.43	0.94	3.50	1.82
2d	0.01	1.23	0.02	23.42	2.32	0.42	1.24	4.14	2.42
2e	0.02	1.69	0.02	23.23	2.05	0.42	1.09	4.05	2.17
2f	0.01	1.45	0.02	22.90	1.19	0.46	0.88	2.36	1.08
2g	0.02	1.70	0.02	22.52	1.86	0.39	0.68	3.61	2.30
2h	0.01	2.53	0.01	25.39	1.75	0.43	0.75	3.98	2.86
2i	0.04	2.23	0.01	18.66	2.13	0.49	0.94	3.17	1.99
2j	0.01	2.34	0.02	22.58	1.83	0.52	1.17	3.81	2.32
2k	0.01	2.80	0.02	21.66	1.97	0.49	1.34	4.47	2.27
2l	0.04	2.58	0.01	21.26	1.93	0.44	1.21	3.87	2.22
2m	0.03	2.43	0.02	22.90	3.07	0.56	1.36	4.53	2.04
3a	0.03	3.74	0.03	24.89	2.36	0.40	1.76	4.88	2.61
3b	0.03	2.66	0.04	21.99	3.43	0.47	1.13	3.78	1.91
3c	0.07	2.39	0.03	26.74	2.28	0.59	1.43	4.86	2.77
3d	0.05	2.23	0.01	23.57	2.20	0.53	1.30	4.01	2.81
Average	<i>0.03</i>	<i>2.46</i>	<i>0.02</i>	<i>23.18</i>	<i>2.23</i>	<i>0.49</i>	<i>1.17</i>	<i>4.18</i>	<i>2.26</i>
Std dev	<i>0.02</i>	<i>1.02</i>	<i>0.01</i>	<i>2.02</i>	<i>0.60</i>	<i>0.08</i>	<i>0.29</i>	<i>1.11</i>	<i>0.44</i>

C.1.5 Small pilot-scale leach tests

Table C.22. ICP results for test 4a(i).

t (hr)	Concentration (mg/L)							Volume (L)
	Al	Cu	Fe	Ni	Pb	Sn	Zn	
1.0	190.3	73.3	26.8		11.7	21.9	13.0	17.00
2.8	236.1	90.4	52.4	4.8	16.8	33.4	11.3	16.99
3.6	223.6	93.4	18.2	5.1	22.4	34.7	10.2	16.98
5.0	256.9	127.9	20.0	7.7	23.3	37.9	13.3	16.97
8.0	260.8	228.2	18.6	11.7	23.9	36.9	19.7	16.96
18.1	321.2	1034.0	14.5	19.2	37.8	50.2	116.9	16.95
24.3	318.8	1314.5	13.4	19.7	37.7	53.7	149.4	16.94
26.2	312.3	1399.1	15.3	19.6	41.3	52.5	166.7	16.93
42.8	302.3	2093.6	37.0	21.8	72.0	73.4	265.9	16.92
49.4	292.8	2040.5	17.0	21.3	76.0	78.7	262.5	16.91
66.6	250.8	1716.8	24.0	18.4	112.6	181.3	222.9	16.90

Table C.23. ICP results for test 4b(i).

t (hr)	Concentration (mg/L)							Volume (L)
	Al	Cu	Fe	Ni	Pb	Sn	Zn	
0.8	11.8	72.2	15.3	0.0	4.5	28.6	13.1	17.64
1.3	24.3	165.2	16.8	6.1	0.0	36.0	27.2	17.63
3.3	201.2	184.4	23.6	6.6	10.1	17.2	15.2	17.62
5.2	214.7	307.1	19.4	8.1	15.2	18.0	19.6	17.61
7.3	232.1	473.5	18.2	9.4	22.2	18.7	31.4	17.60
22.1	259.4	1435.4	14.2	14.0	77.8	27.2	133.3	17.59
28.1	232.7	1530.7	17.2	13.5	74.3	27.1	151.6	17.58
45.8	232.5	1965.0	16.1	15.0	89.5	49.1	188.4	17.57
51.8	231.6	2012.2	18.0	14.8	103.7	73.8	191.9	17.56

Table C.24. ICP results for test 4a(ii).

t (hr)	Concentration (mg/L)							Volume (L)
	Al	Cu	Fe	Ni	Pb	Sn	Zn	
4.0	27.0	355.3	15.4	6.7	0.0	20.7	36.8	10.12
6.5	37.3	532.0	13.5	8.0	0.0	24.4	67.1	10.11
16.1	59.2	1617.4	11.9	12.4	5.2	47.2	193.1	10.10
23.9	66.9	1967.3	12.2	13.1	10.8	66.9	227.7	10.09
28.7	64.1	1979.7	12.3	12.6	6.6	63.3	219.0	10.08
40.2	66.4	2136.7	13.6	12.5	14.8	86.7	224.6	10.07

Table C.25. ICP results for test 4b(ii).

t (hr)	Concentration (mg/L)							Volume (L)
	Al	Cu	Fe	Ni	Pb	Sn	Zn	
0.3	11.6	74.1	16.1	0.0	0.0	26.7	16.3	10.39
1.5	23.5	165.3	16.7	23.2	0.0	33.3	26.9	10.38
6.8	37.9	337.4	13.6	8.7	0.0	36.6	64.4	10.37
24.2	53.3	1192.2	15.7	13.2	8.7	57.3	213.8	10.36
30.1	53.7	1436.2	13.1	13.7	6.6	65.0	235.2	10.35
47.7	66.2	1956.9	12.4	16.3	11.6	84.3	288.9	10.34

C.2 Precious metal leach tests

C.2.1 Experimental design

Table C.26. ICP results for experimental design tests, at t = 48 hours.

Temp	Gly (M)	pH	Au (mg/L)	Volume (L)	Feed (mg)
60	0.5	11.5	0.075443	0.682	3.28
60	0.1	11.5	0.021092	0.671	3.84
60	0.5	12.5	0.061882	0.683	3.37
60	0.1	12.5	0.02055	0.677	3.37
75	0.1	11.5	0.020388	0.673	5.10
75	0.5	11.5	0.029827	0.686	3.97
75	0.1	12.5	0.024992	0.677	3.97
75	0.5	12.5	0.027508	0.685	3.97

C.2.2 Additional tests

Table C.27. ICP results for glycine tests without the addition of cyanide.

	Test 6a	Test 6b	Test 7a	Test 7b	Test 6a	Test 6b	Test 7a	Test 7b
t (hr)	Au (mg/L)				Volume (L)			
0.5	0.074	0.277	0.000	0.000	0.5089	0.505	0.502	0.5
1.0	0.085	0.147	0.000	0.000	0.51	0.515	0.502	0.495
2.0	0.091	0.116	0.009	0.016	0.5166	0.519	0.499	0.49
4.2	0.093	0.062	0.008	0.015	0.5356	0.546	0.502	0.485
8.0	0.086	0.050	0.014	0.017	0.5686	0.585	0.515	0.48
12.0	0.075	0.028	0.016	0.015	0.5856	0.633	0.541	0.475
24.0	0.109	0.000	0.032	0.020	0.6446	0.761	0.588	0.47
36.0	0.065	0.000	0.038	0.016	0.6596	0.821	0.623	0.465
48.0	0.047	0.000	0.030	0.025	0.7156	0.924	0.656	0.46
60.0	0.043	-	0.049	-	0.7498	-	0.713	-
72.0	0.041	0.000	0.054	0.041	0.7688	0.995	0.73	0.455
84.0	0.040	-	0.070	-	0.8298	-	0.765	-
96.0	0.032	0.000	0.066	0.068	0.9005	1.055	0.81	0.45

Table C.28. ICP results for test 6c (cyanide-glycine test), with initial volume of 500 mL.

t (hr)	Metal concentration (mg/L)								
	Ag	Al	Au	Cu	Fe	Ni	Pb	Sn	Zn
0.5	2.5	0.1	0.7	40.8	0.2	0.9	0.0	4.7	0.0
1.0	2.0	1.1	0.5	108.4	1.9	1.5	0.0	3.1	0.0
2.0	1.5	2.4	0.6	179.9	4.1	2.7	0.0	5.0	2.7
4.0	1.1	4.7	0.5	302.4	8.4	4.8	0.0	9.1	7.6
7.5	1.0	9.8	0.5	382.4	11.2	6.2	0.0	14.8	9.7
12.0	1.7	15.5	0.8	479.4	13.5	8.4	0.0	24.4	11.9
24.0	1.2	32.0	0.6	705.2	15.7	18.8	0.0	49.0	13.9
36.0	2.3	45.3	1.1	968.3	15.3	23.6	0.0	26.8	12.1
48.0	4.0	63.7	1.8	1472.4	15.3	24.9	0.0	8.8	18.9
60.0	4.8	66.7	2.5	1549.4	14.5	24.1	0.0	3.4	21.8
71.7	4.4	73.9	2.5	1735.9	15.3	25.3	0.0	1.5	26.3
79.0	4.7	78.2	2.7	1848.4	14.8	26.3	0.0	0.8	31.9
96.0	5.1	81.0	3.1	1959.1	16.2	26.5	0.0	0.3	35.6
Mass in feed (mg)	4.1	537.3	3.8	1714.7	573.8	82.0	121.0	408.0	166.9

C.2.2 Silver dissolution

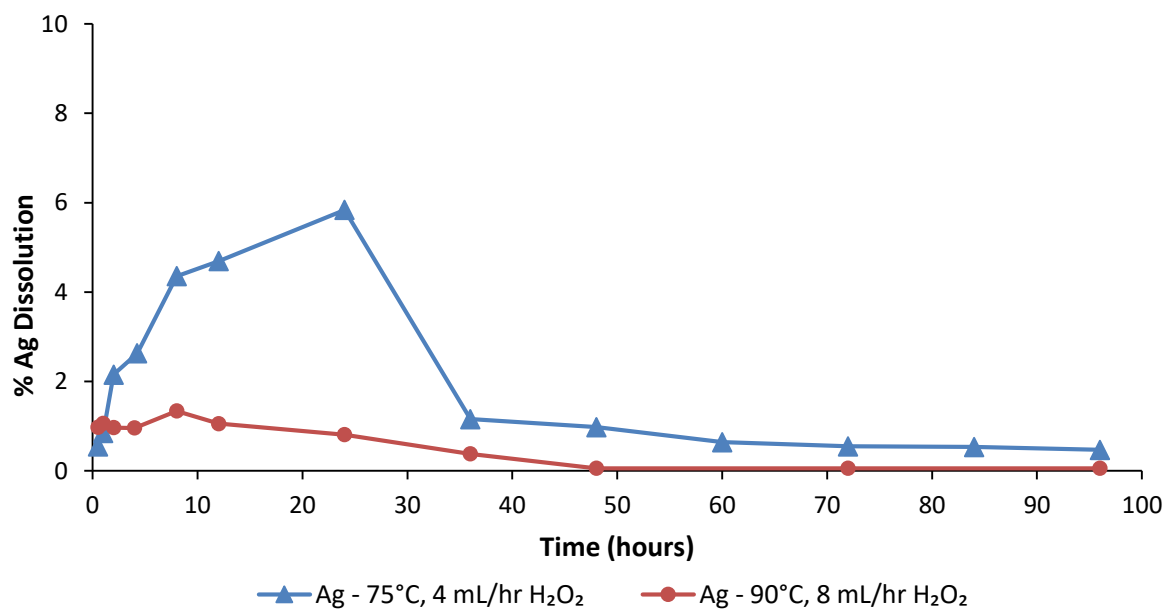


Figure C.1. Percentage silver dissolution as a function of time temperature and peroxide flowrate, for the tests performed at pH 12.5 and 0.5 M glycine.

Appendix D: Sample calculations

D.1 Mass balance to determine feed composition

Complete metal dissolution is assumed in the aqua regia tests.

The mass of metal i in the feed, $m_{i,feed}$, can be calculated using Equation B.1 to B.3.

During the glycine leach tests: at $t = 0$, the first sample is taken, $s=1, j=1$; for the second sample taken $s=2, j=2$; the final sample taken corresponds to $s=f, j=f$.

$$m_{i,feed} = m_{i,j=f} + m_{i,aqua\ regia} \quad [B.1]$$

The mass of species i in the aqua regia PLS after 24 hours, $m_{i,aqua\ regia}$, can be calculated from Equation B.2:

$$m_{i,aqua\ regia} = C_{i,aqua\ regia} V_{aqua\ regia} \quad [B.2]$$

$$m_{i,j} = (V_1 - \sum_{s=1}^{j-1} V_{sample,j}) \cdot C_{i,j} + (\sum_{s=1}^{j-1} V_{sample,s} \cdot C_{i,s}) \quad [B.3]$$

where $C_{i,j}$ is the mass concentration of species i in solution in the sample number j

$(V_1 - \sum_{s=1}^{j-1} V_{sample,j})$ is the volume of the solution prior to sample j being taken. The volume of peroxide and NaOH (from the pH controller), is added to $(V_1 - \sum_{s=1}^{j-1} V_{sample,j})$ where applicable.

$V_{sample,s}$ is the volume of the sample taken at sample number s .

The first term on the right hand side of Equation B.3 is the mass of that particular metal in solution at time j ; the second term is the mass of that particular metal that has been removed from the vessel in the samples taken prior to sample j .

D.2 Percentage dissolution

The fractional dissolution of metal i at time instance j , $X_{i,j}$, is the fraction of that species in the feed that is present in the leach solution at time j :

$$X_{i,j} = \frac{m_{i,j}}{m_{i,feed}} \quad [\text{B.4}]$$

with $m_{i,j}$ and $m_{i,feed}$ calculated using Equation B.1 to B.3.

$X_{i,j}$ is multiplied by 100 to obtain the percentage dissolution.

D.3 Rate calculations

Leach rates reported by Oraby and Eksteen (2015a) for a gold foil test (performed at 60°C, 0.5 M glycine, 1% H₂O₂, pH 11) were used to calculate the theoretical gold dissolution based on the surface area of the gold foils used in this project. These rates are summarised in Table 2.9.

From Table 2.9, for first 48 h, the average leach rate is calculated to be 0.347 µmol/m²s.

For 48 h – 96 h, leach rates are not provided; this was determined using the concentration versus time data reported by Oraby and Eksteen (2015a). The concentration versus time plot during this time period was approximately linear. Between 48 h and 96 h, ±6 mg Au (15 mg/L Au x 0.4 L) dissolved.

Calculating leach rate from literature based on concentration versus time data for 48 – 96 h, with foil surface area of 20 cm²:

$$\frac{6 \text{ mg}}{\frac{\text{mmol}}{10^3 \mu\text{mol}} \times 0.002 \text{ m}^2 \times \frac{196.967 \text{ mg}}{\text{mmol}} \times 48 \text{ h} \times \frac{3600 \text{ s}}{\text{h}}} = \frac{0.088 \mu\text{mol}}{\text{m}^2 \text{ s}}$$

Calculating theoretical mass of gold that should dissolve in this work, based on surface area of 1.56 cm²:

Mass of gold dissolved between 0 - 48 h:

$$\frac{0.347 \mu\text{mol}}{\text{m}^2 \text{ s}} \times \frac{\text{mmol}}{10^3 \mu\text{mol}} \times 0.000156 \text{ m}^2 \times \frac{196.967 \text{ mg}}{\text{mmol}} \times 48 \text{ h} \times \frac{3600 \text{ s}}{\text{h}} = 1.84 \text{ mg}$$

Mass of gold dissolved between 48 - 96 h:

$$\frac{0.088 \mu\text{mol}}{\text{m}^2 \text{ s}} \times \frac{\text{mmol}}{10^3 \mu\text{mol}} \times 0.000156 \text{ m}^2 \times \frac{196.967 \text{ mg}}{\text{mmol}} \times 48 \text{ h} \times \frac{3600 \text{ s}}{\text{h}} = 0.47 \text{ mg}$$